

FURTHER CHARACTERIZATION OF IRAS DOPED SILICON DETECTORS

(NASA-CR-152014) FURTHER CHARACTERIZATION  
OF IRAS DOPED SILICON DETECTORS (Naval Ocean  
Systems Center) 147 p HC A07/MF A01

N77-30985

CSSL 20L

Unclass

G3/76 44013

INFRARED DEVICES GROUP  
ELECTRONIC MATERIAL SCIENCES DIVISION  
NAVAL OCEAN SYSTEMS CENTER  
SAN DIEGO, CALIFORNIA 92152

JUNE 1977

THIS WORK PERFORMED FOR  
NASA AMES RESEARCH CENTER  
UNDER NASA P. R. No. A-39498B



## TABLE OF CONTENTS

	<u>Page</u>
1.0 INTRODUCTION _____	1
2.0 MEASUREMENT CONSIDERATIONS _____	2
3.0 SBRC Si:Sb DETECTOR MEASUREMENTS -----	3
4.0 DIELECTRIC RELAXATION EFFECTS _____	16
5.0 CHARACTERIZATION OF SPONTANEOUS NOISE SPIKES AND GAMMA-INDUCED SPIKES --	25
5.1. RIC/MSD Si:P _____	26
5.1.1. Dependence of Spontaneous Noise Spike Event Rate _____	27
5.1.2. Spontaneous Noise Spike Pulse Amplitude Distribution _____	31
5.1.3. Gamma Event Pulse Height Distribution _____	42
5.1.4. Spike Event Pulse Shapes _____	50
5.1.5. Software Circumvention of Spikes _____	55
5.2. RIC/MSD Si:As Hardware Circumvention of Gamma Spikes _____	58
5.3. SBRC Si:Sb - Spontaneous Noise Spikes _____	65
6.0 DC-COUPLED OUTPUT MEASUREMENTS _____	79

## FURTHER CHARACTERIZATION OF IRAS DOPED-SILICON DETECTORS

### 1.0 INTRODUCTION

The data in this report are the results of further measurements made on several doped-silicon detectors in support of the IRAS program. Previous measurements for the IRAS program were reported in NASA Contractor Report No. 151,941, "Characterization of IRAS Doped-Silicon Detectors," December 1976. Funding for this additional work was provided by NASA Purchase Request No. A-39498B from Ames Research Center.

This report presents data on a new Si:Sb detector manufactured by Santa Barbara Research Center (SBRC) as well as new data on several of the previously measured detectors. The data in this report falls into four general sections:

Section 3: Data on the new SBRC Si:Sb detector.

Section 4: Data showing the effects of detector bias on dielectric relaxation.

Section 5: Characterization of spontaneous noise and gamma-induced spikes and their circumvention.

Section 6: Data showing the time response of two detectors to step changes in the background photon flux density.

Section 5 should be of particular interest since little data on transient phenomena are readily available. The data contained in Section 6 is quite extensive and indicates several potential system problems.

## 2.0 MEASUREMENT CONSIDERATIONS

A complete description of the measurement apparatus and electronics was given in the previous report. The experimental set-up for the measurements reported here was identical to that previously used with one minor exception. While all data in the previous report were obtained with the cold MOSFET pre-amplifier operation as a source follower, some of the data in this report were obtained operating the MOSFET as the input stage of a transimpedance amplifier (TIA). In the TIA configuration the detector load resistor becomes the resistor in the feedback loop. This results in an increase in system bandwidth. The bandwidth in the TIA configuration is limited by the value of the feedback resistor and its shunt capacitance.

Data was obtained at very low background photon flux densities in several instances. This data is labeled "ZILCH" on the graphs. This term is used to indicate the lowest possible photon flux density available in a given measurement apparatus. For the data reported here, a zilch background is less than  $2 \times 10^7$  photons per second per  $\text{cm}^2$ .



### 3.0 SBRC Si:Sb DETECTOR MEASUREMENTS

The data presented in this Section were obtained in exactly the same manner as previously reported data. Spectral response, frequency response, noise spectra, etc., are shown in Figs. 1-12. The gap in the spectral response (Fig. 1) between 34.5 and 36.0 microns was due to a lack of energy caused by atmospheric water vapor absorption. The residual long wavelength response (greater than 30 $\mu$ m) is approximately 10%. Note that the optimum bias data shown in Fig. 2 was obtained at an operating temperature of 4.5K. While the optimum bias at 4.5K is 9 volts, there is evidence (see Section 5.3) that higher biases might be advantageous at lower temperatures. The signal wave-shape shown in Fig. 11 may be of interest. Spontaneous noise spikes are clearly shown in Figs. 10, 11, and 12.

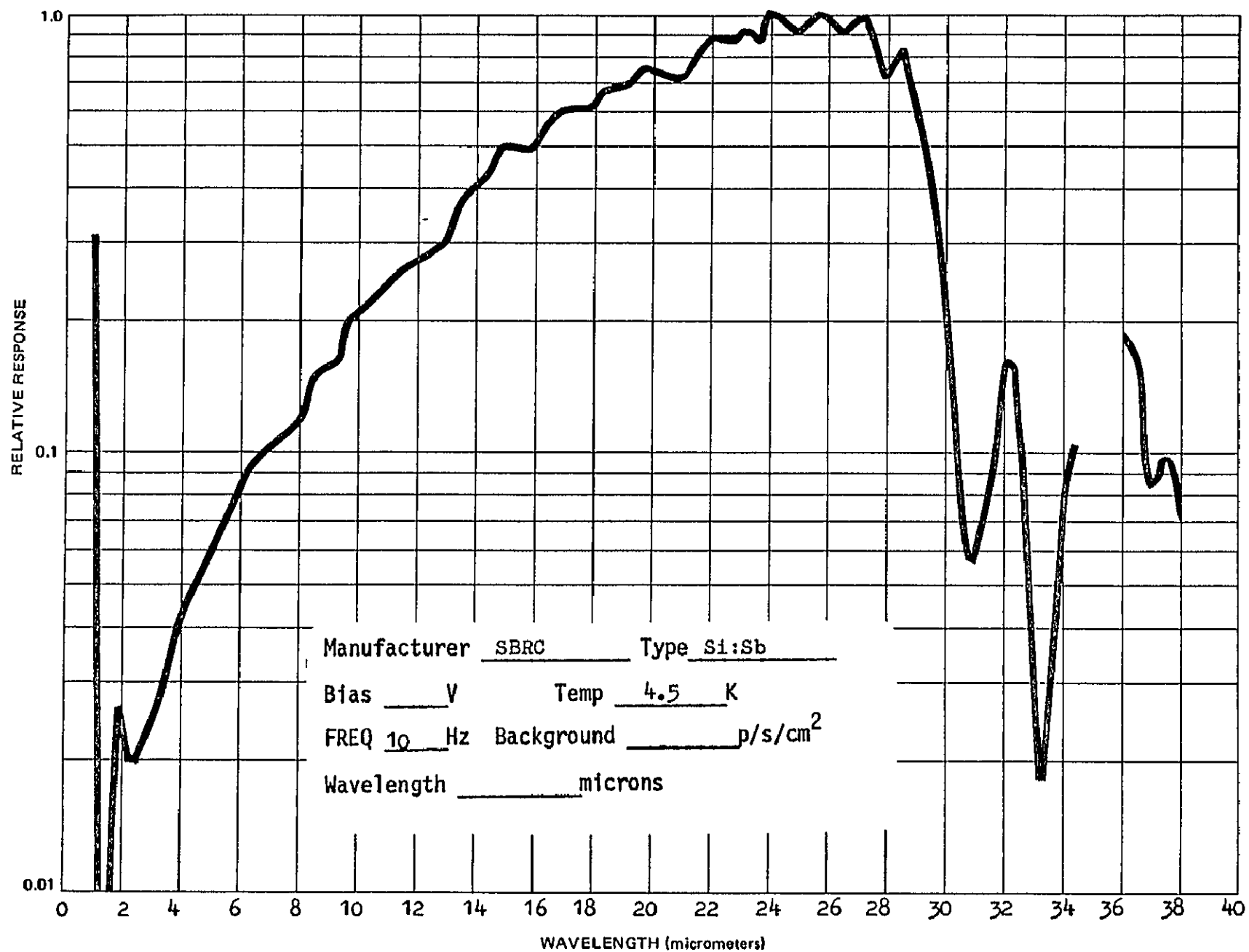


Figure 1

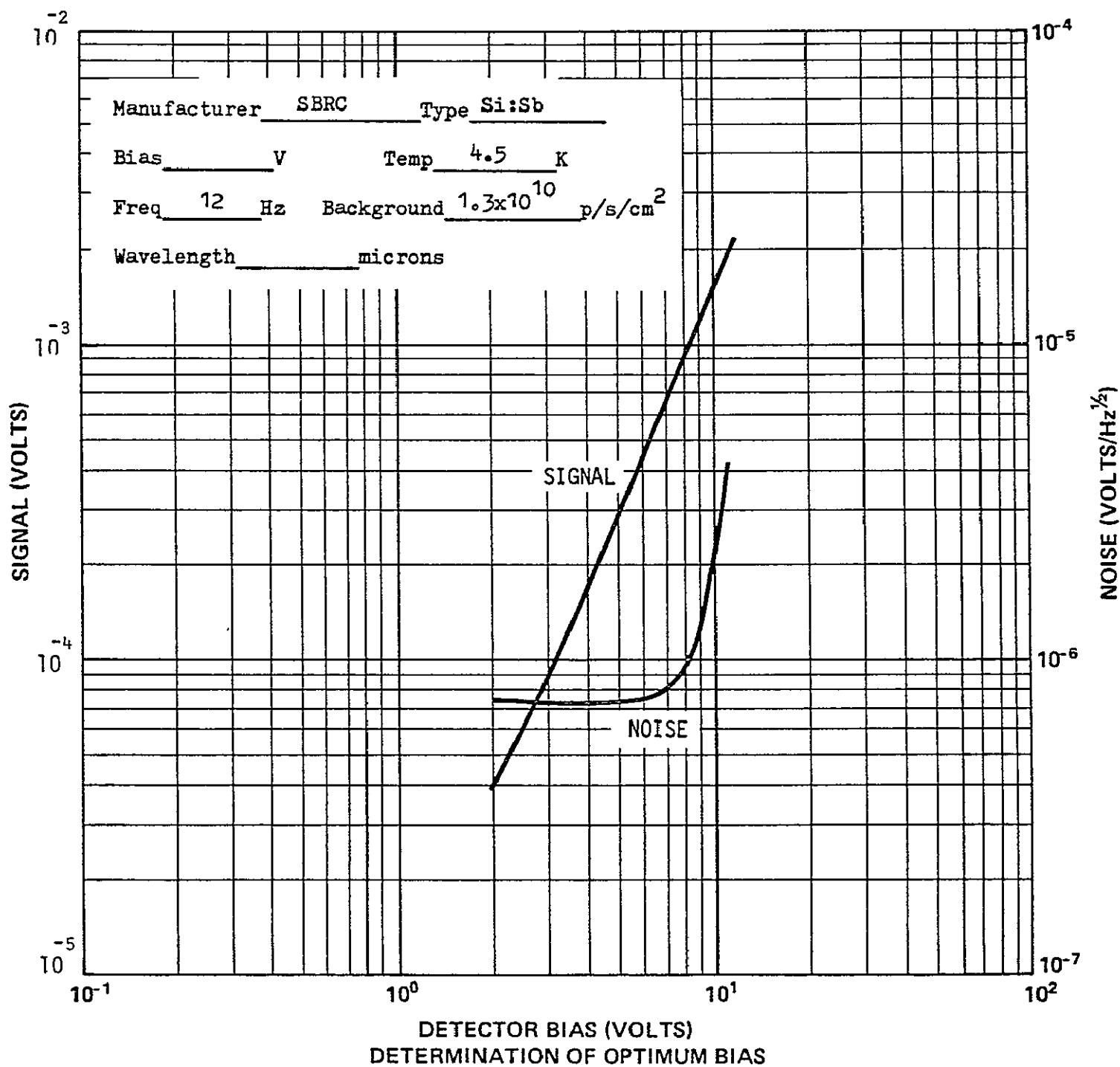


Figure 2

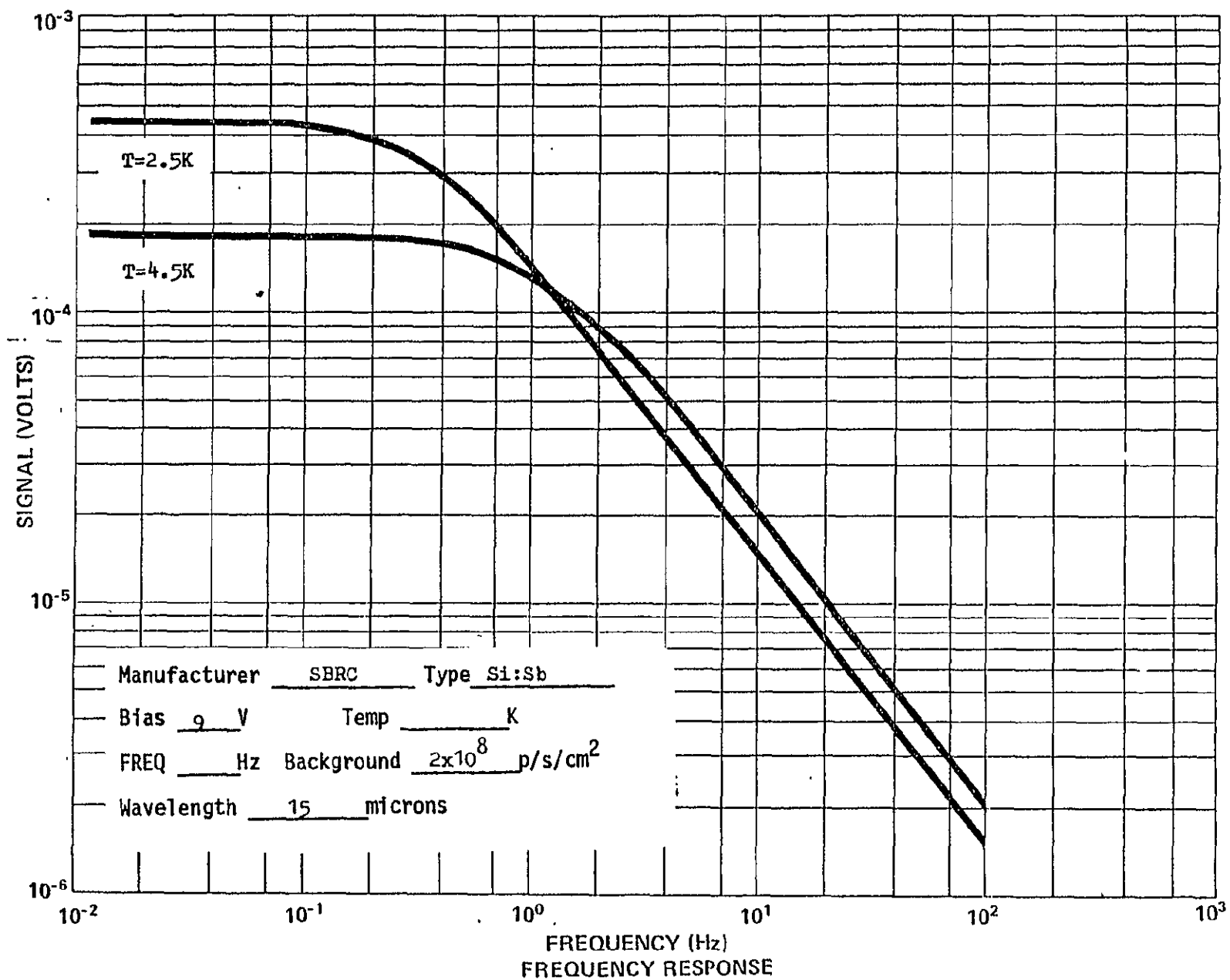


Figure 3

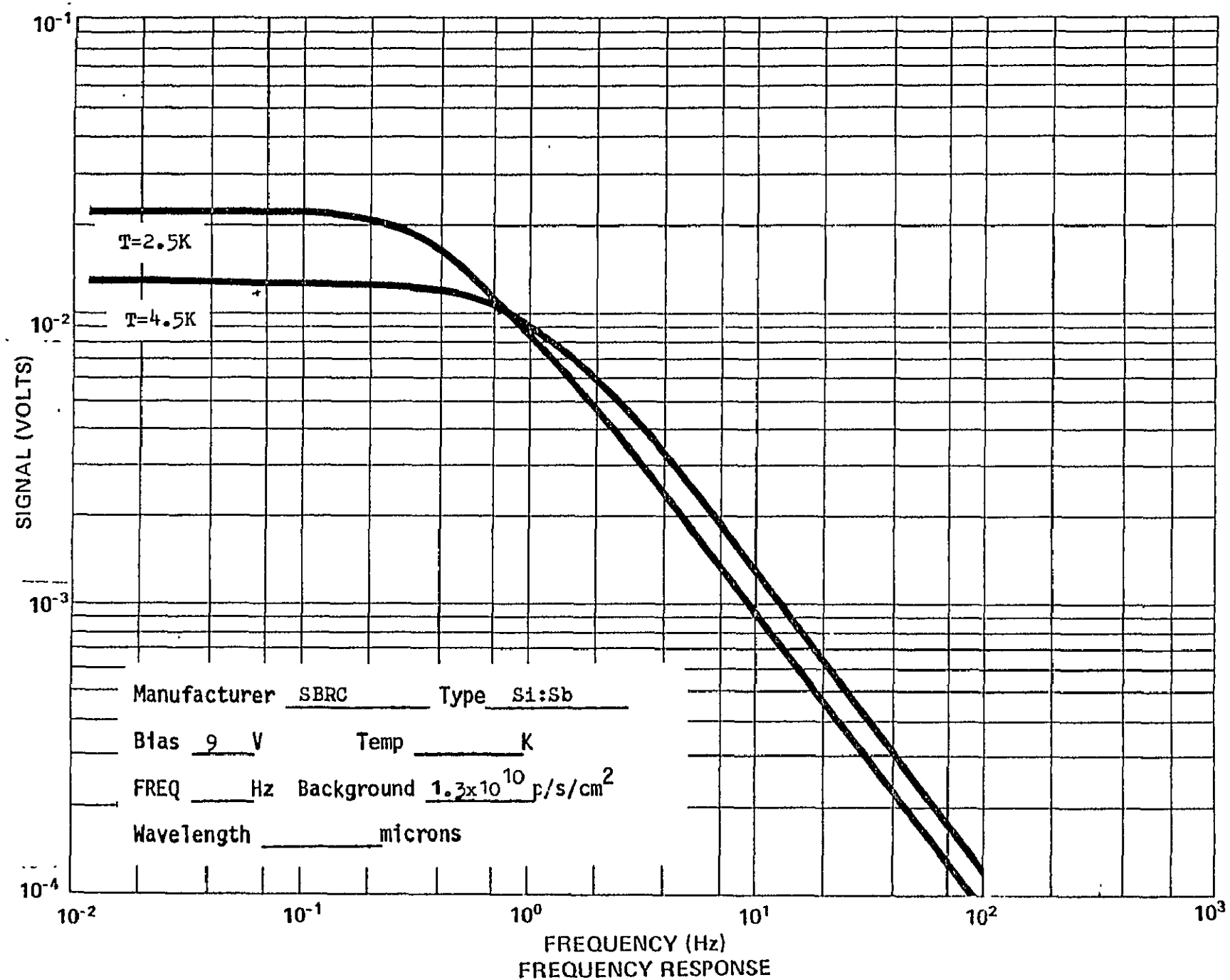


Figure 4

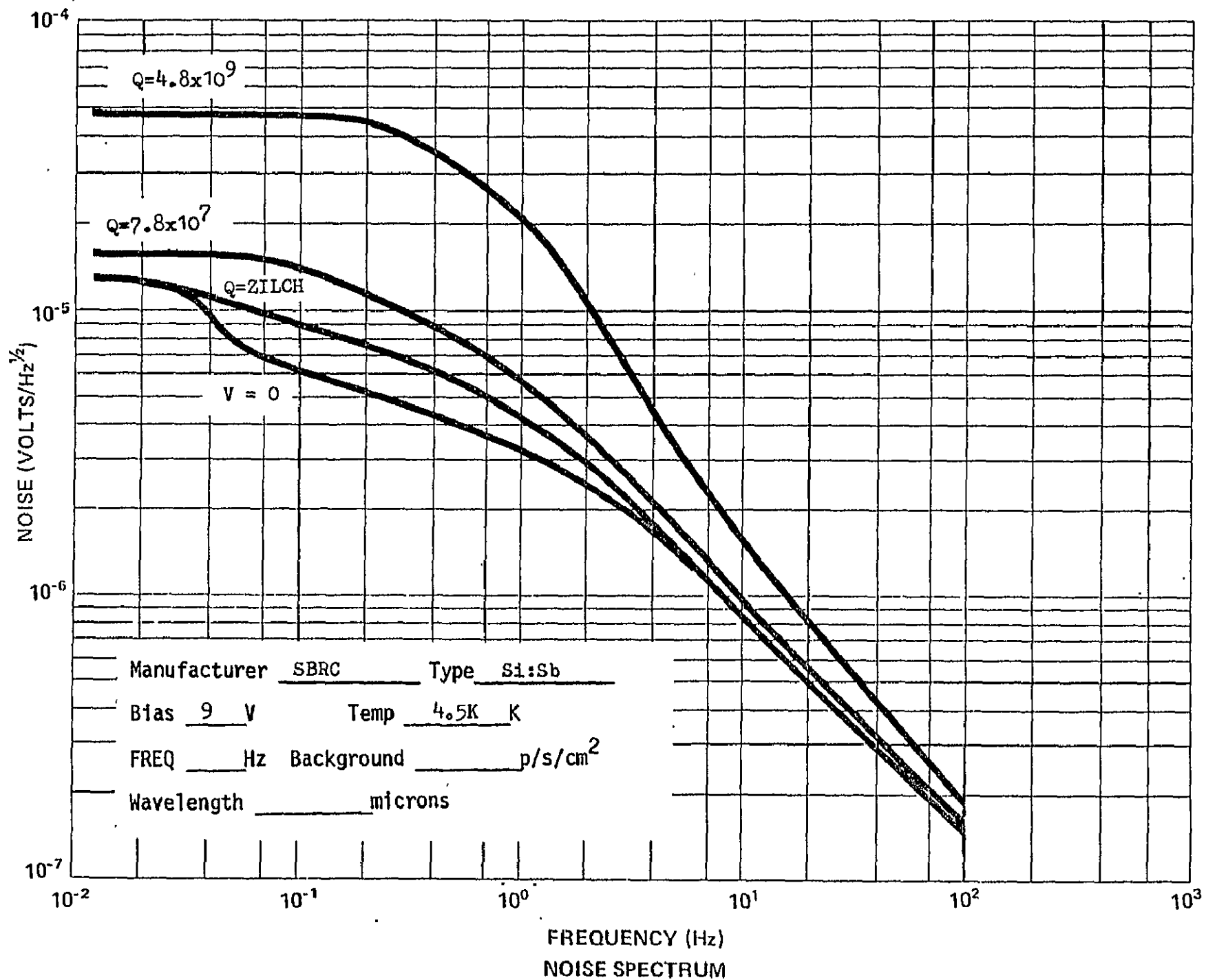


Figure 5

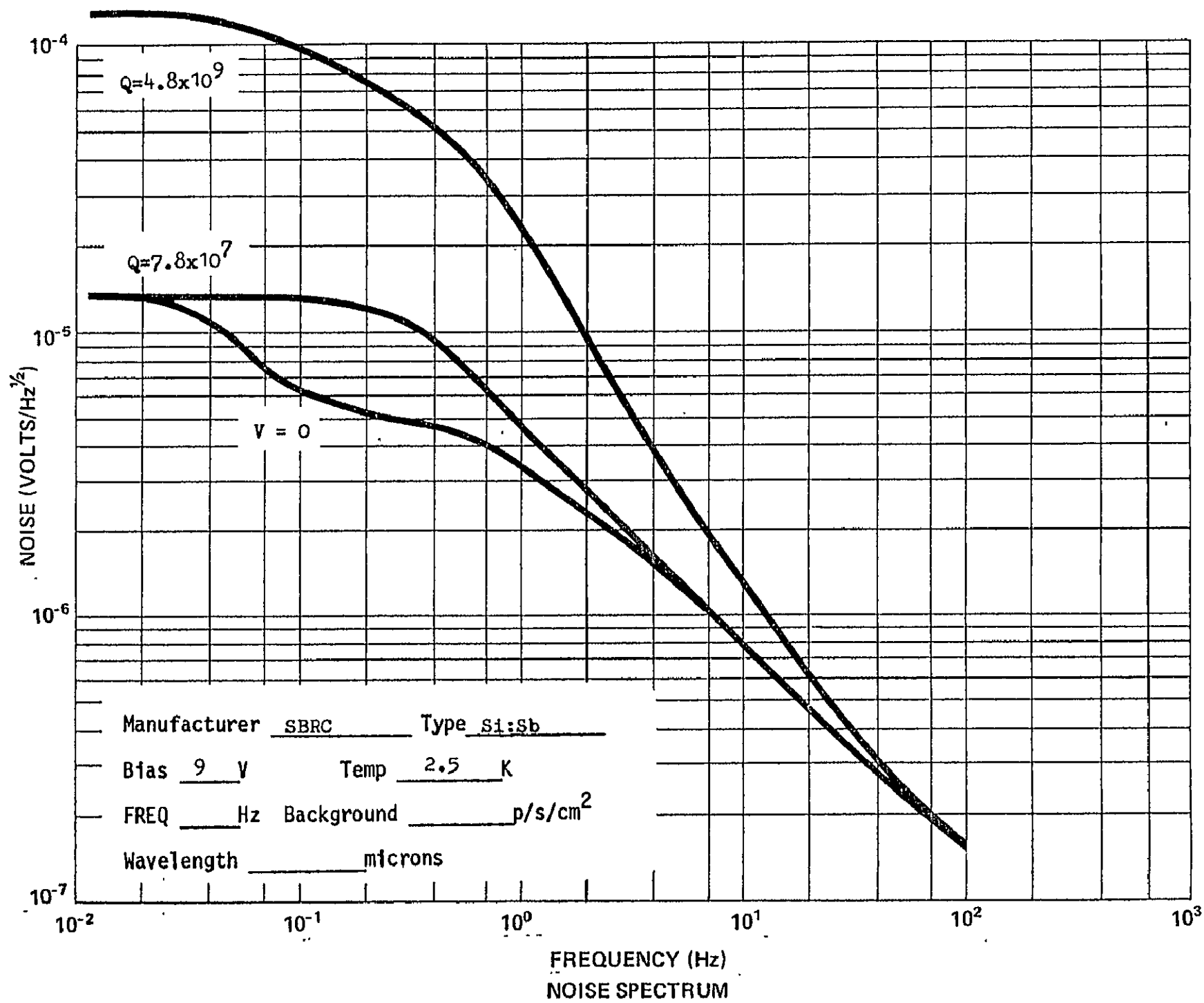


Figure 6

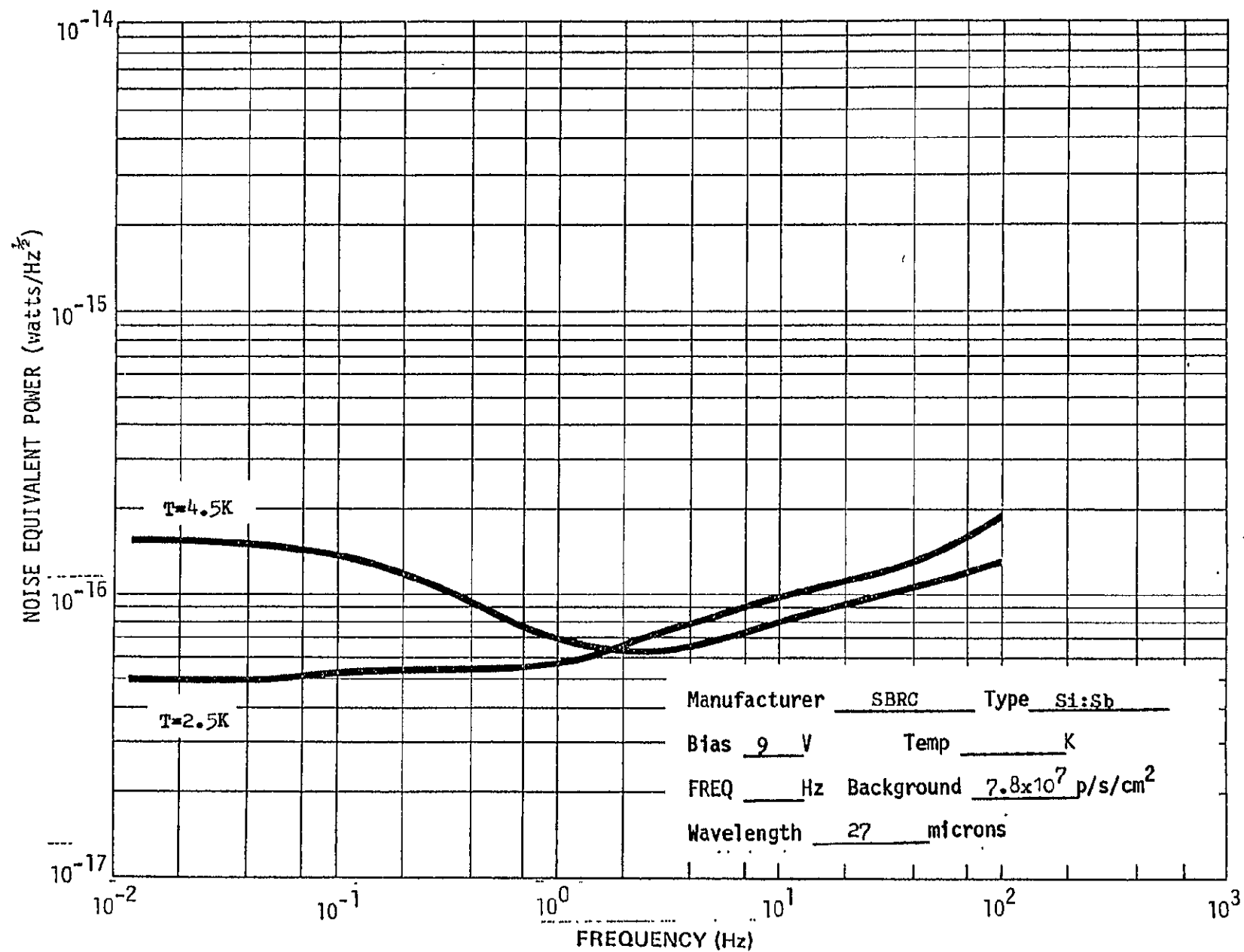


Figure 7



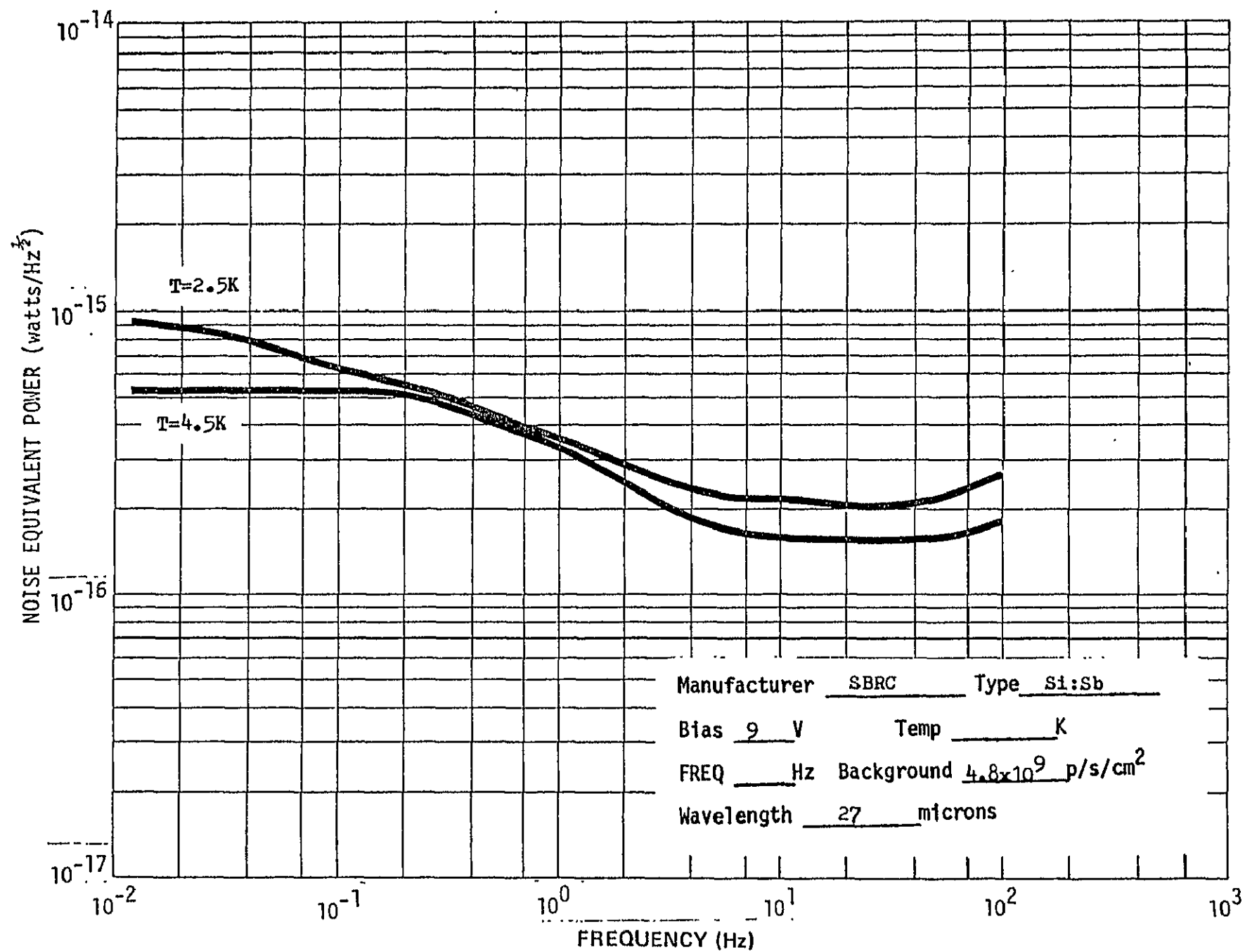


Figure 8

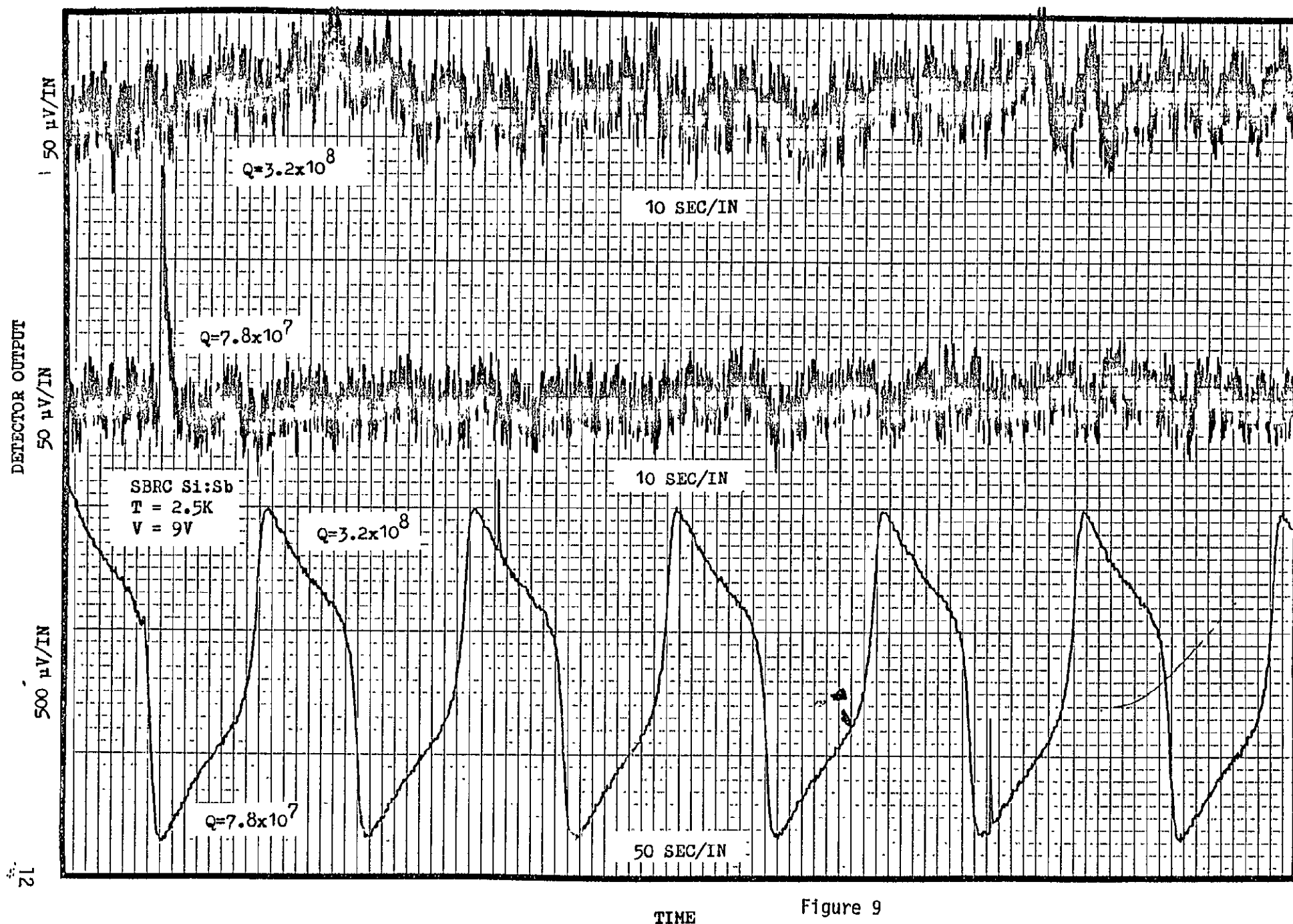


Figure 9

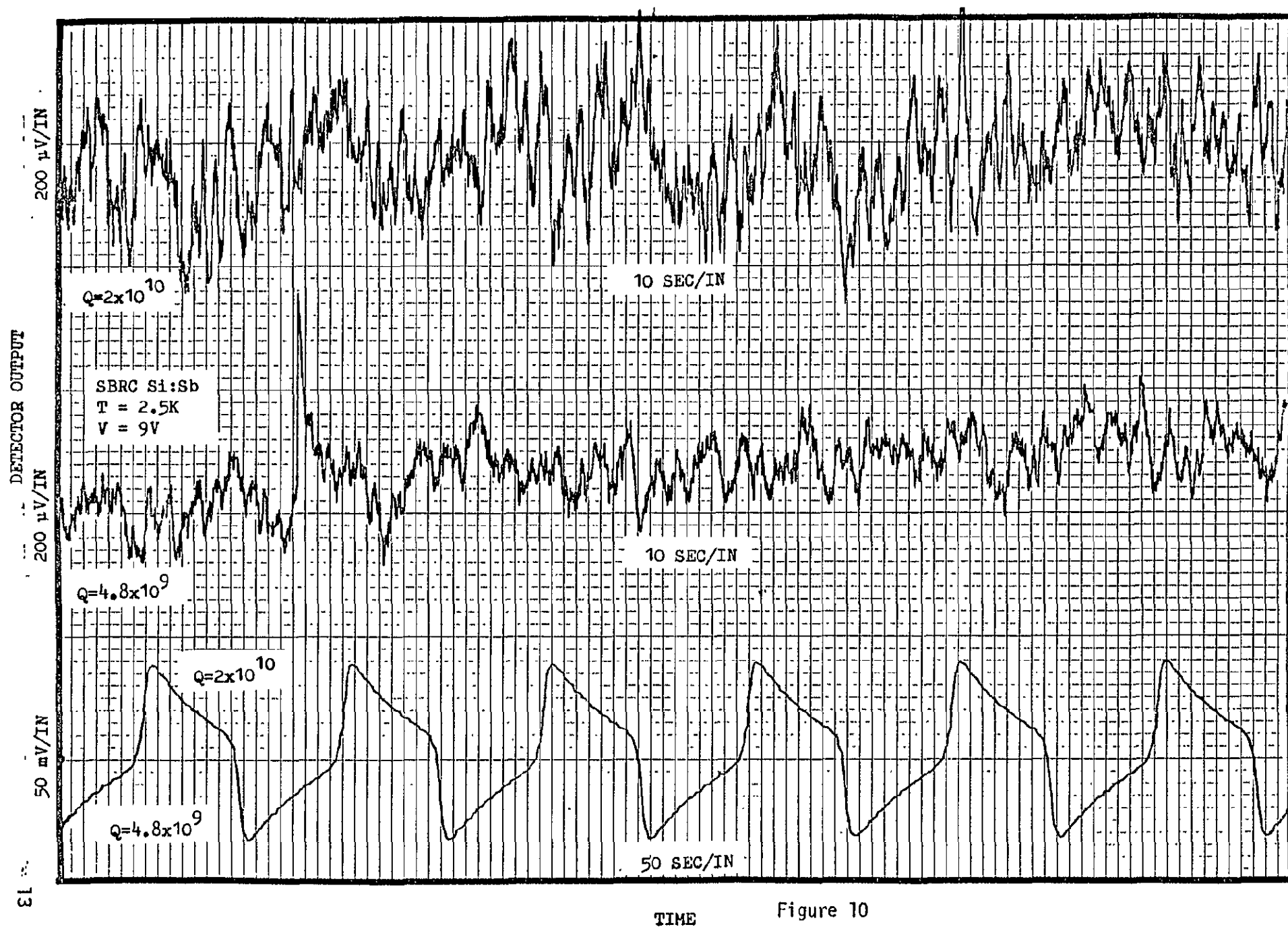
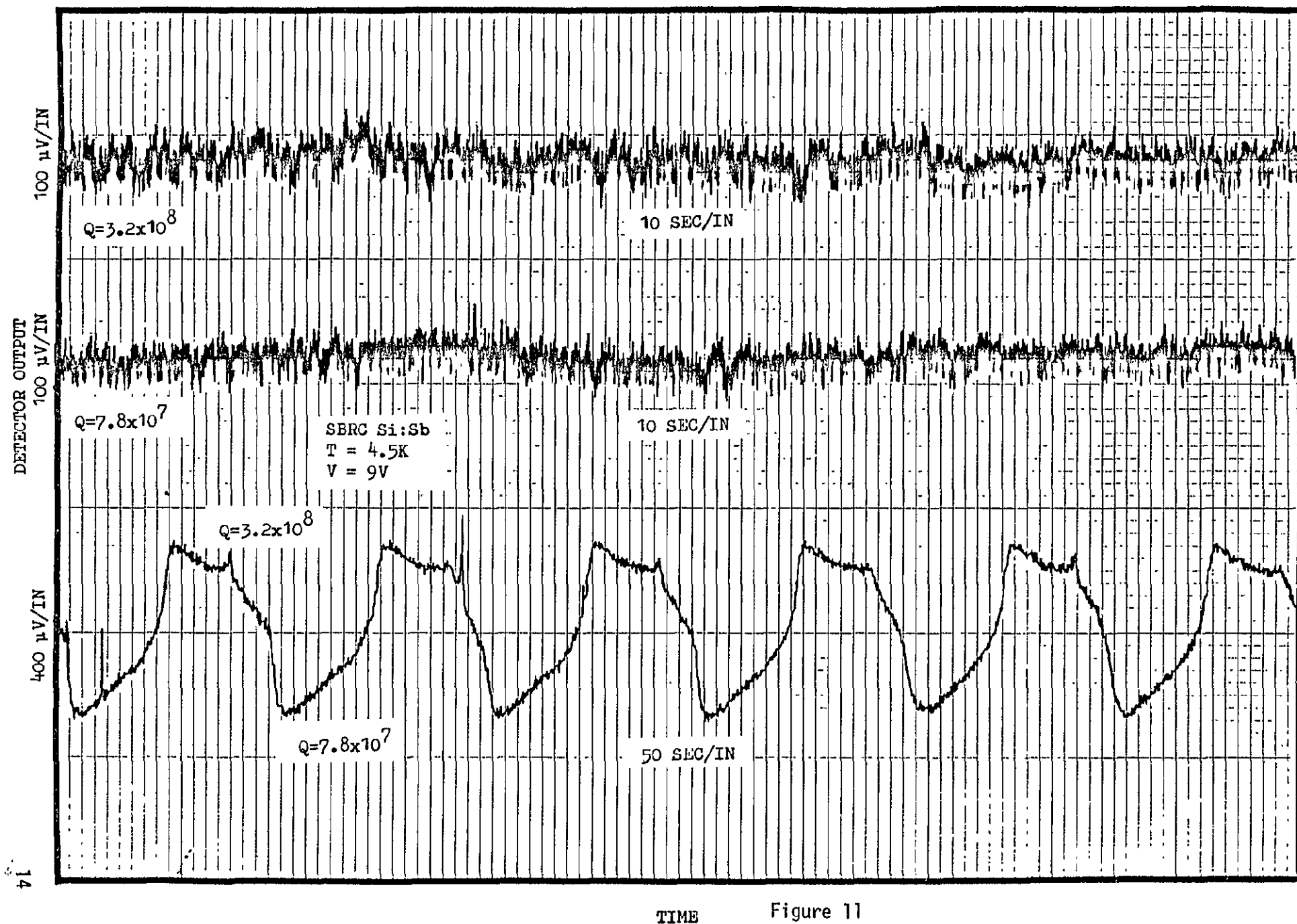


Figure 10



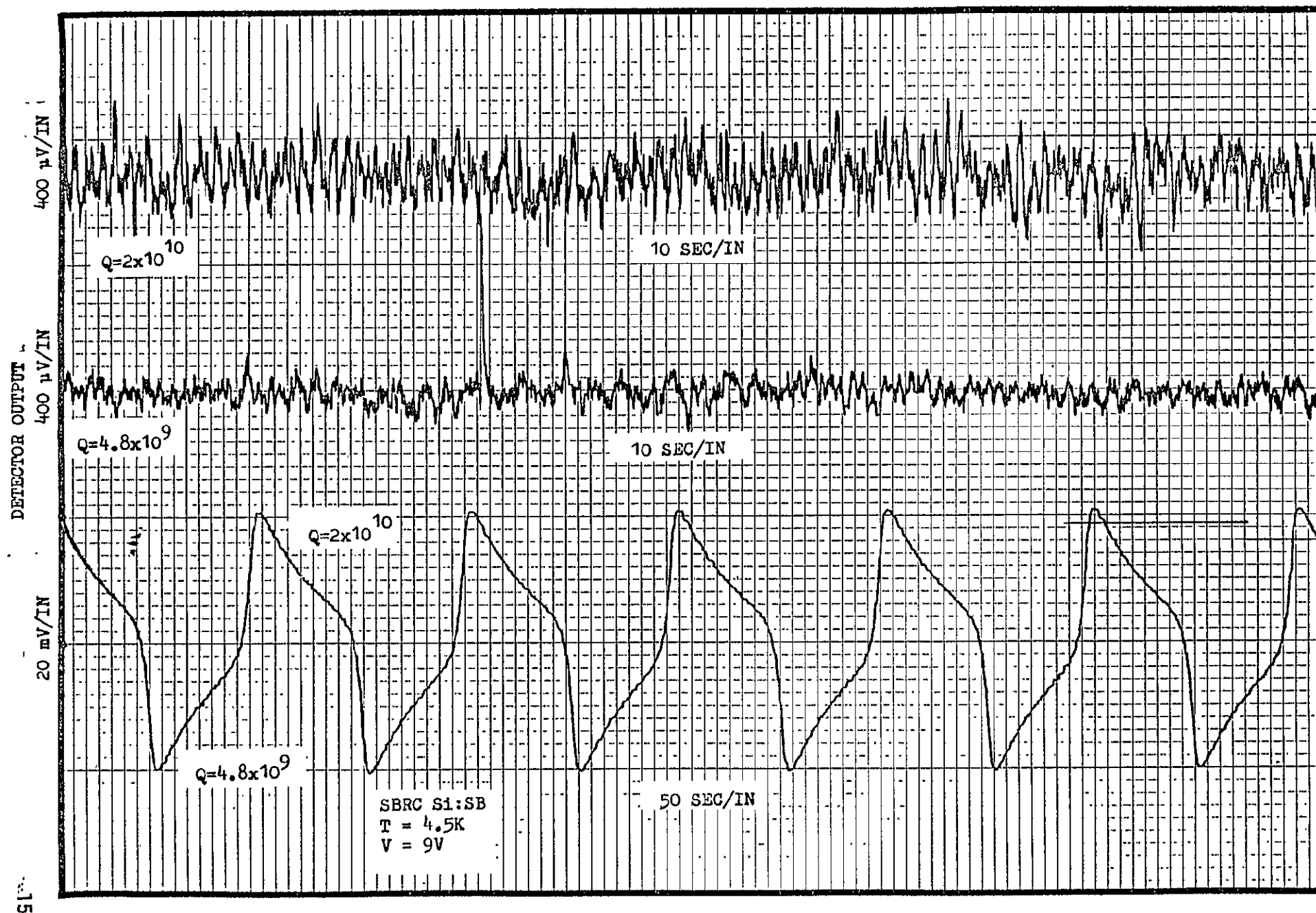


Figure 12

#### 4.0 DIELECTRIC RELAXATION EFFECTS

All extrinsic photoconductors operating under reduced photon backgrounds exhibit an effect known as "dielectric relaxation." A detector will have a high responsivity at low frequencies and a low responsivity at high frequencies. The frequency at which the transition between the two responsivities occurs seems to be related to the electrical conductivity of the detector. Detector conductivity, in turn, is a function of bias voltage, background photon, flux, and operating temperature.

To illustrate the effect of these three variables on the dielectric relaxation frequency, each parameter was varied while measuring the frequency response of two detectors between 0.012 and 12.0 Hz. Data for a RIC/MSD Si:Sb detector are shown in Figs. 13-16 and data for a SBRC Si:As detector are shown in Figs. 17-20. For each detector, measurements were made at two backgrounds, two operating temperatures, and several bias voltages. Measurements at the higher background were made using a TIA. A source follower configuration was used at the lower background. The dotted lines on the lower background graphs indicate the true detector response (correction was made for the input RC roll-off of the MOSFET). Note that for both detectors, the transition frequency between the low and high frequency responsivities moves to higher frequency with increasing background, temperature, and bias. Also for a fixed background and temperature, the ratio between the high and low frequency responsivities increases with increasing bias voltage.

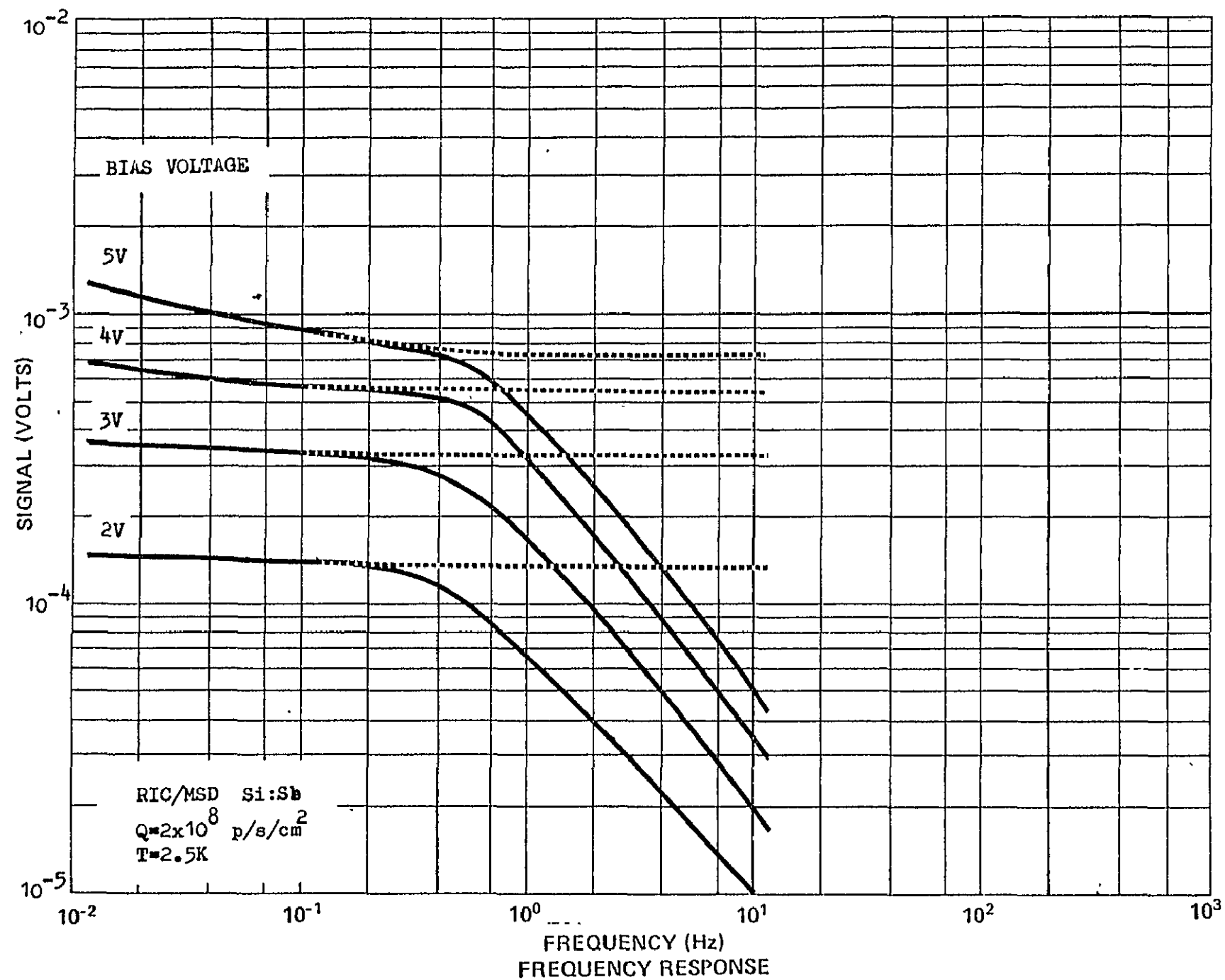


Figure 13

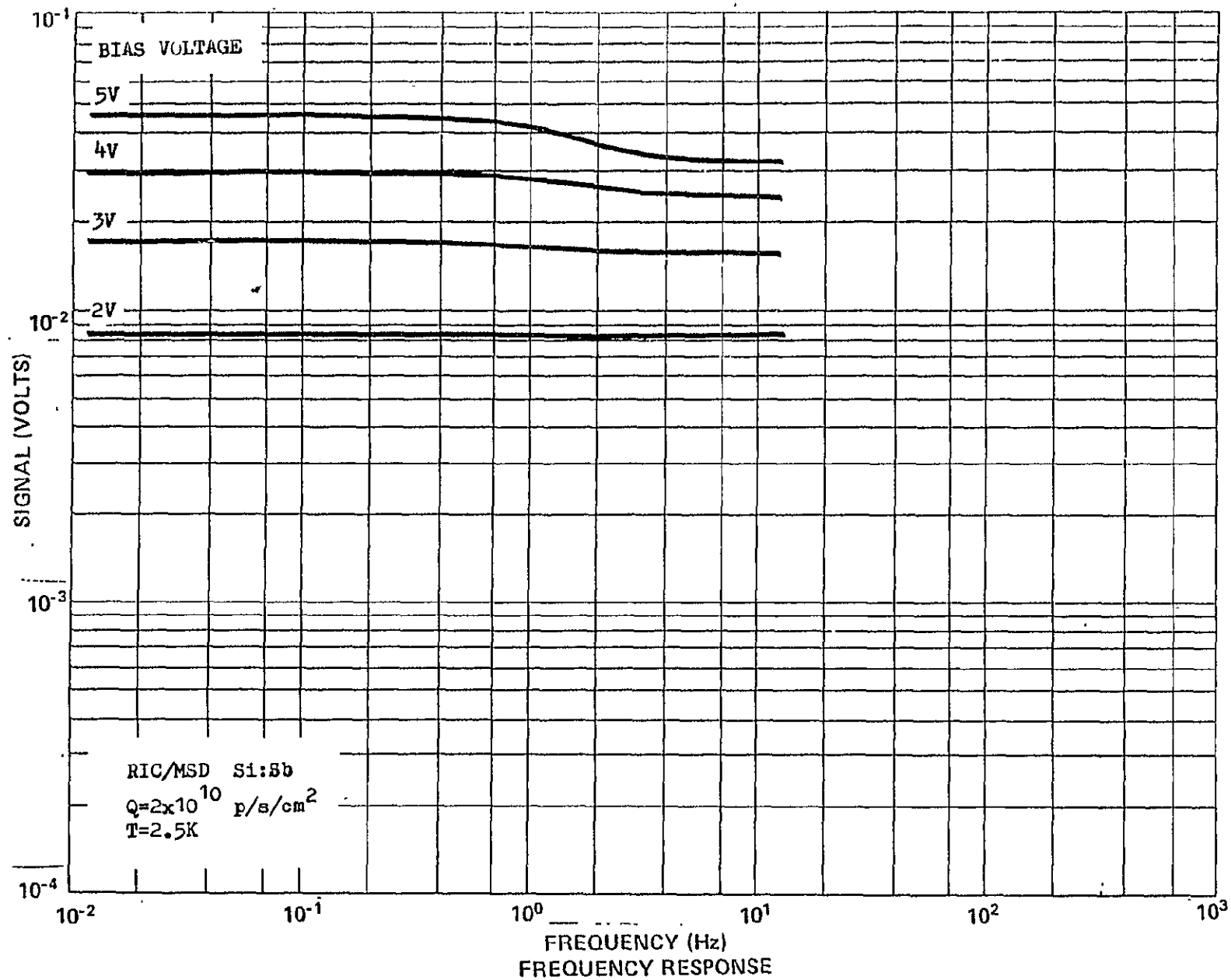


Figure 14



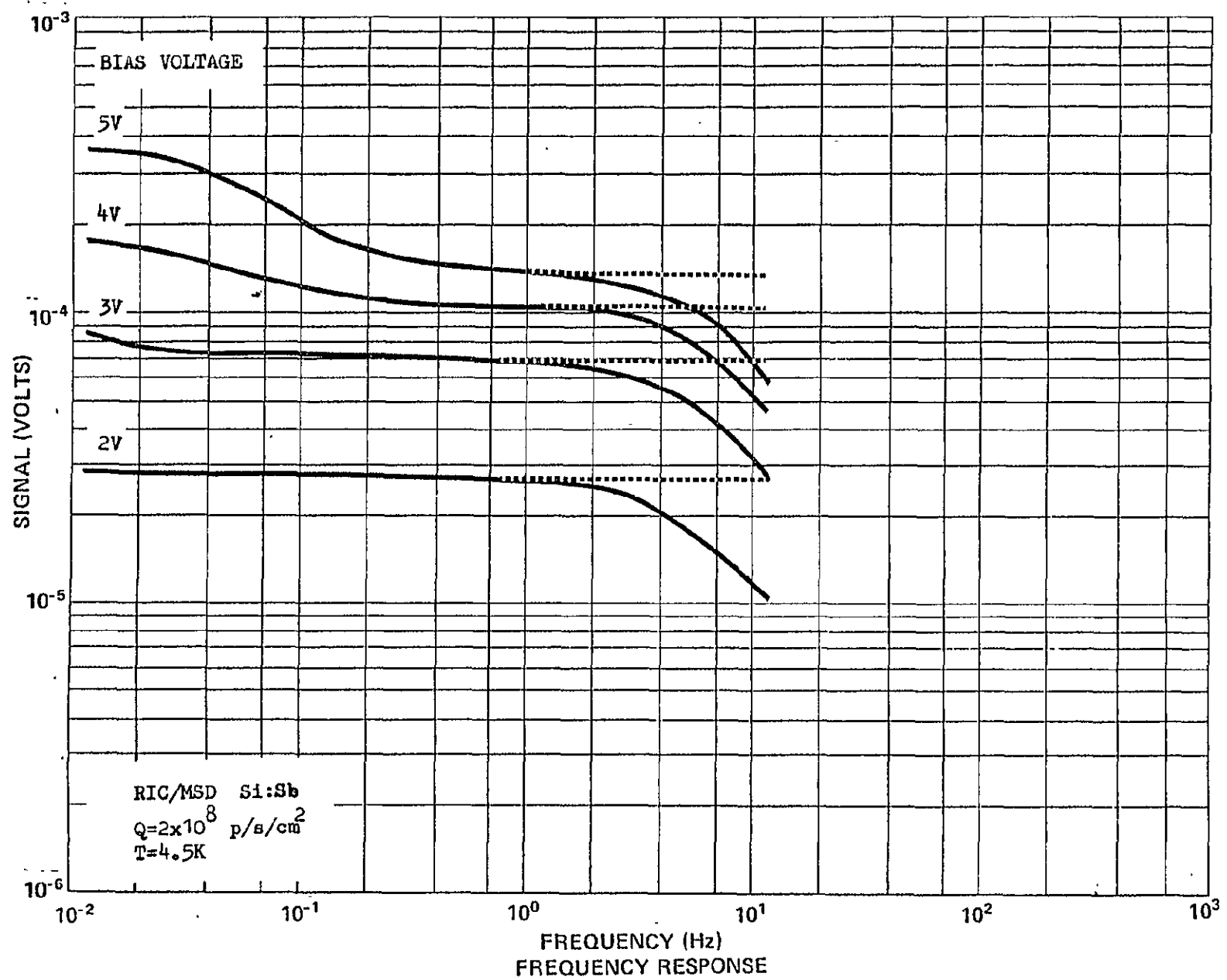


Figure 15

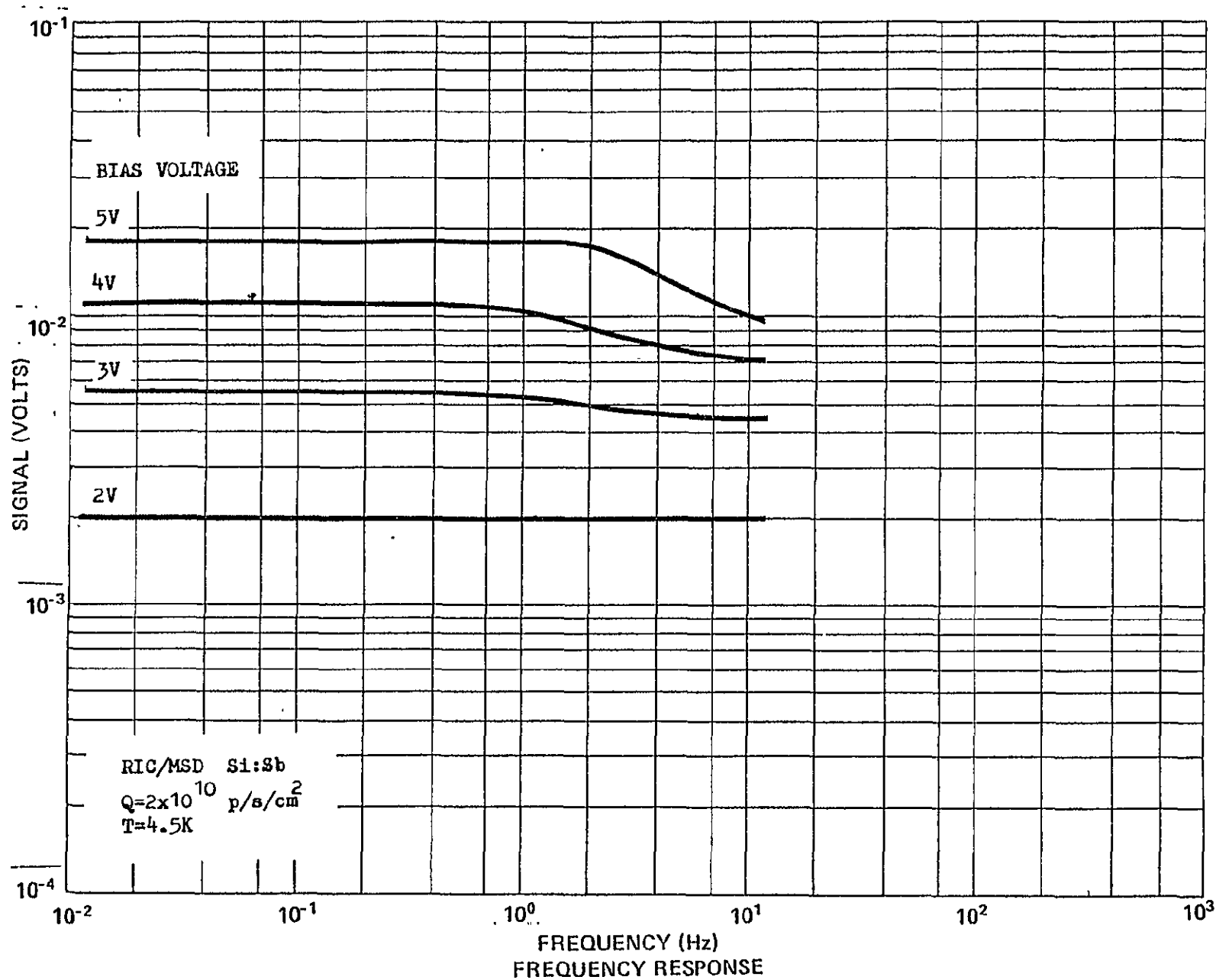


Figure 16

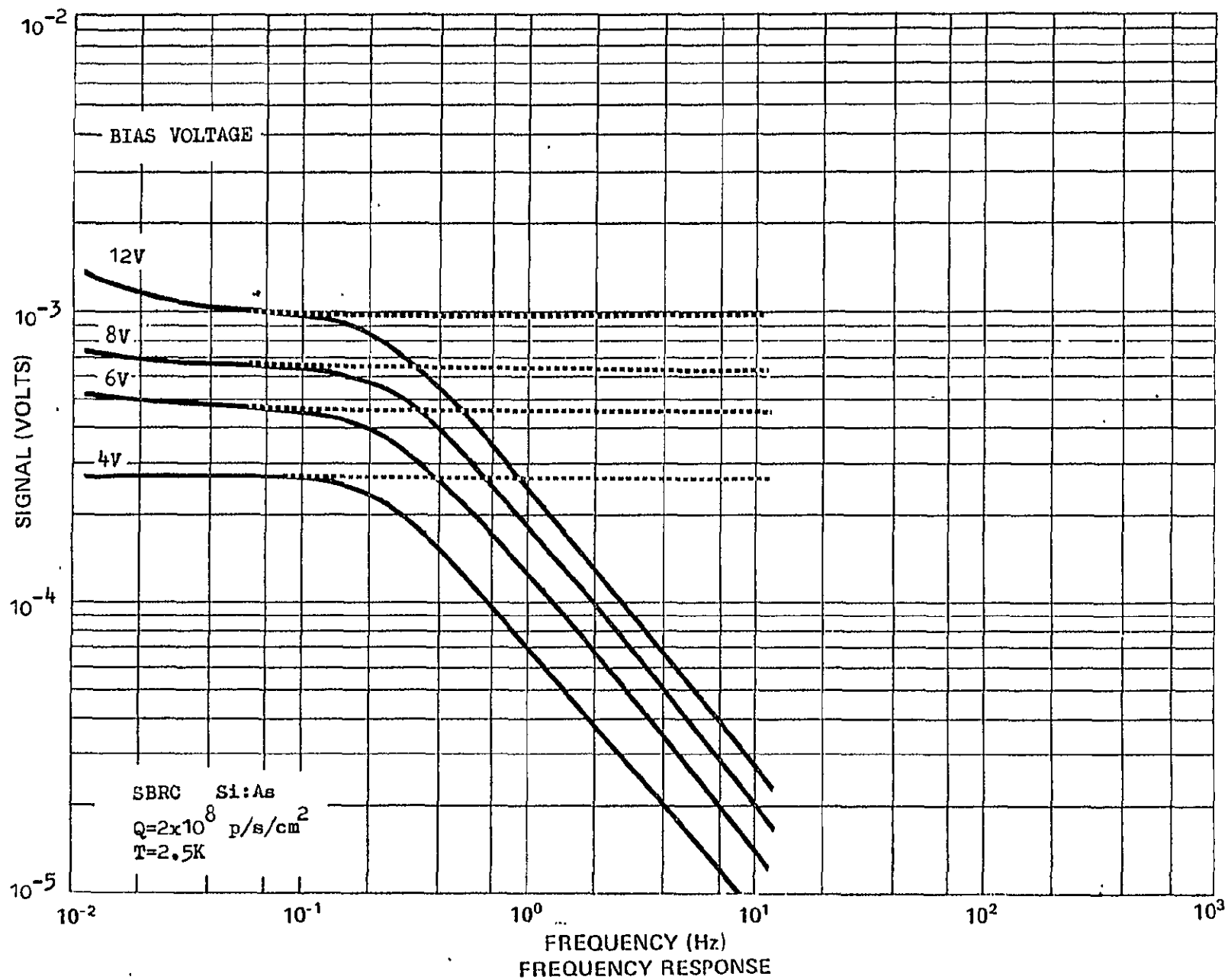


Figure 17

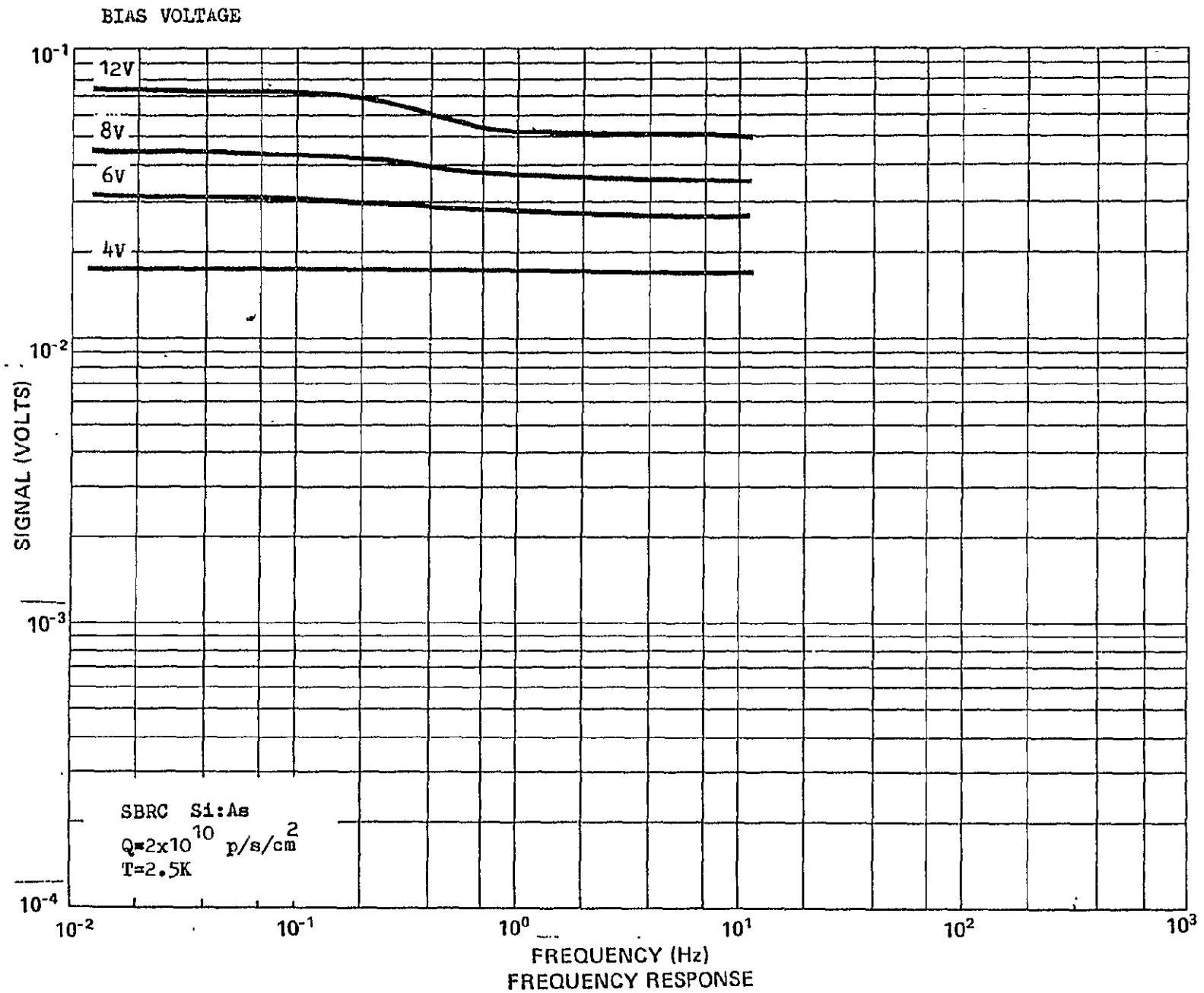


Figure 18

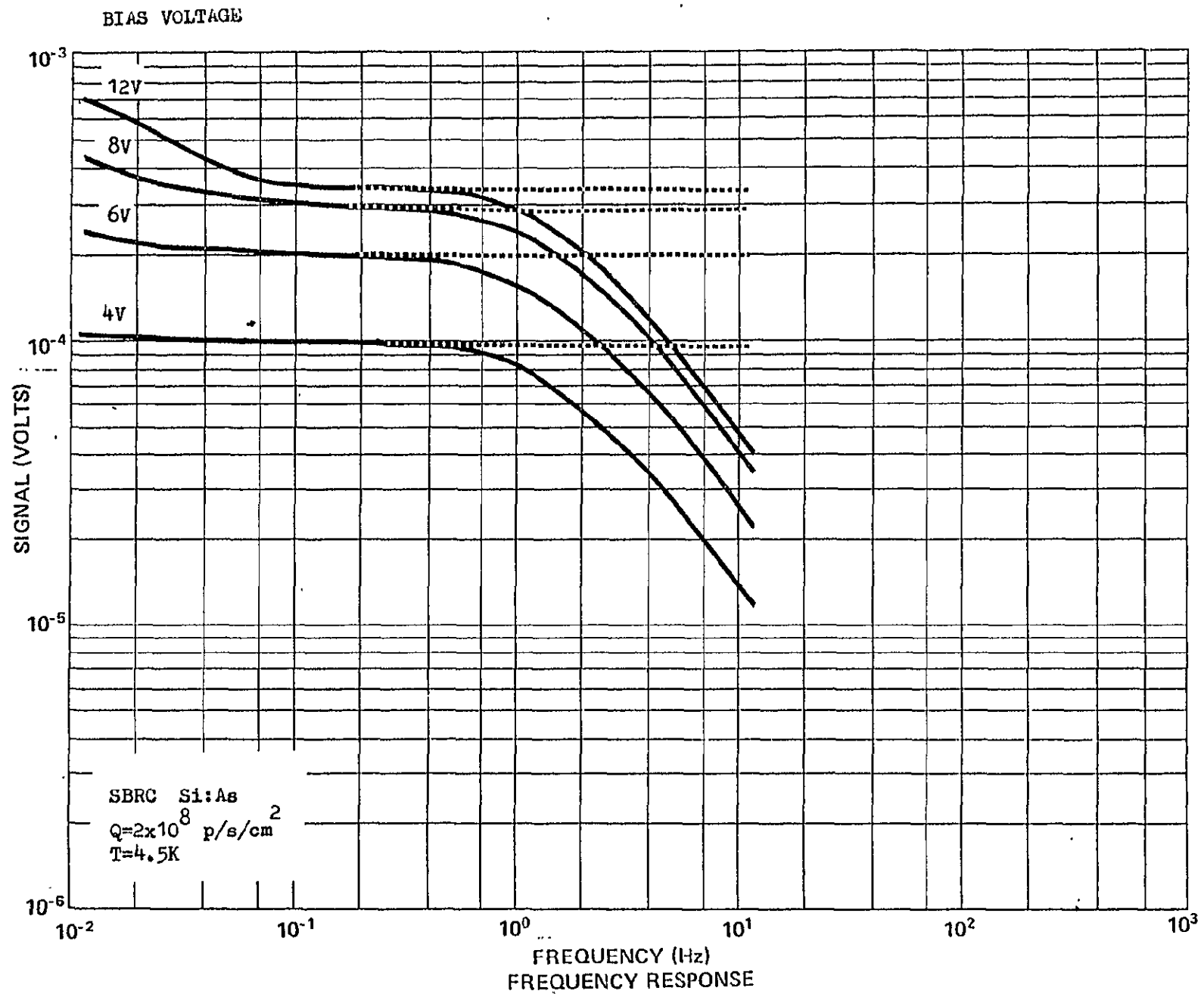


Figure 19

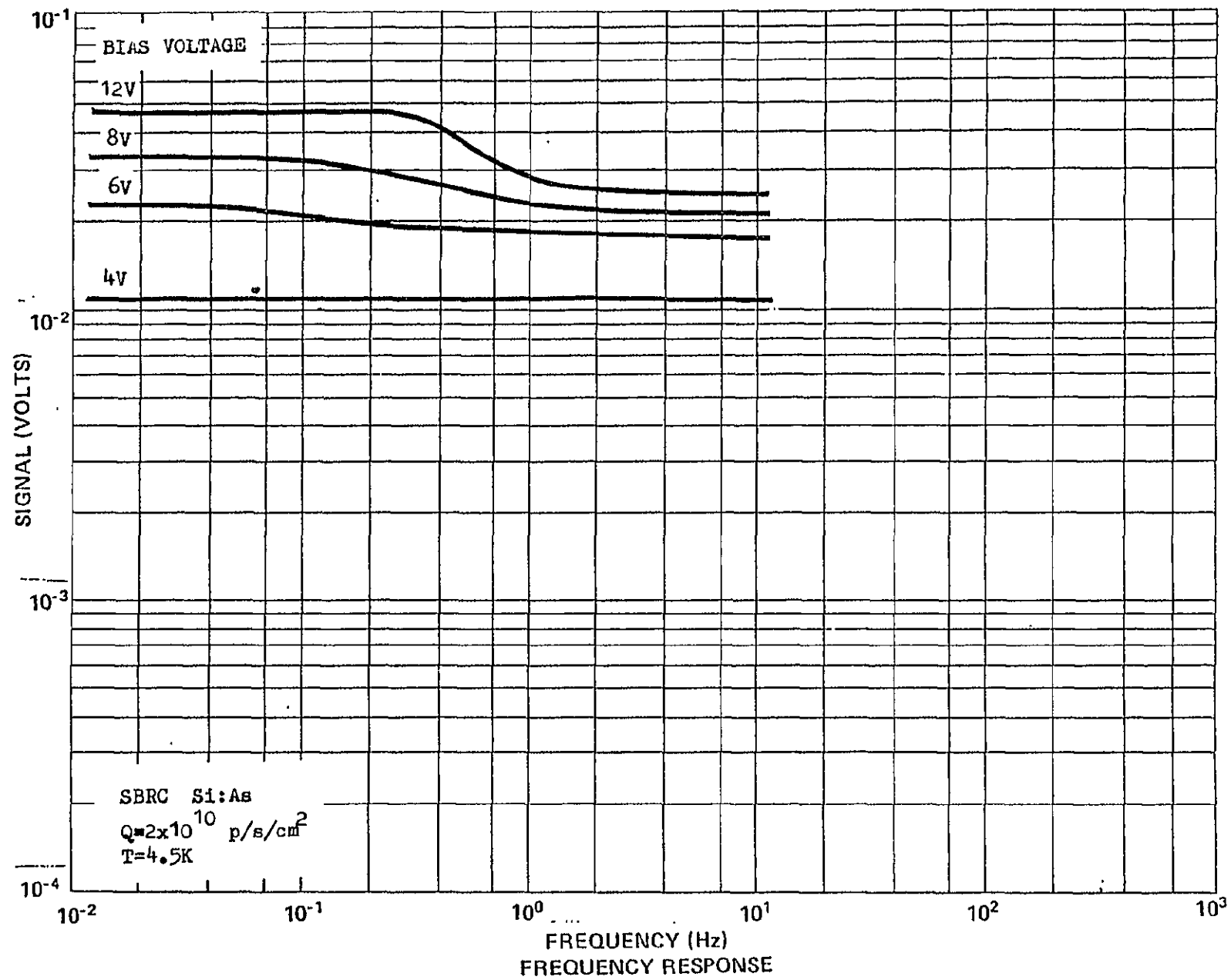


Figure 20

## 5.0 CHARACTERIZATION OF SPONTANEOUS NOISE SPIKES AND GAMMA INDUCED SPIKES

Some extrinsic photoconductors operating in a reduced IR background environment exhibit "spontaneous noise spiking." These noise spikes are usually characterized by a rapid rise time and a decay time set by the system bandwidth. It has been shown that ionizing radiation absorbed in these detectors exhibits similar effects. This Section deals with the characterization of these two types of spikes and with two means of circumventing the noise spike problem. Data were obtained on three different detectors and the data in this Section are grouped by detector.

#### 5.1.0. RIC/MSD Si:P

This detector was chosen for the characterization of spontaneous noise spikes because of its rather high event rate. Gamma-induced spikes were also measured by placing a small Cobalt 60-gamma source close to the detector.



### 5.1.1. Dependence of Spontaneous Noise Spike Event Rate

A TIA configuration was used to obtain the data in this Section. The output of the TIA was fed into a counter which was triggered by spikes whose amplitudes were greater than the detector noise level. Counts were accumulated for a period of 5 minutes for each data point.

Figure 21 shows the spontaneous noise spike event rate as a function of bias voltage for two temperatures and several backgrounds. The same data are replotted in Figs. 22 and 23 as functions of background at the two temperatures. The event rate is seen to be a strong function of both background and bias, but the functional dependence is different at the two temperatures.

46 6012

SPONTANEOUS Events/Minute

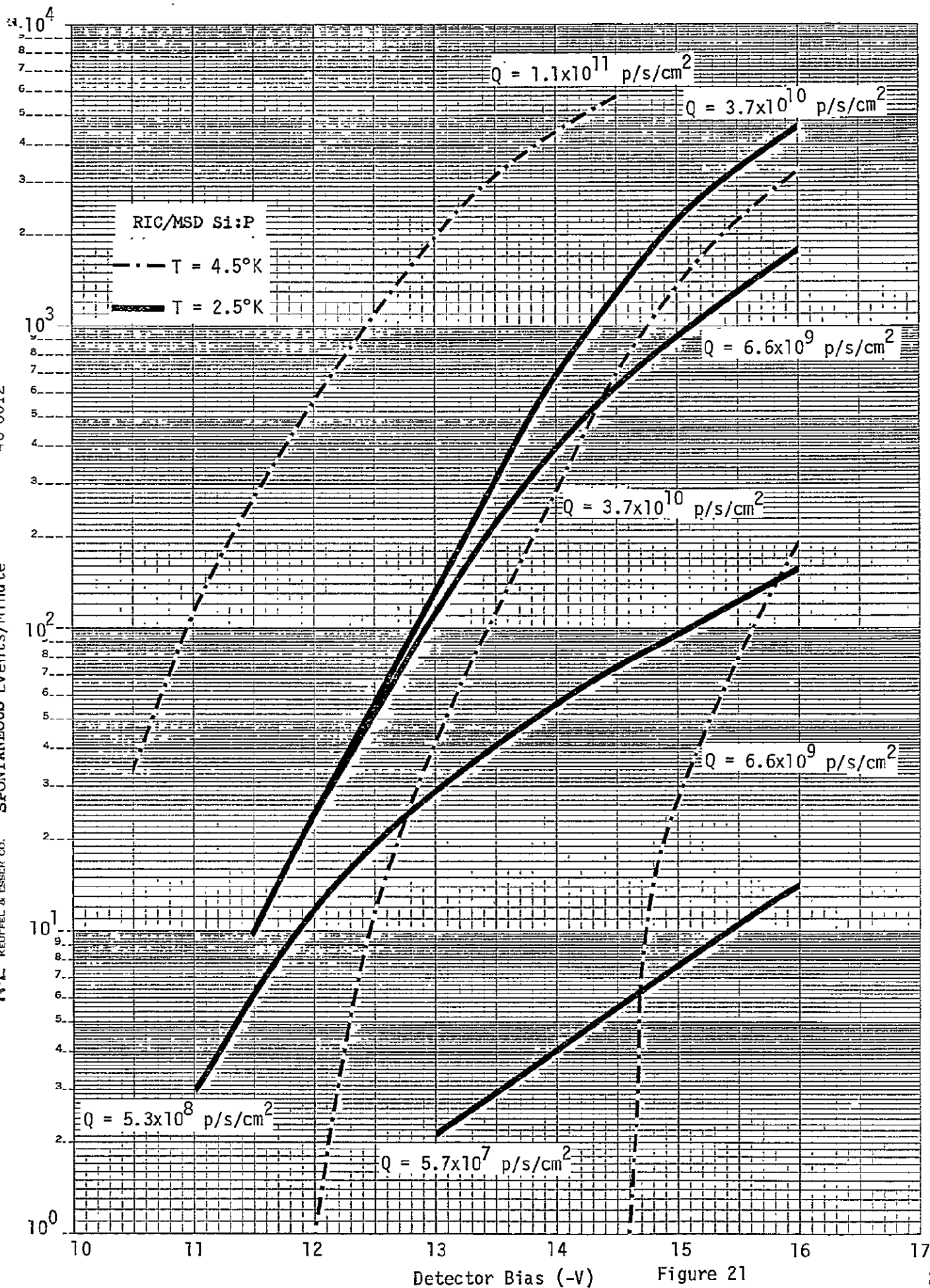
K.E. SEMI-LOGARITHMIC /  
KEUFEL & ESSER CO.

Figure 21

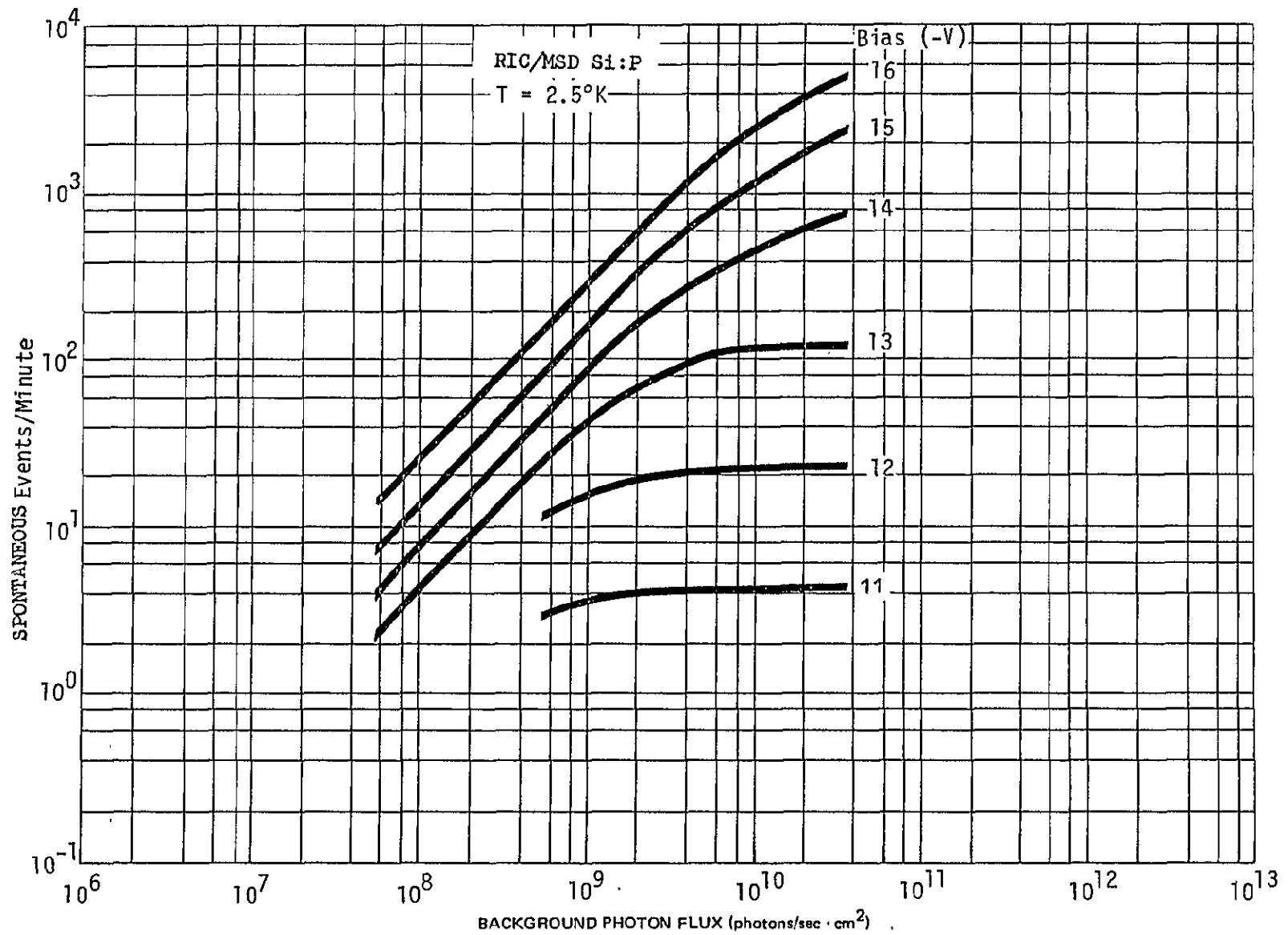


Figure 22

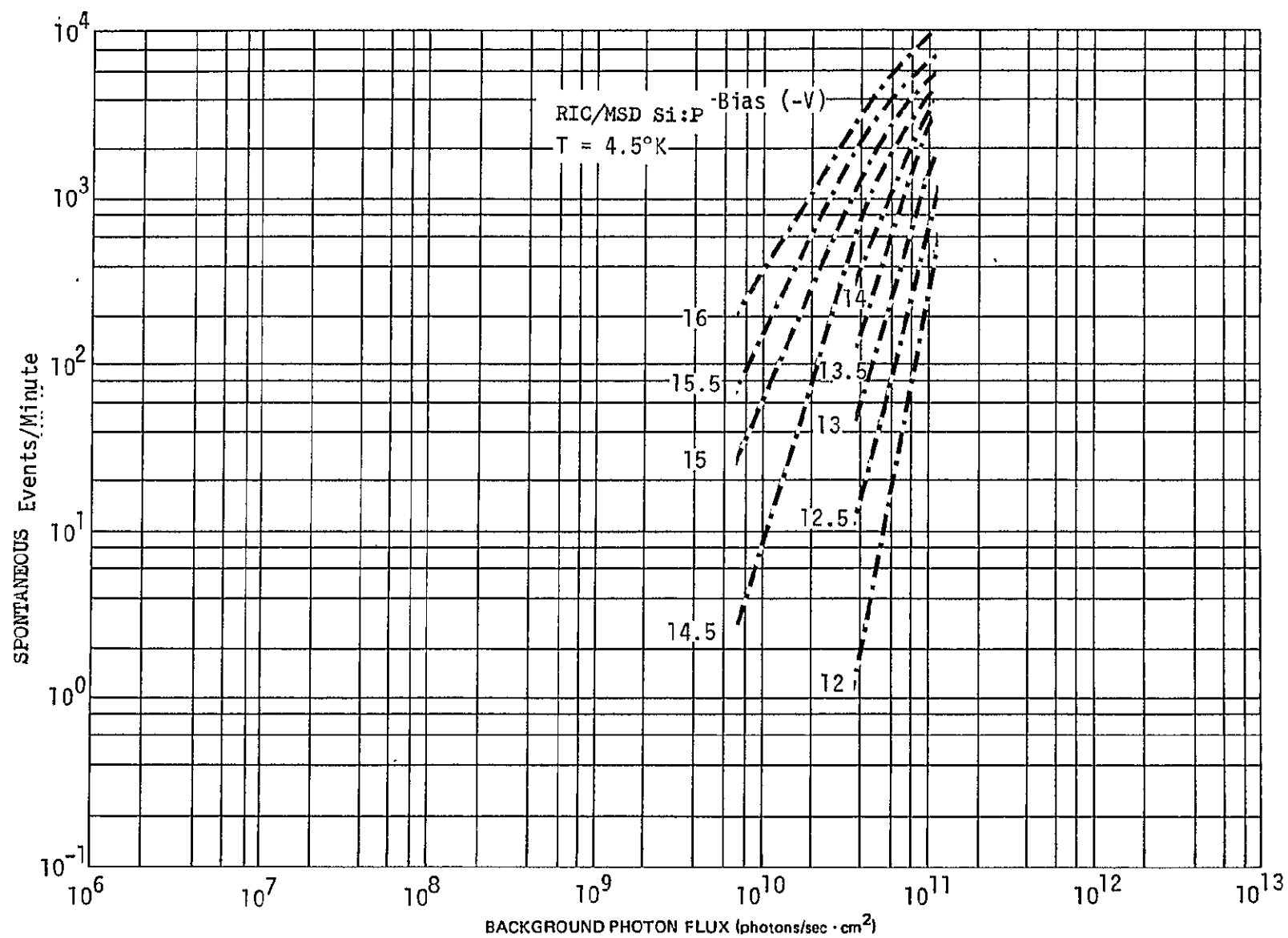


Figure 23

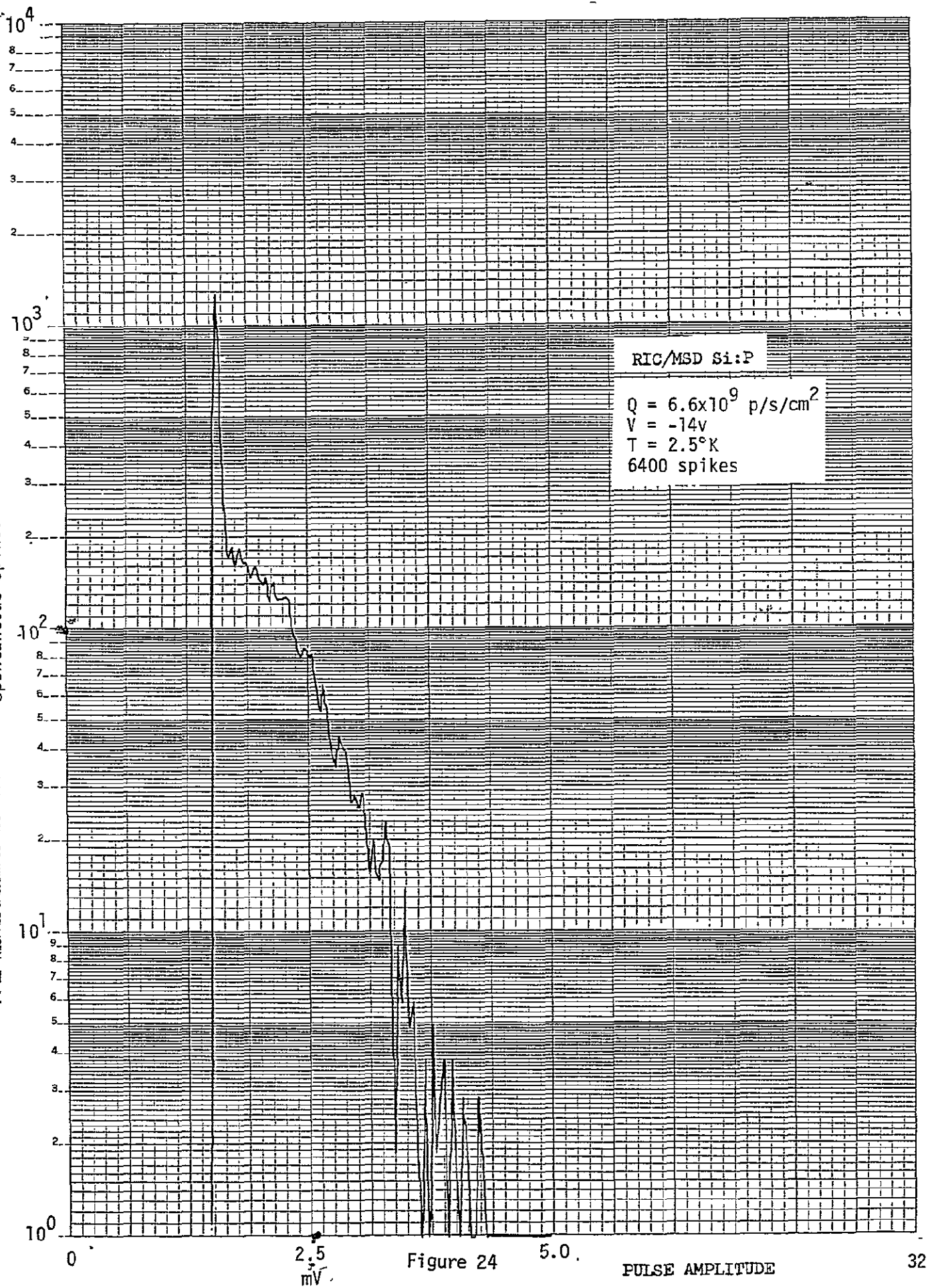
### 5.1.2. Spontaneous Noise Spike Pulse Amplitude Distribution

A TIA was used to obtain the data presented in this Section. The output of the TIA was also fed through the trigger circuit of a Hewlett-Packard 5451B Courier Analyzer. The trigger level was set to minimize triggering on "normal" noise. The 5451B performed the amplitude distribution. Figures 24-27 show the resulting spontaneous pulse amplitude distributions at a temperature of 2.5K, at two biases and two backgrounds. These distributions seem to be fairly gaussian with a shift to higher amplitudes with increasing bias.

Figures 28-33 show the pulse amplitude distributions at an operating temperature of 4.5K, two backgrounds, and several biases. Note that the distributions are quite different than those obtained at 2.5K. At the lower backgrounds and at the higher backgrounds with low biases, the amplitudes fall into two groups - one group just above the threshold level and the other group at a higher value. However, at the highest biases and backgrounds, the distributions tend to become continuous. The pulse amplitudes again increase with increasing bias voltage.

46 6012

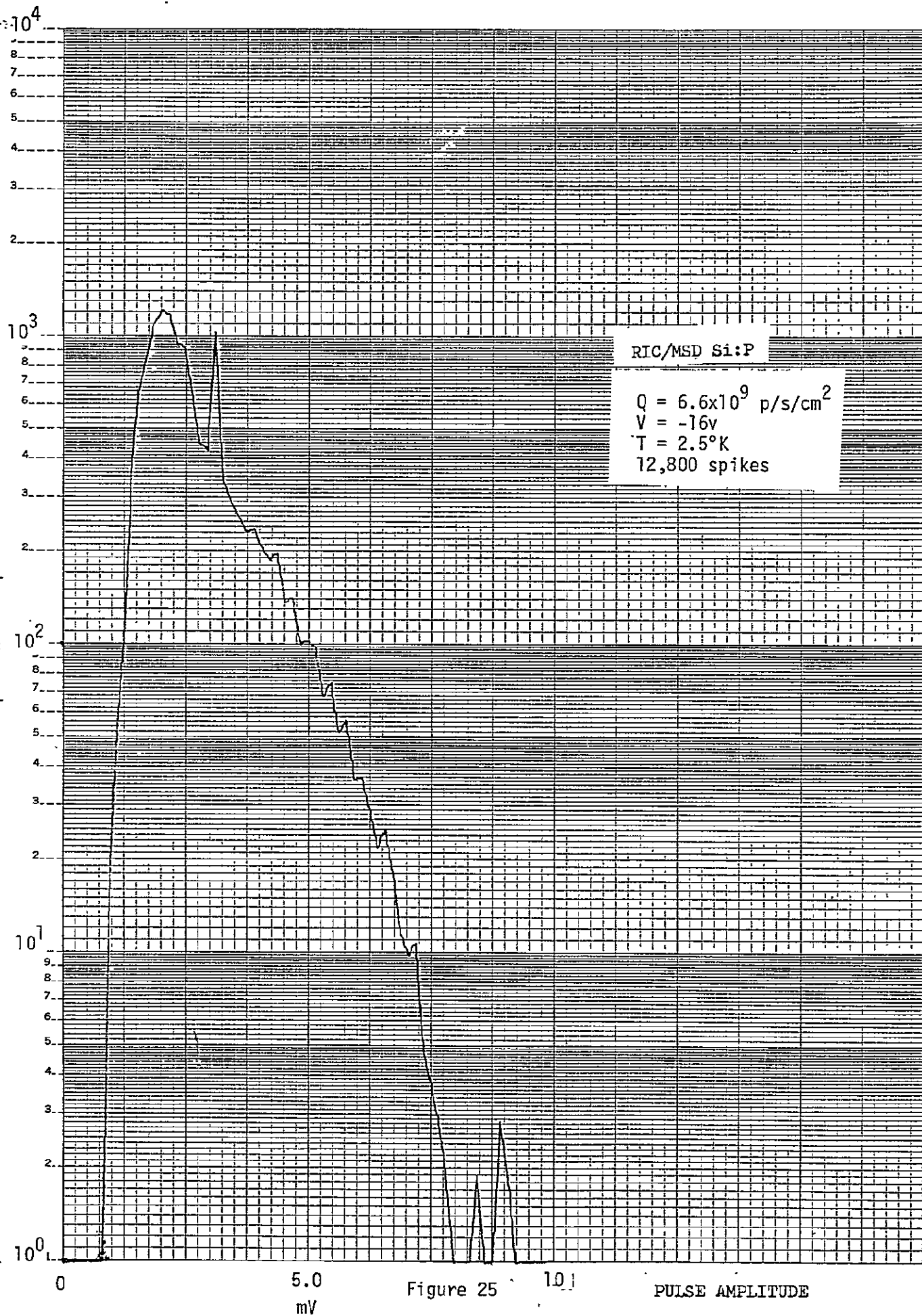
Spontaneous Spikes

K&E SEMI-LOGARITHMIC 4 CYCLES X 70 DIVI  
KEUFFEL & ESSER CO. MADE IN U.S.A.

46 6012

KE SEMILOGARITHMIC 4 CYCLES X 70 DIVIS  
KEUFTEL & ESSER CO. MADE IN U.S.A.

Spontaneous Spikes



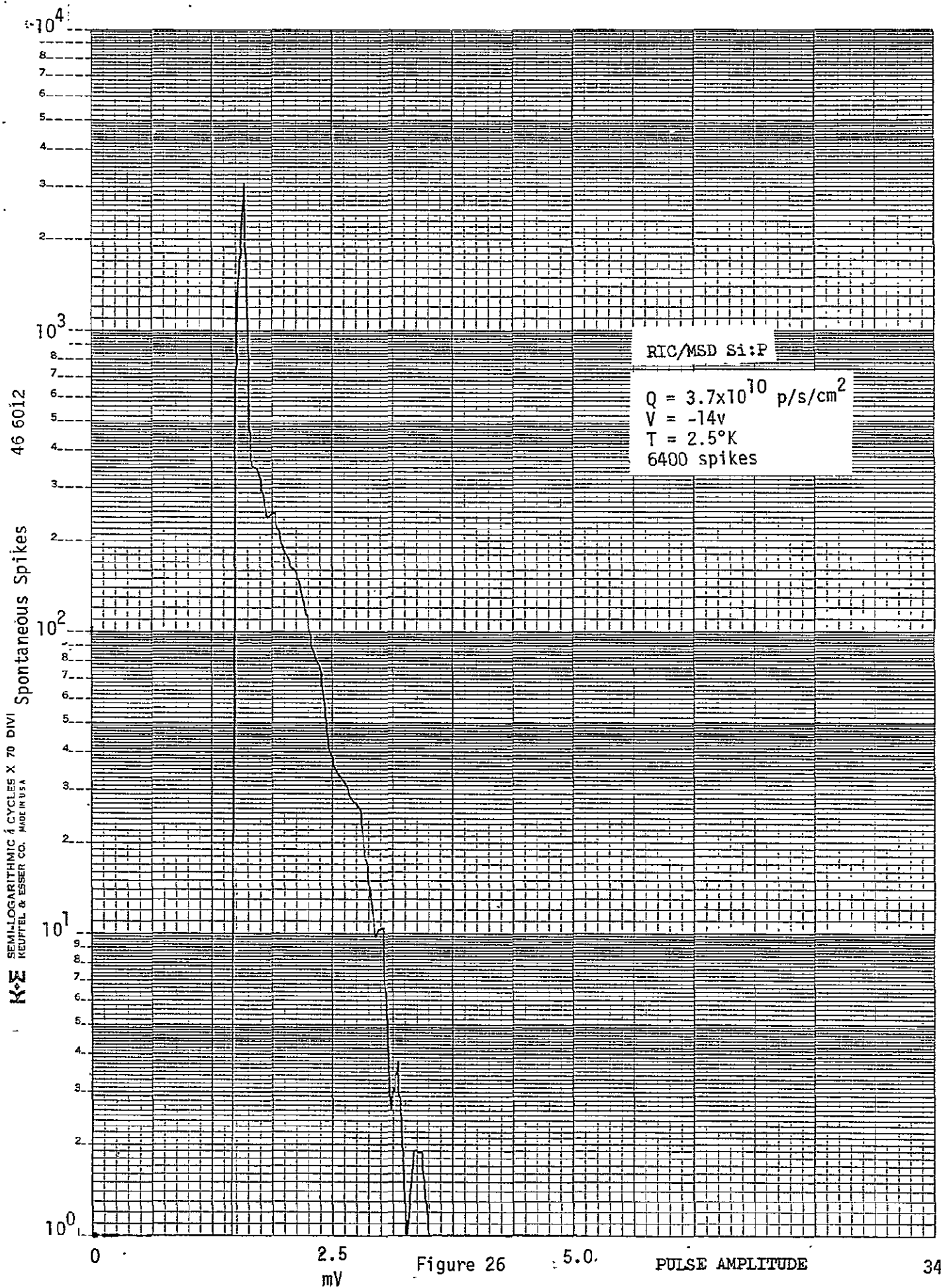
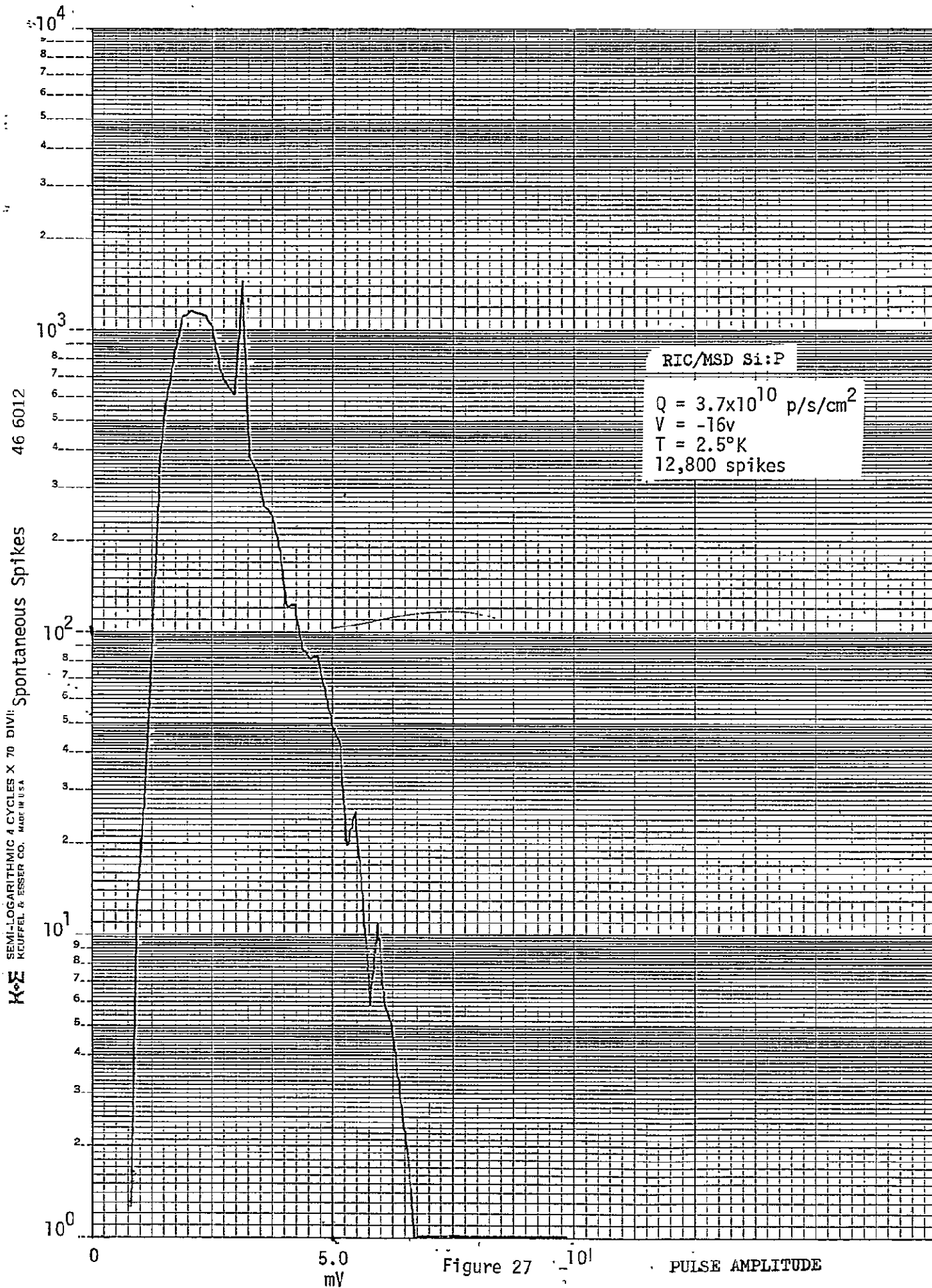


Figure 26





46 6012  
KOE SEMI-LOGARITHMIC 4 CYCLES X 70 DIVIS  
KEUFFEL & ESSER CO. MADE IN U.S.A.

Spontaneous Spikes

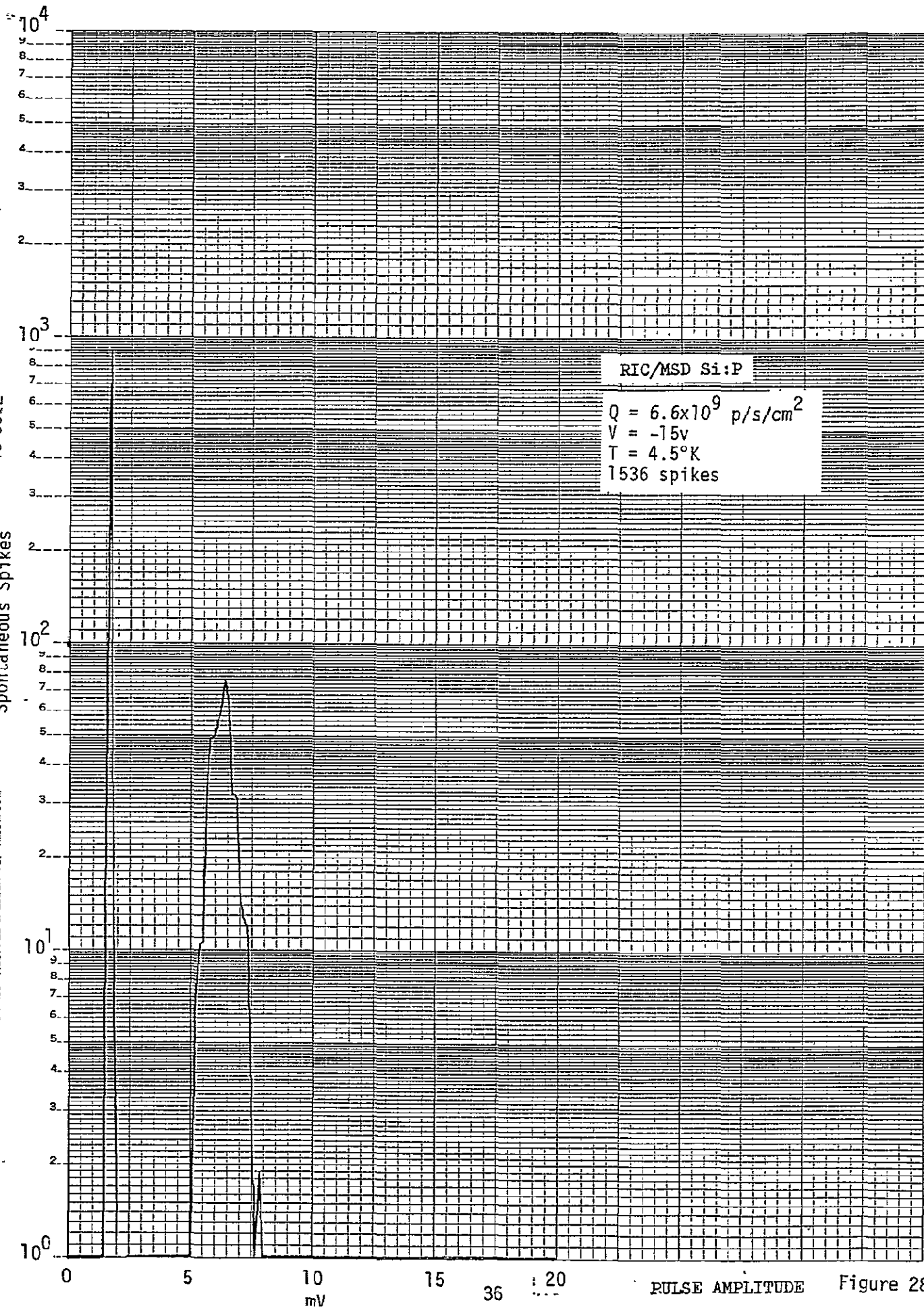


Figure 28

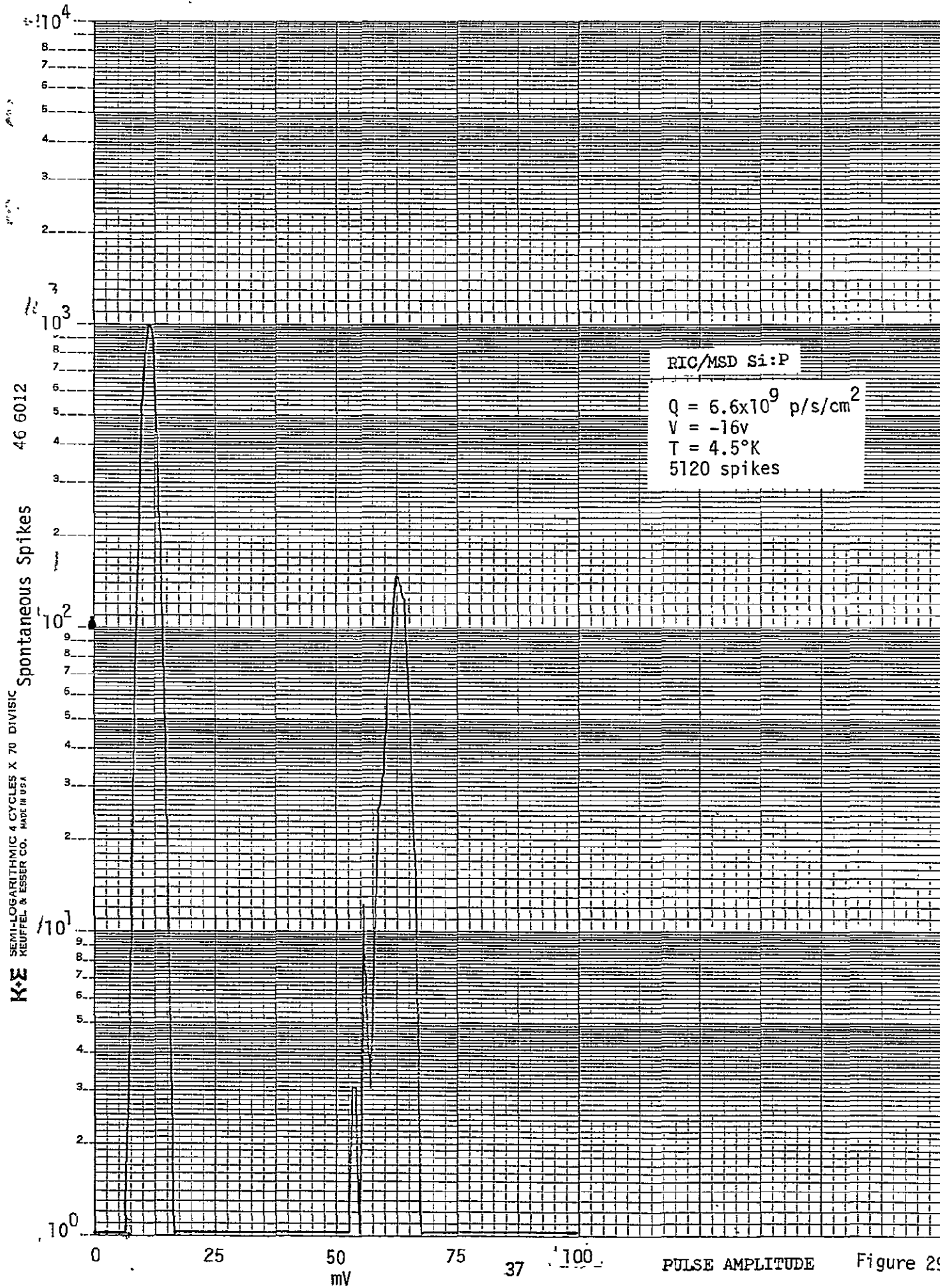
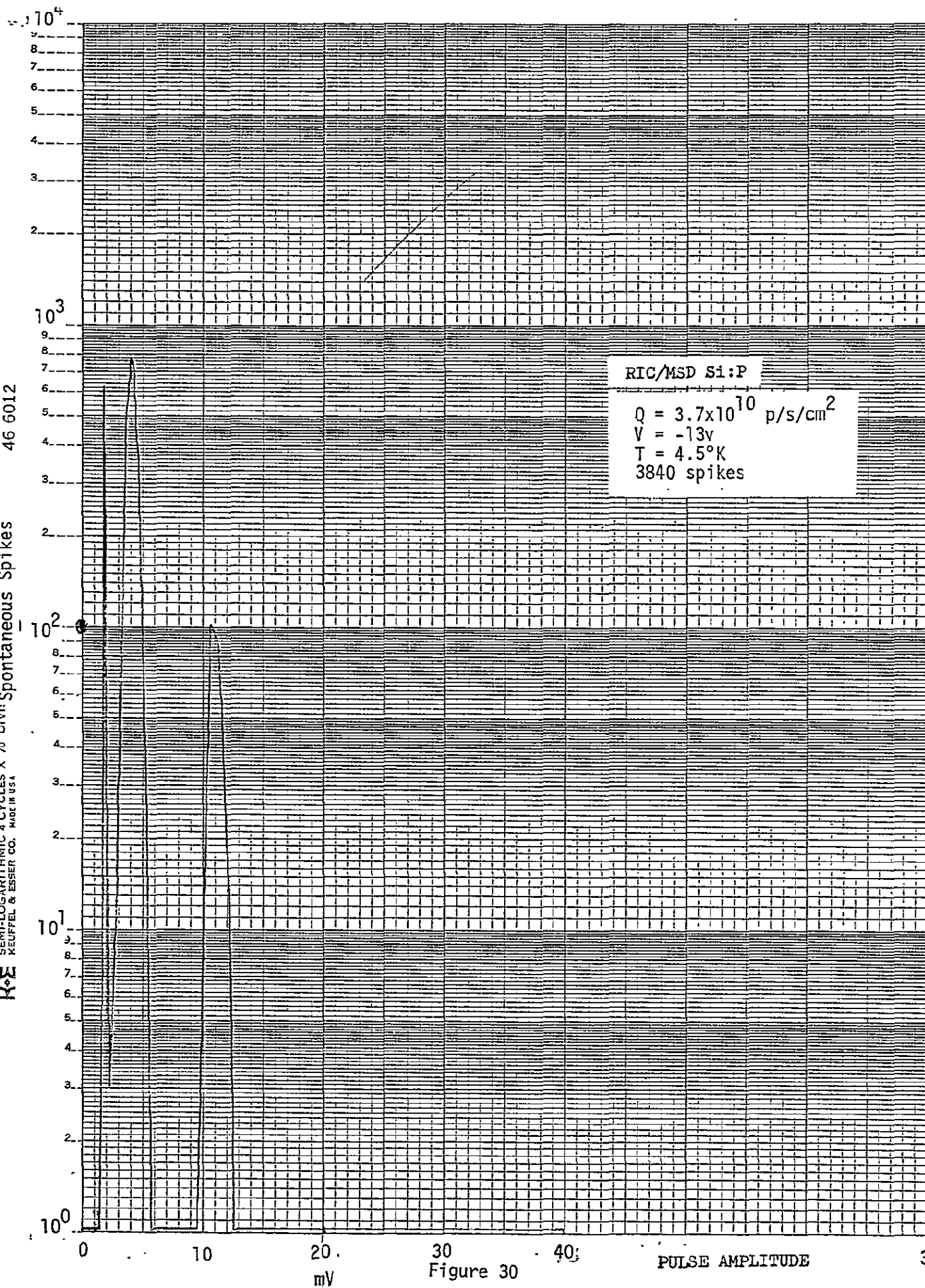


Figure 29

46 6012

SEMI-LOGARITHMIC 4 CYCLES X 70 DIVISION Spontaneous Spikes  
KEUFFEL & ESSER CO. MADE IN USA



K·E SEMI-LOGARITHMIC 4 CYCLES X 70 DIVISIONS SPONTANEOUS SPIKES  
KEUFFEL & ESSER CO. MADE IN U.S.A.

46 6012

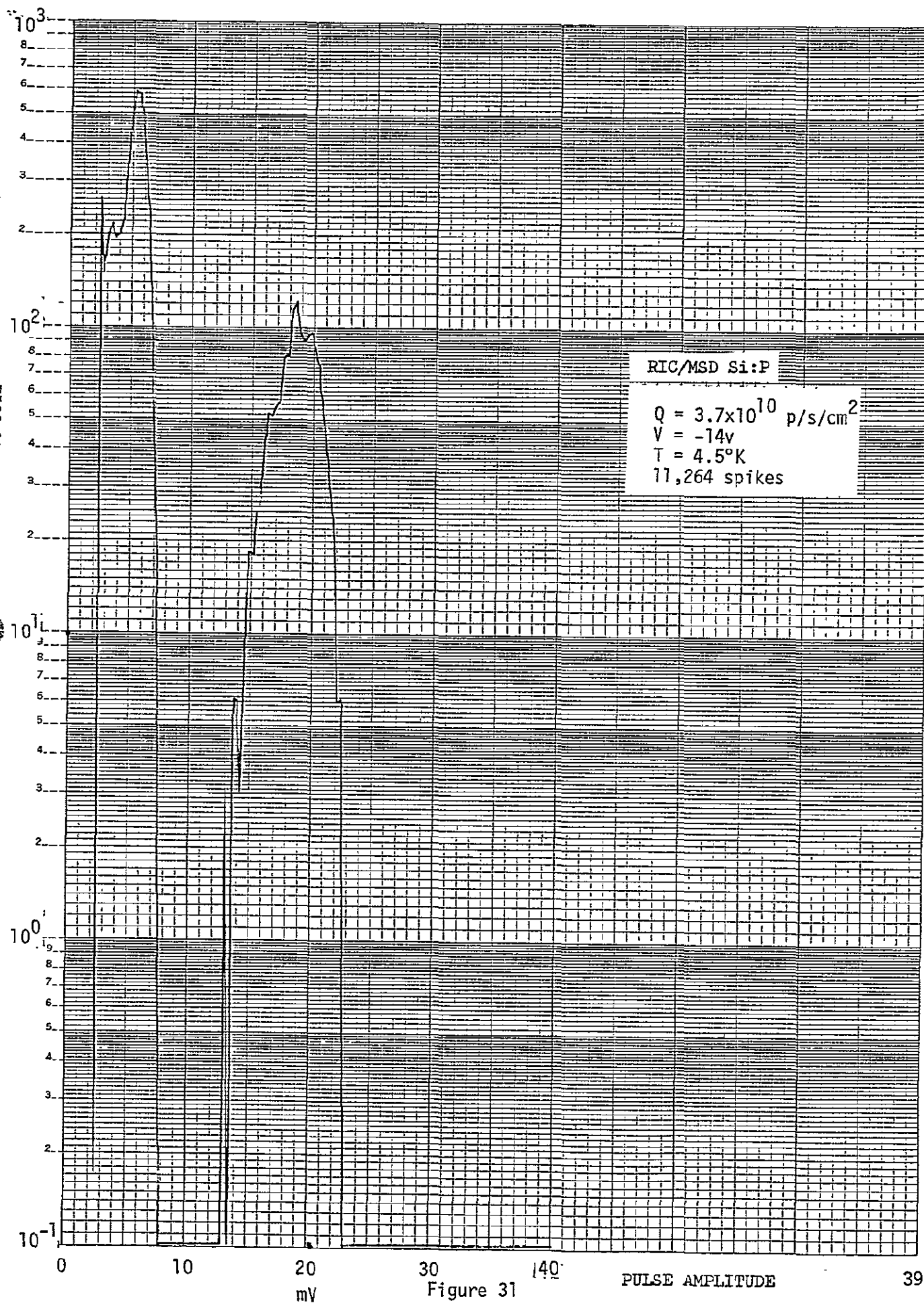
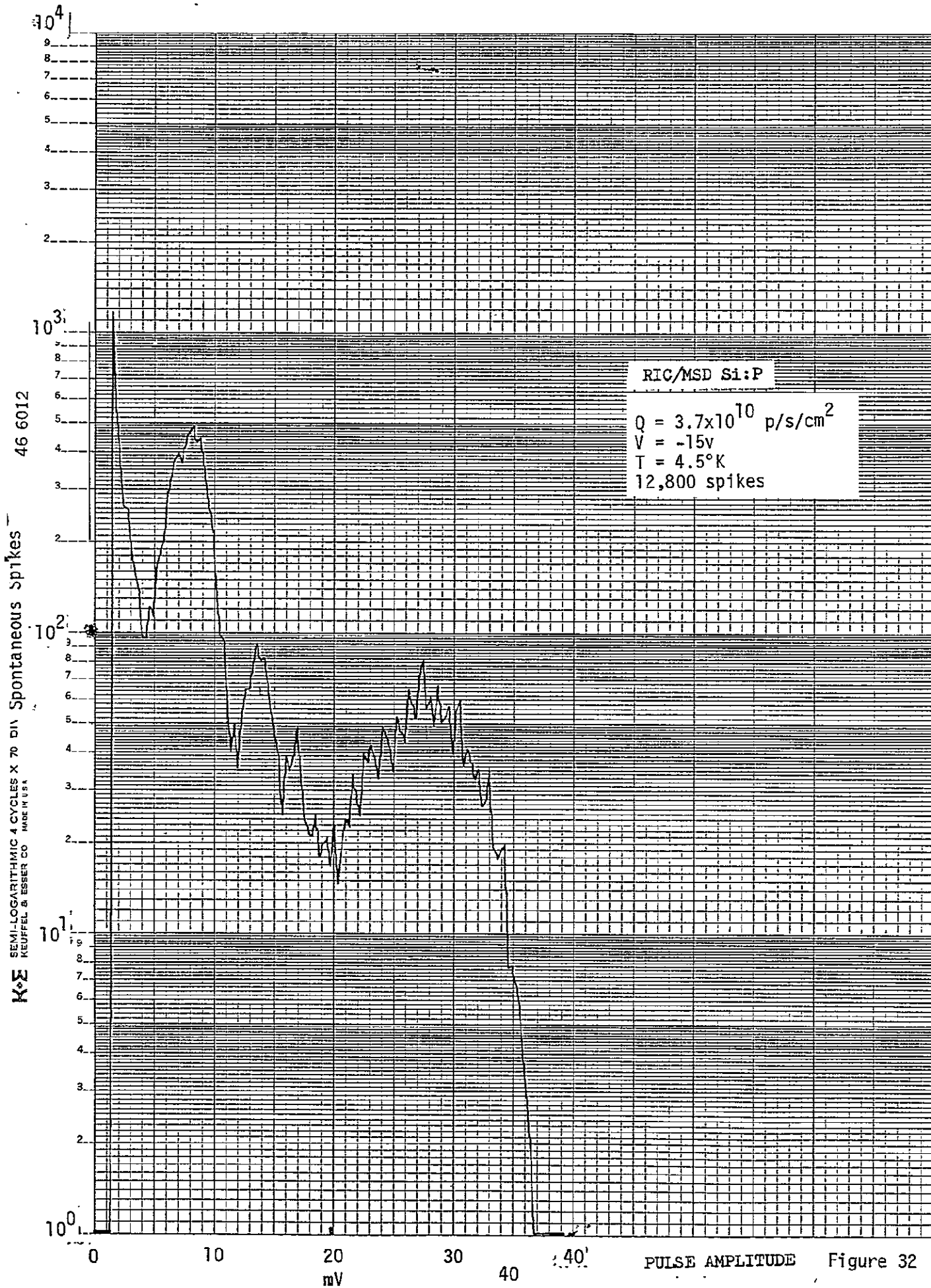
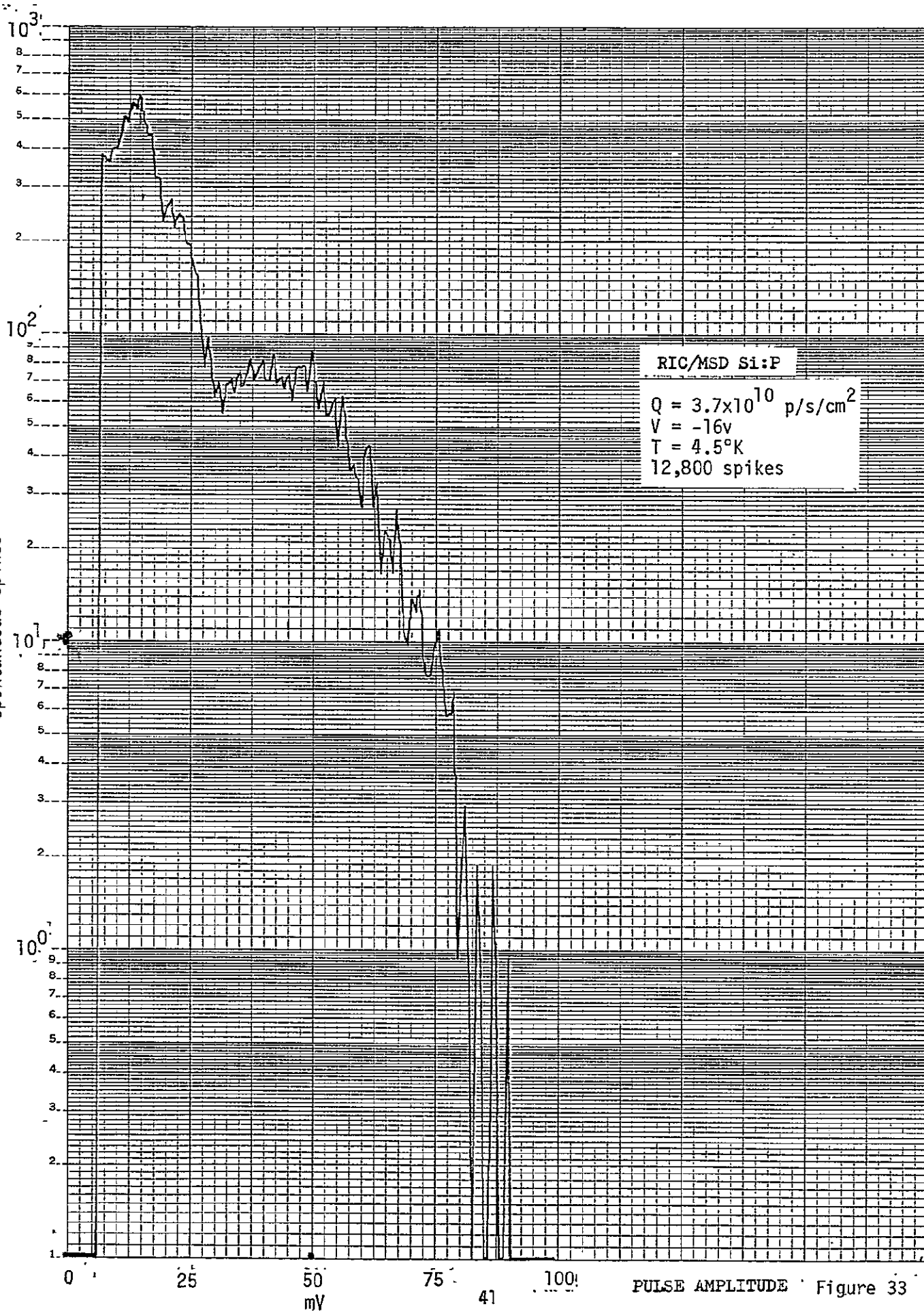


Figure 31



46 6012

Spontaneous Spikes

K·Σ SEMI-LOGARITHMIC 4 CYCLES X 70 DIV  
KEUTTEL & ESSER CO. MADE IN U.S.A.

### 5.1.3. Gamma Event Pulse Height Distribution

This Section presents several graphs (Figs. 34-40) showing the amplitude distribution of pulses produced by Cobalt 60-gammas. Data was obtained under a zilch optical background to minimize the number of spontaneous noise spike events. Measurements were made at temperatures of 2.5K and 4.5K and at several bias values using a TIA. The resulting distributions appear to be quite gaussian and resemble the distributions of spontaneous spikes at 2.5K except that the pulse amplitudes are larger.



46 6012

Gamma Pulses

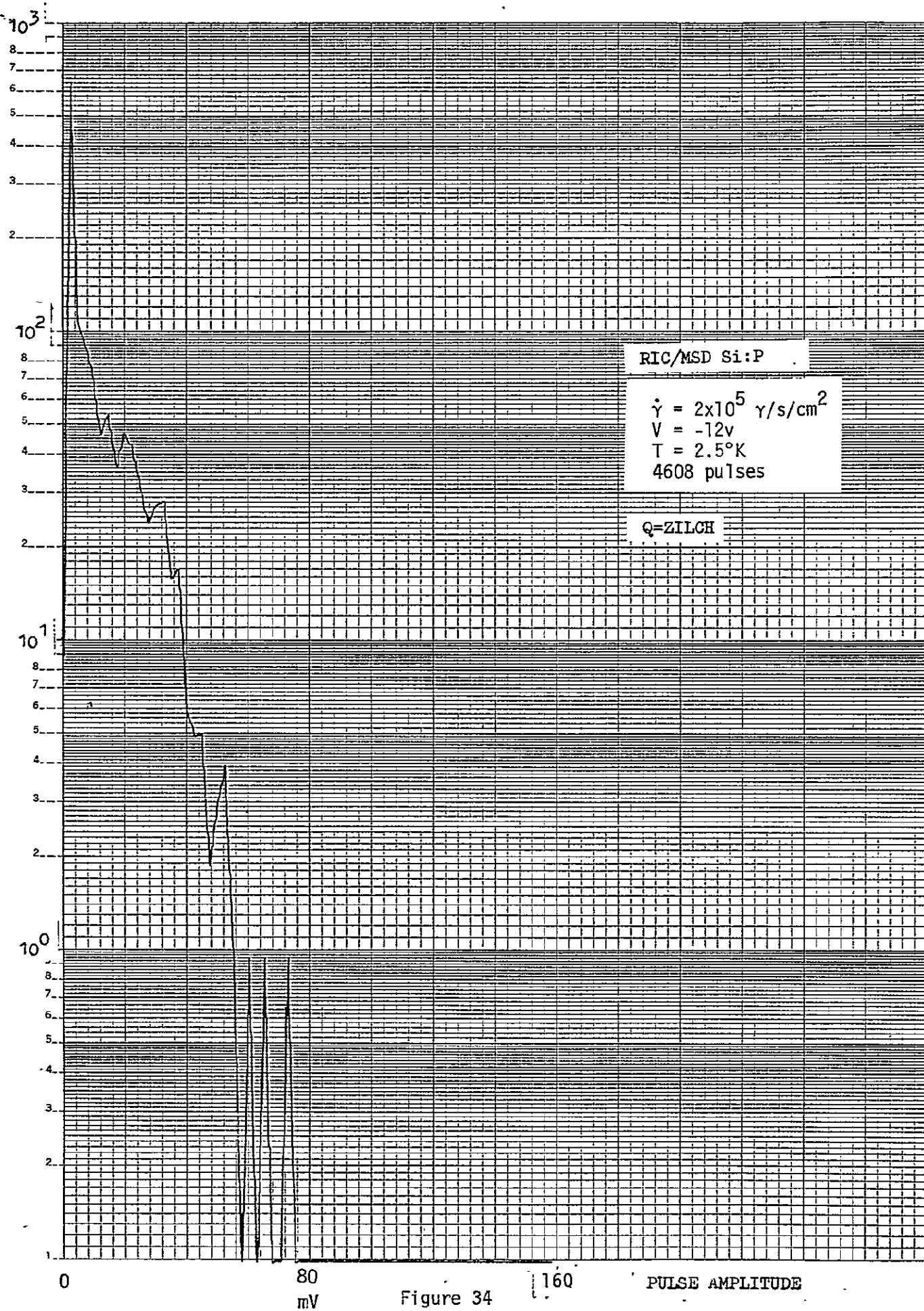
K-E SEMI-LOGARITHMIC CYCLES X 70 DIVISION  
KEUFFEL & ESSER CO. MADE IN U.S.A.

Figure 34

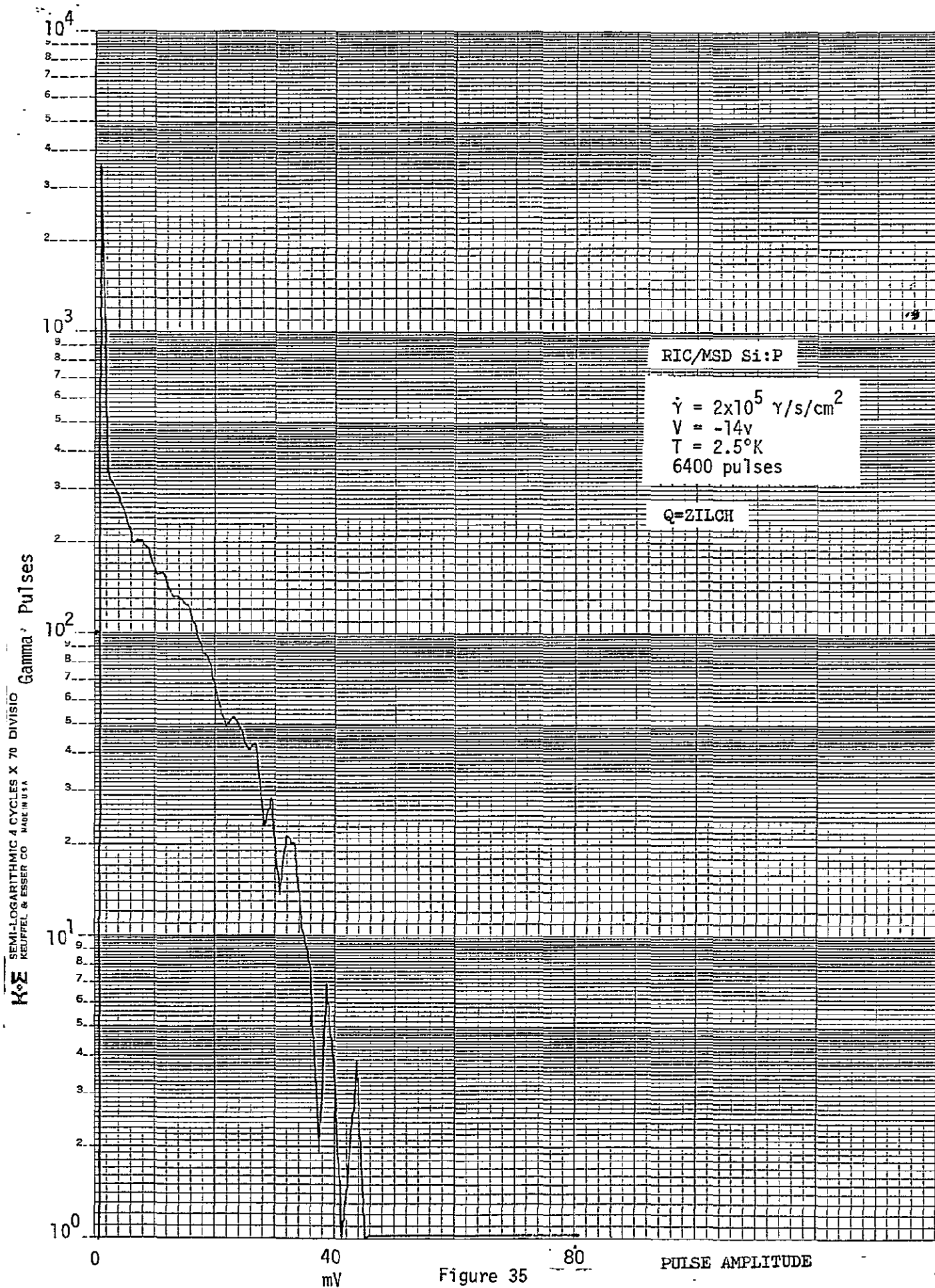


Figure 35

46 6012

Gamma Pulses

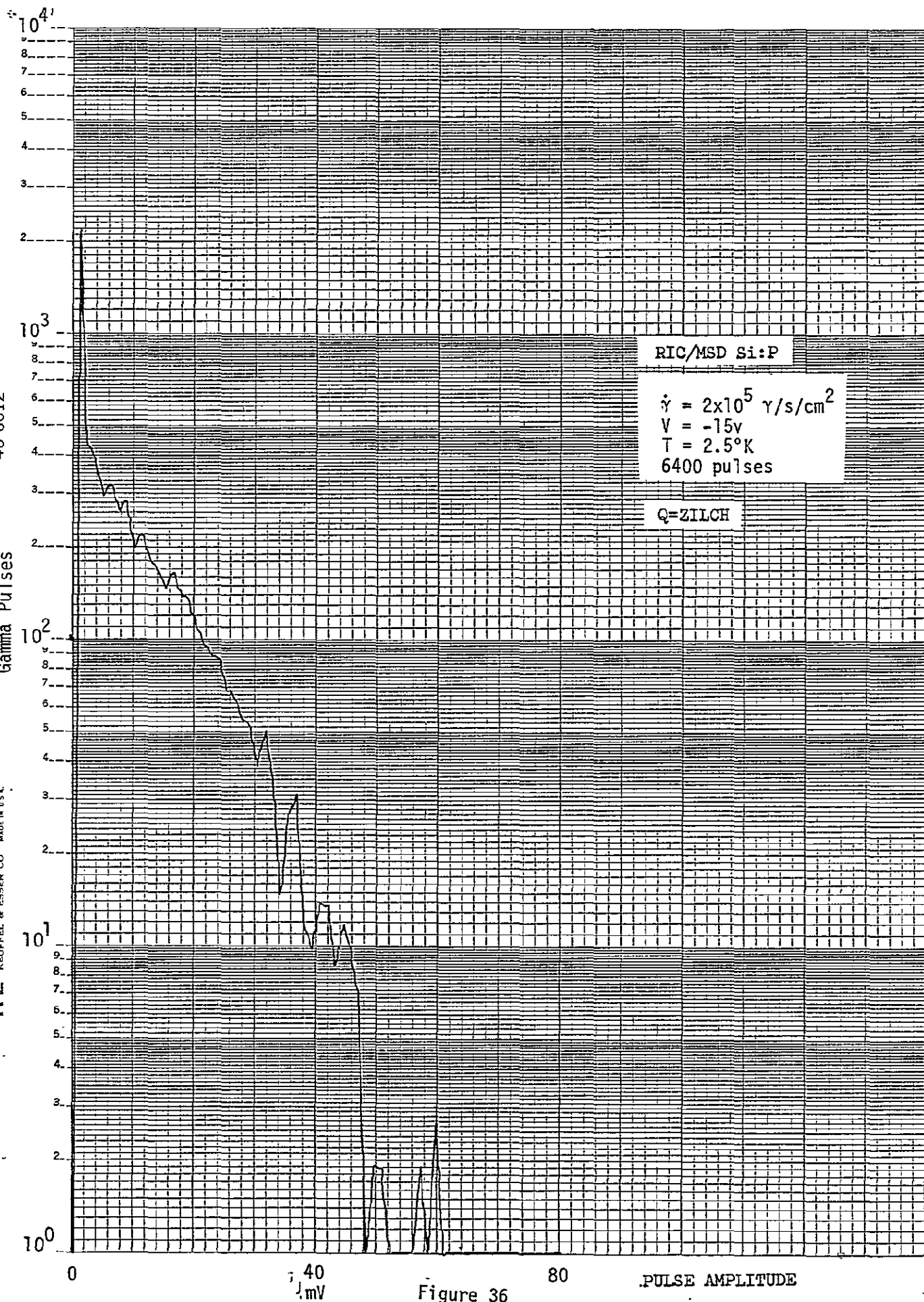
K.E. SEMI-LOGARITHMIC 4 CYCLES X 70 DIVISIONS  
KEUFFEL & ESSER CO. MADE IN U.S.A.

Figure 36

PULSE AMPLITUDE

46 6012

K&E SEMI-LOGARITHMIC 4 CYCLES X 70 DIVISION  
KEUFFEL & ESSER CO. MADE IN U.S.A.

Gamma Pulses

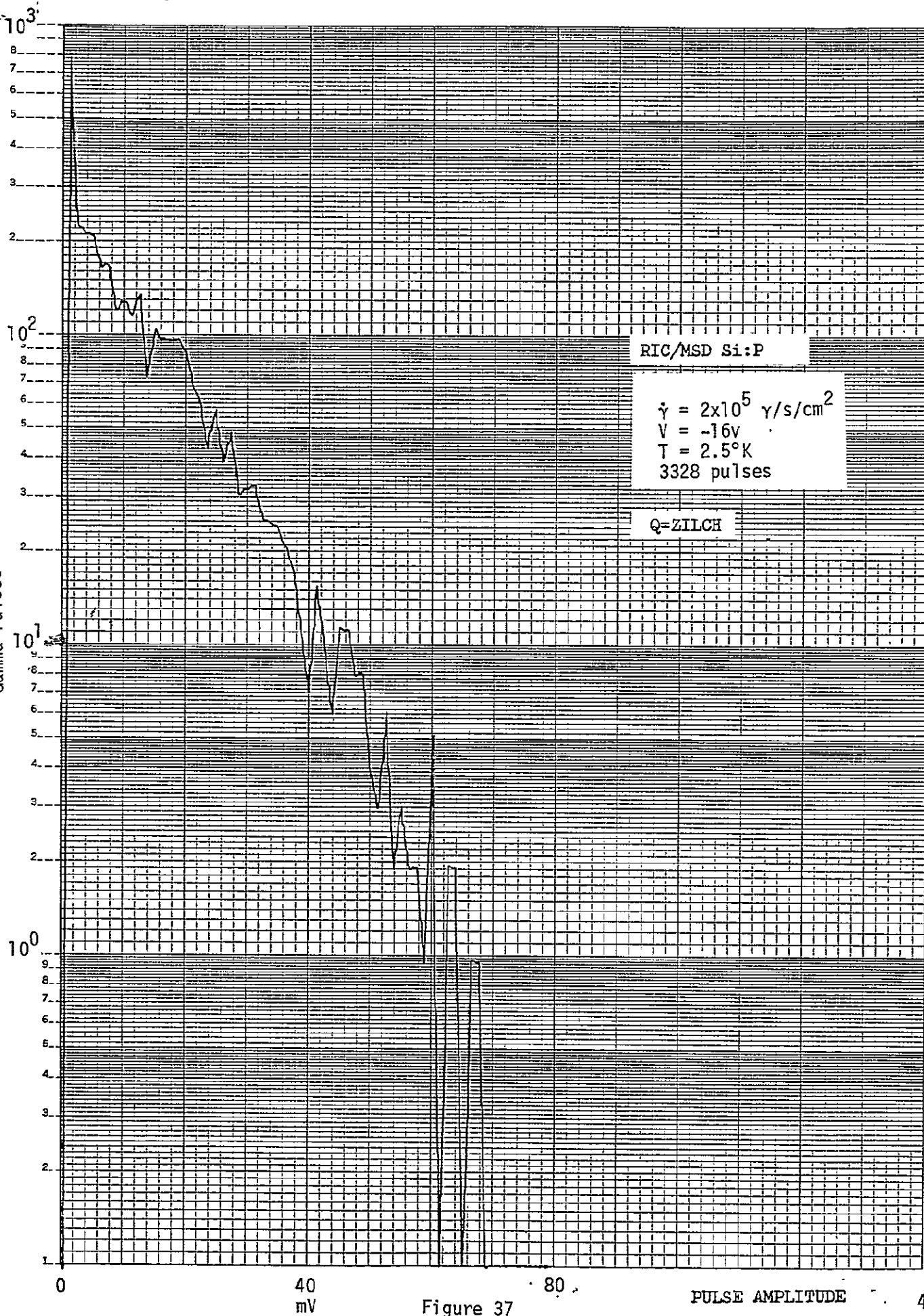


Figure 37

PULSE AMPLITUDE

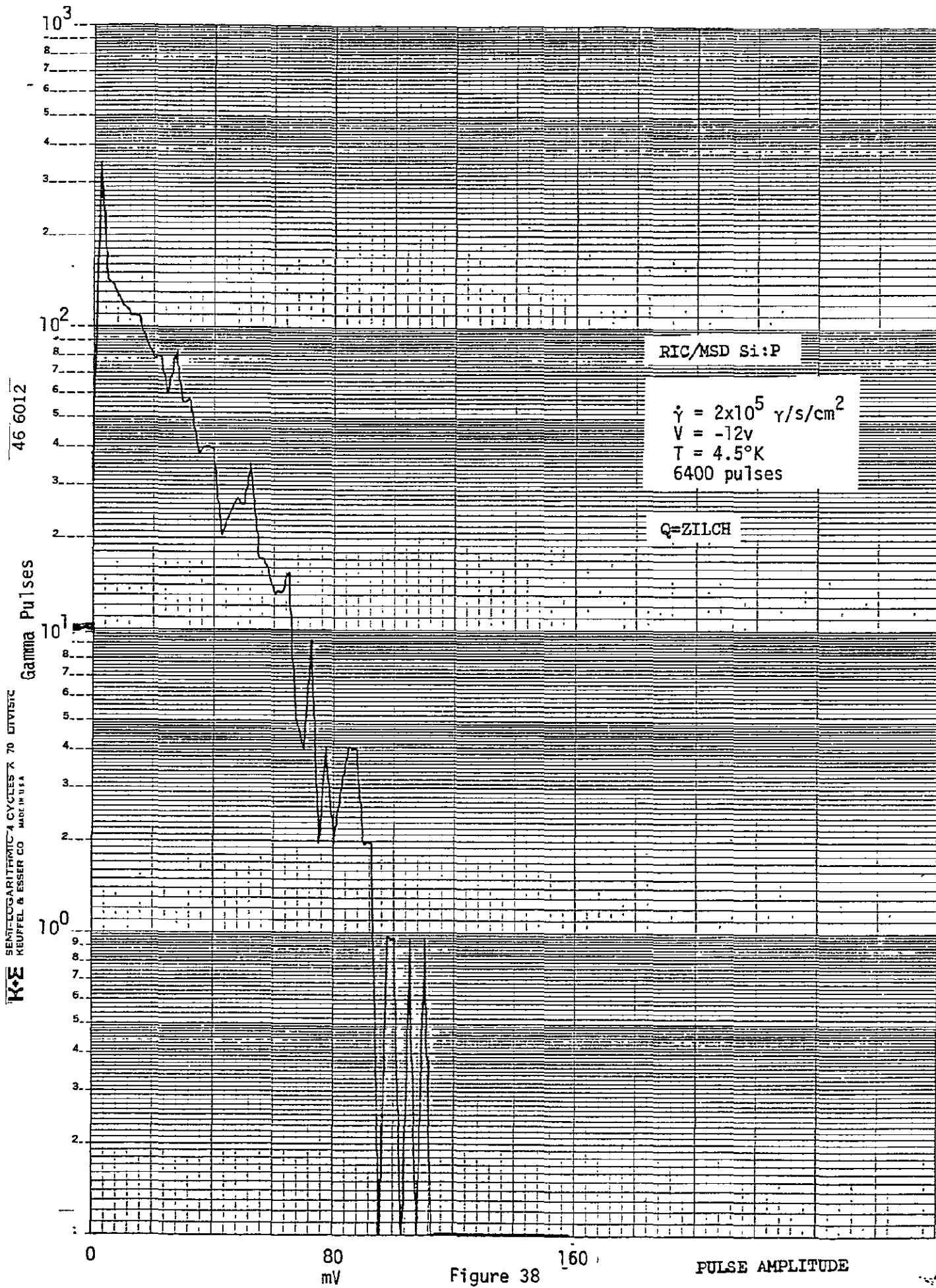


Figure 38

46 6012

Gamma Pulses

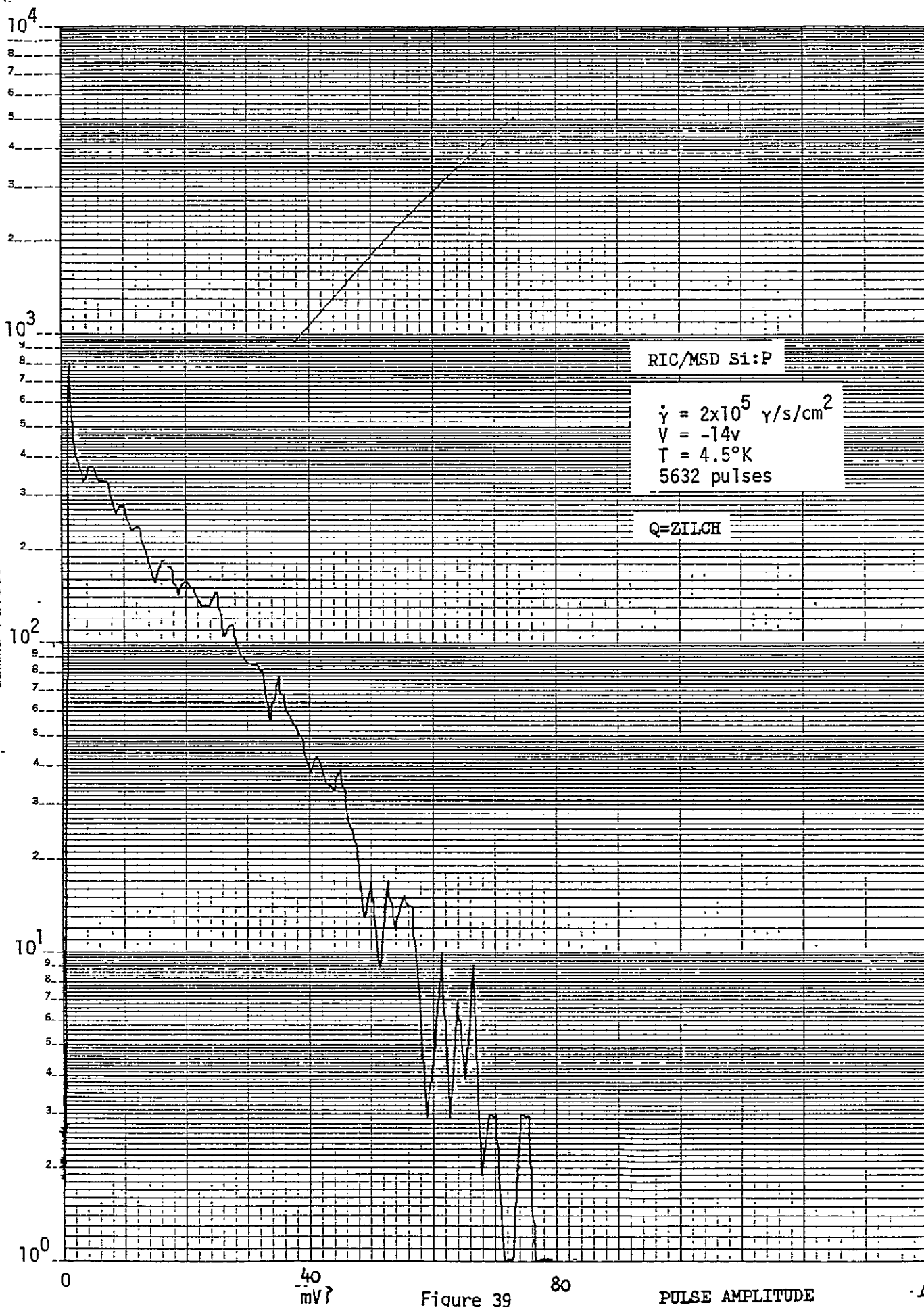
K.E. SEMICONDUCTOR TECHNOLOGY  
KEUFFEL & ESSER CO. MADE IN U.S.A.

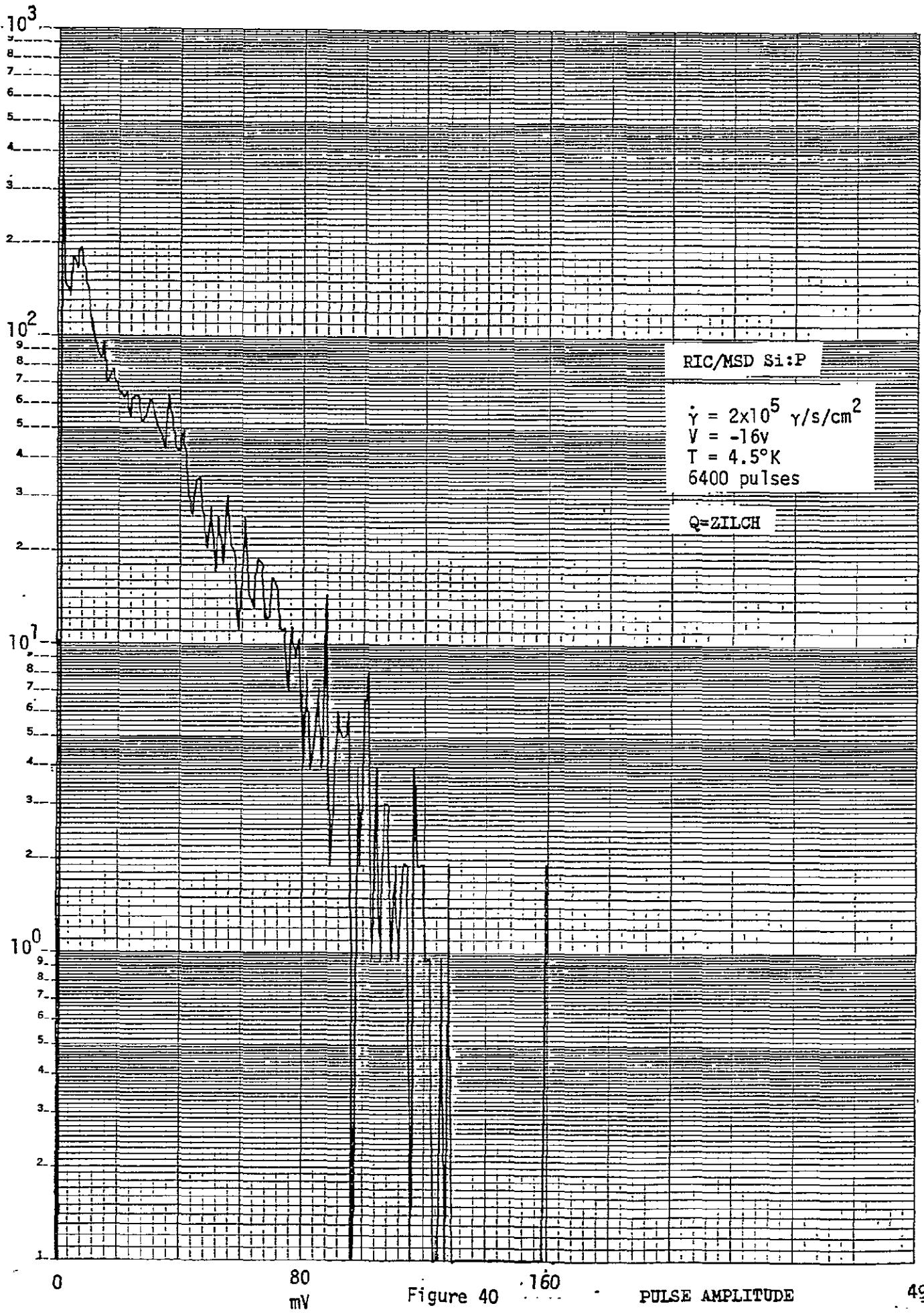
Figure 39

PULSE AMPLITUDE

46 6012

K&E SEMI-LOGARITHMIC 4 CYCLES X 70 DIVISION  
KEUFFEL & ESSER CO. MADE IN U.S.A.

Gamma Pulses



RIC/MSD Si:P

$\dot{\gamma} = 2 \times 10^5 \text{ } \gamma/\text{s}/\text{cm}^2$   
 $V = -16\text{v}$   
 $T = 4.5^\circ\text{K}$   
6400 pulses

Q=ZILCH

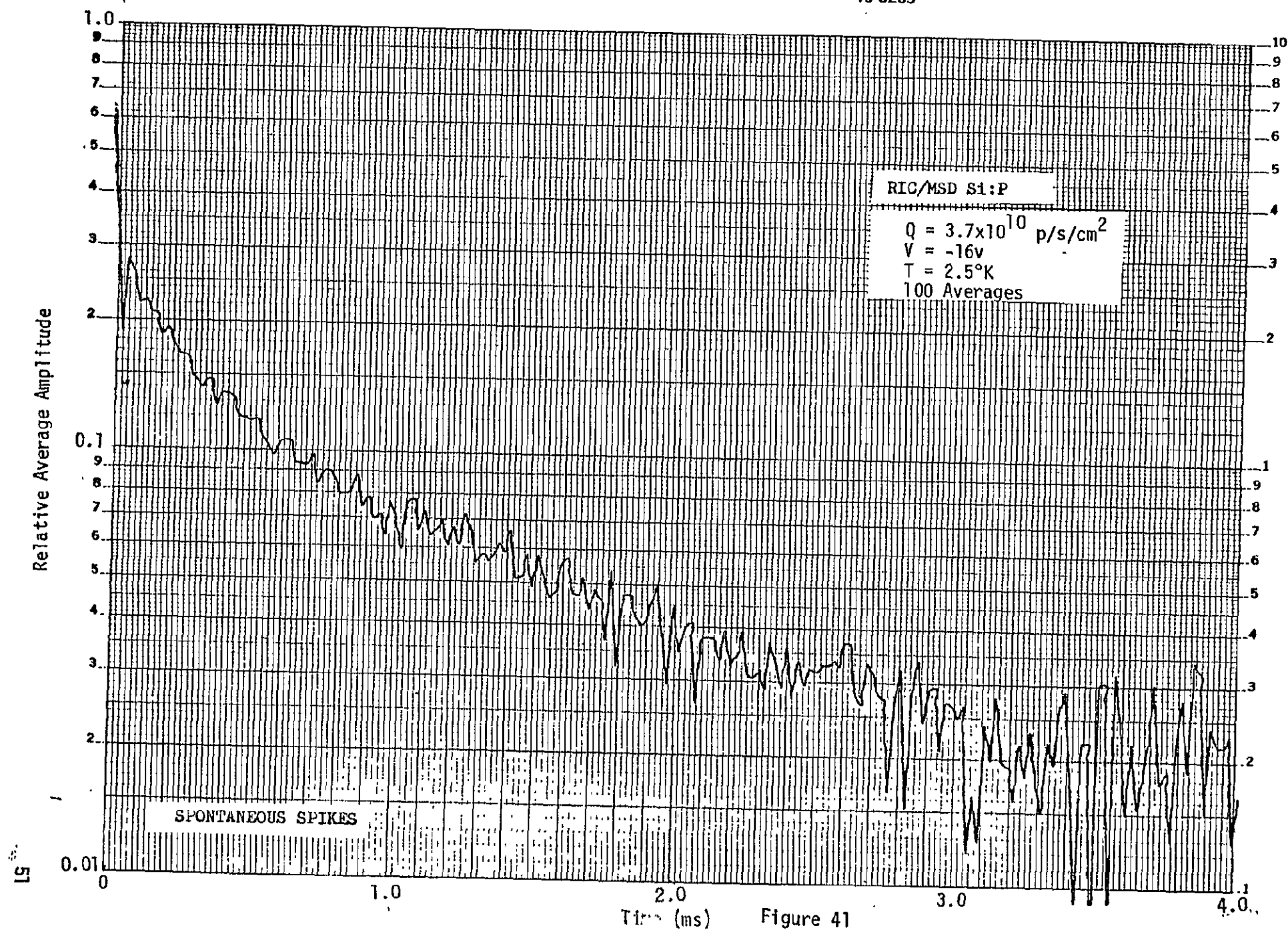
Figure 40

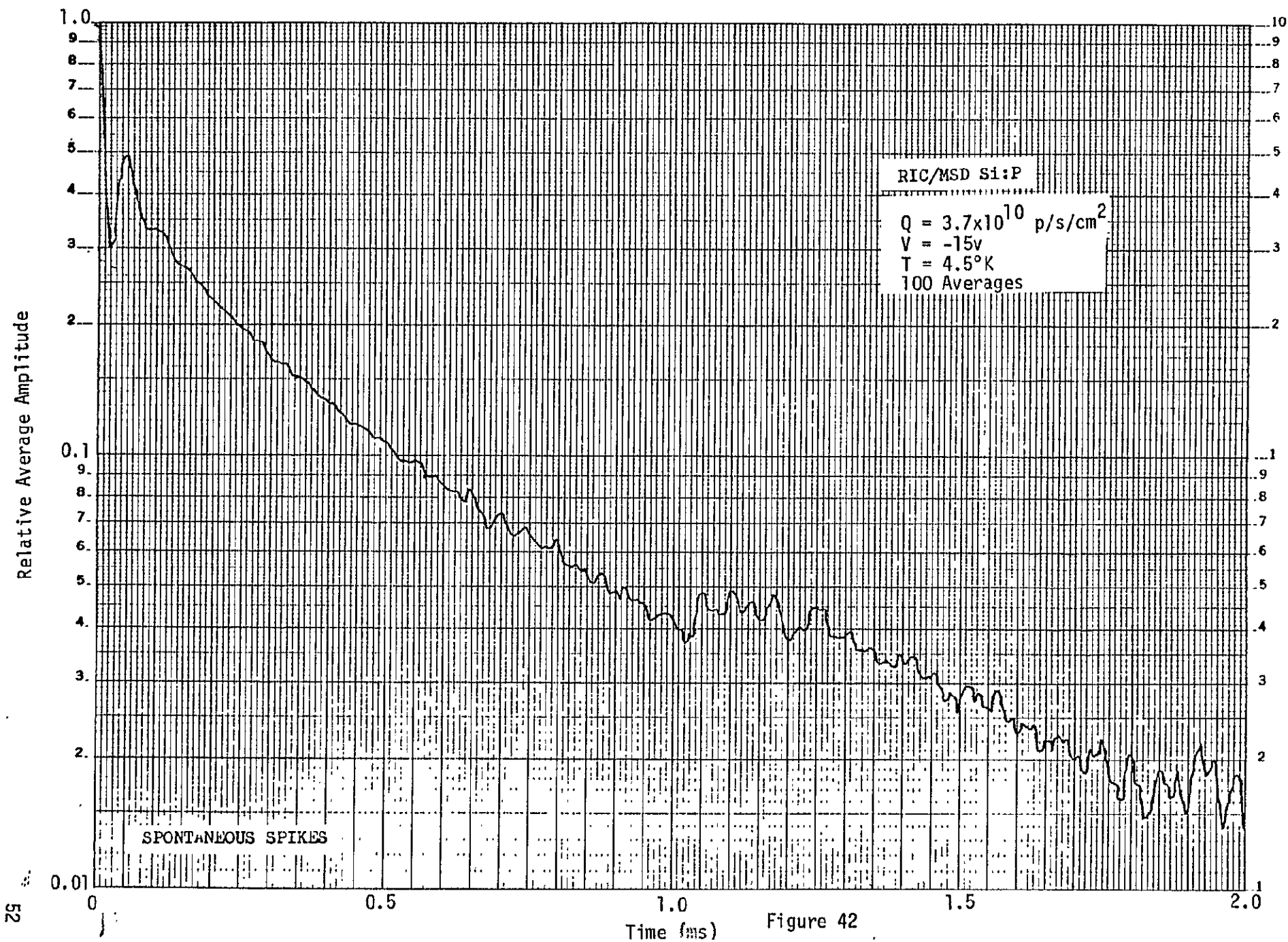
PULSE AMPLITUDE

#### 5.1.4. Spike Event Pulse Shapes

Figures 41 and 42 show the time dependence of spontaneous noise spikes at 2.5K and 4.5K. An average of 100 pulses was used to increase the signal to noise ratio. These spikes are characterized by an initial fast rise (not shown), an initial fast decay with ringing (caused by electronics), and a slow decay. The final slow decay corresponds to the RC time constant of the feedback resistor used in the TIA. The decay times are about 1.9 ms at 2.5K and 0.5 ms at 4.5K which correspond to the value of the feedback resistor and its shunt capacitance of about 0.5 $\mu$ f. Figure 43 shows similar data for gamma-induced spikes at a zilch optical background and at 4.5K. Note that the time dependence of the gamma-induced spikes is identical to that of the spontaneous noise spikes.







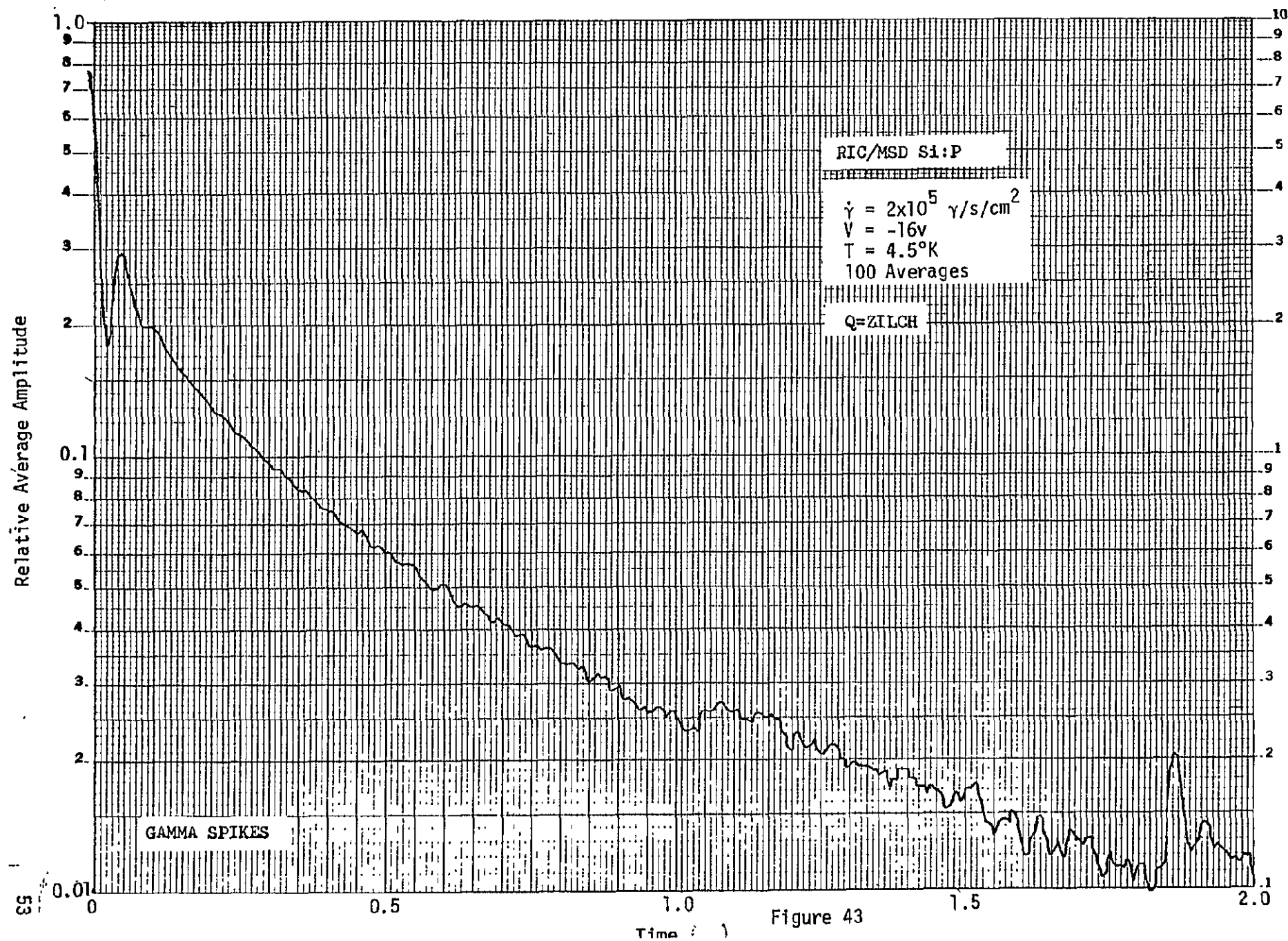


Figure 43

#### 5.1.5. Software Circumvention of Spikes

A computer program was written to remove spikes from time domain data to see how well the resulting noise spectra would match a noise spectra measured without spikes. This program used a relatively simple algorithm to perform the spike removal. It started at the beginning of the time domain data (  $t = 0$  ) and computed the average value of the data from  $t = 0$  up to each consecutive data point. If the value of any data point exceeded a preselected value (somewhat above the peak-to-peak detector noise level), the current average was substituted for that data point and a new current average computed using the substituted value (average remained the same). This process continued until the entire time domain window had been filled. The results of this spike removal technique are shown in Figs. 44 and 45 for time windows of 10 and 100 sec. where the data with and without spikes are shown. Note the relative uniformity in both time spacing and in the amplitudes of the larger pulses.

These data were then used to calculate the noise spectra for both cases and the data are shown in Fig. 46. A source follower configuration was used for these data. Note the decrease in noise for the "deglitched" data. For comparison purposes, the noise spectra at a lower background is also shown. At this background the number of spontaneous noise spikes was greatly reduced. The agreement between the "deglitched" noise at  $3.7 \times 10^{10}$  p/s/cm<sup>2</sup> and the noise at  $6.6 \times 10^9$  p/s/cm<sup>2</sup> is fairly good except between 1 and 50 Hz. The additional noise at the higher frequencies may be due to background noise (which remains after the spikes are removed) or due to small amplitude spikes which were not removed by this technique.

OUTPUT (50  $\mu$ V/IN)

$Q=3.7 \times 10^{10}$  (spikes removed)

RIC/MSD Si:P

T = 4.5K

V = -14V

OUTPUT (200  $\mu$ V/IN)

$Q=3.7 \times 10^{10}$  (with spikes)

150 Hz BANDWIDTH

TIME (1 SEC/IN) . Figure 44

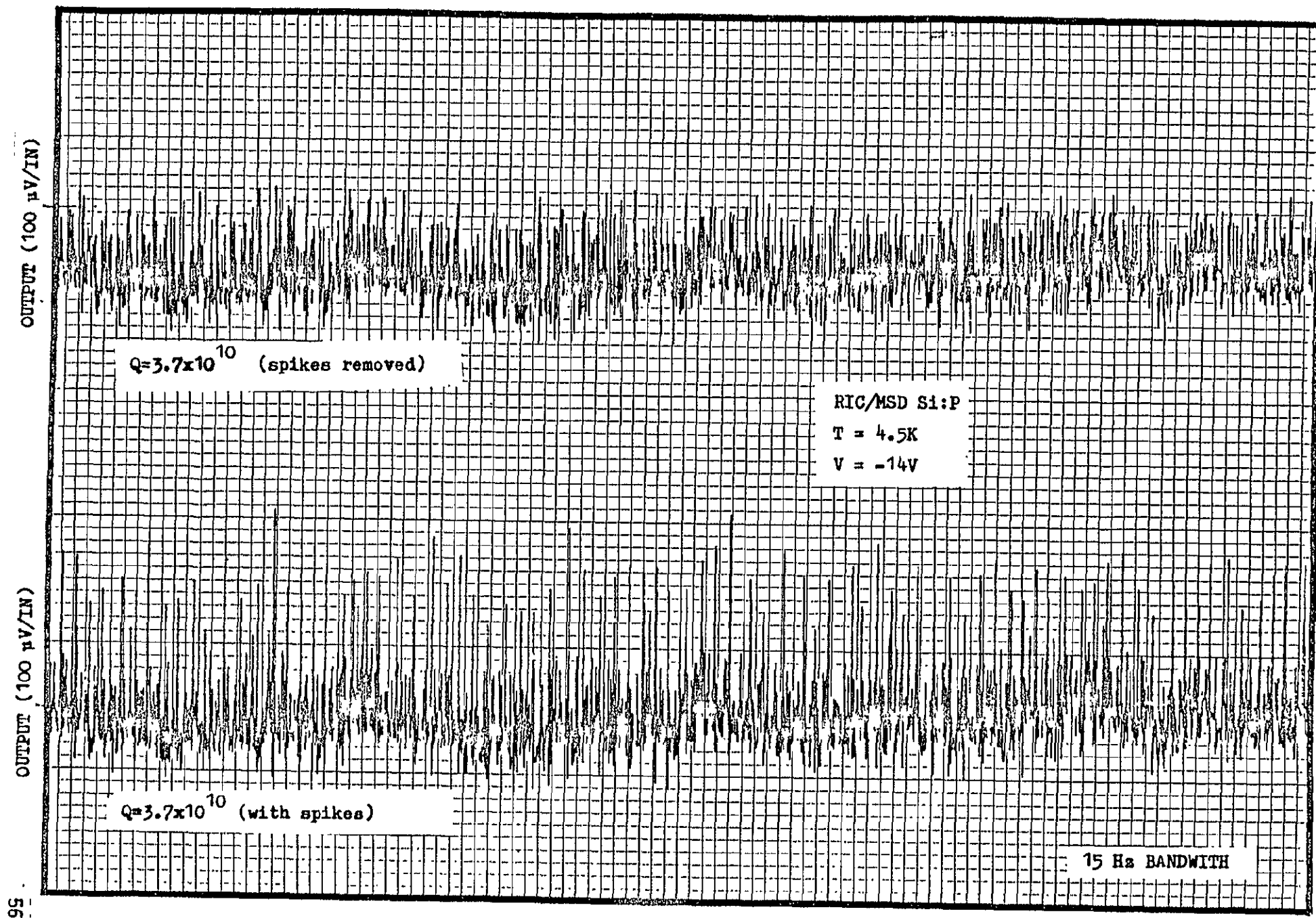


Figure 45

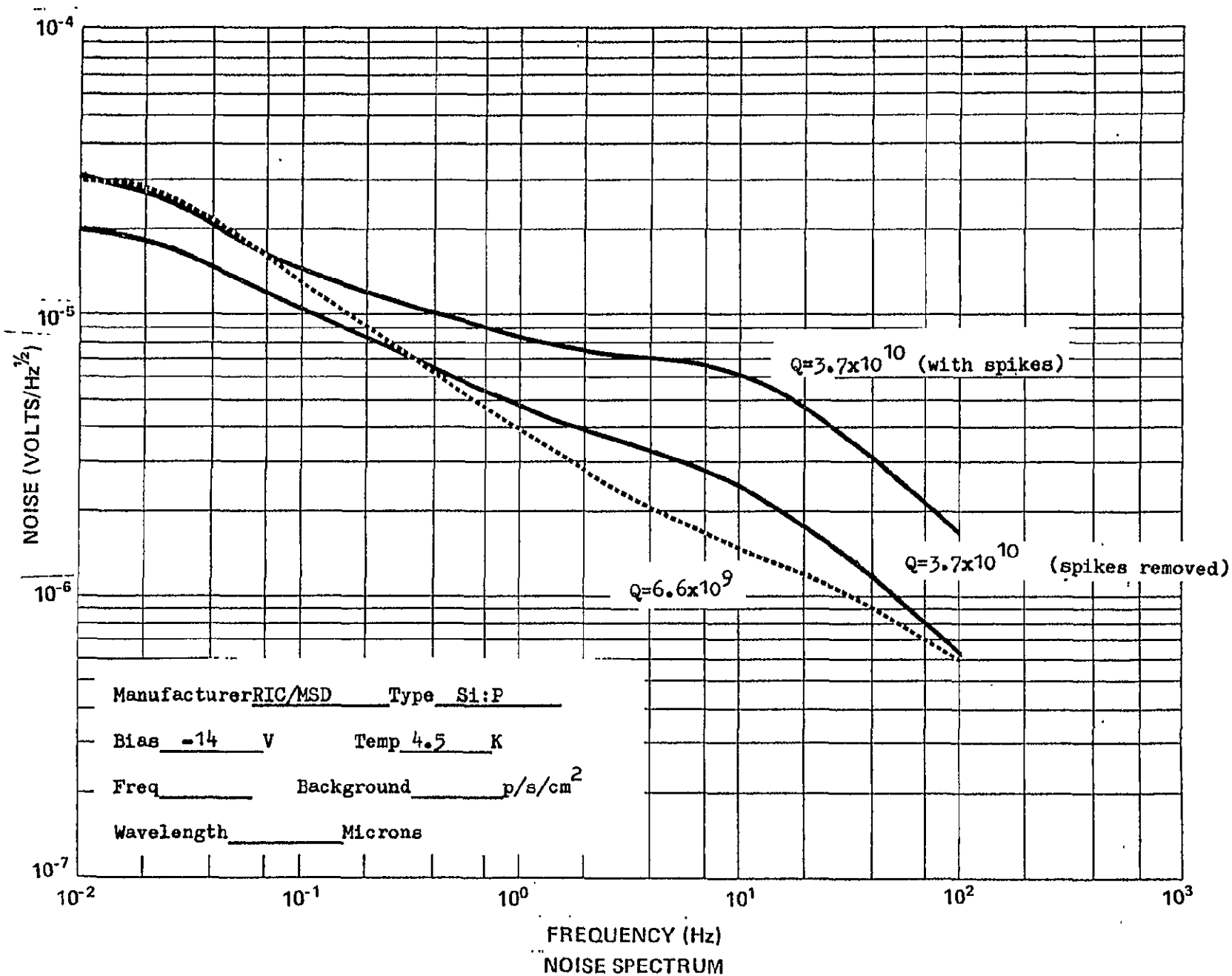


Figure 46

## 5.2. RIC/MSD Si:As Hardware Circumvention of Gamma Spikes

The following data were obtained using an Aerojet Electrosystem Company (AESC) wideband feedback preamplifier (operating as a TIA) ac-coupled to a keyed-clamp circuit that was specifically designed for the suppression of gamma noise pulses.<sup>[1]</sup> Outputs for signal processing were available at the TIA as well as the keyed-clamp gate circuit. Provision was made for deactivating the gate so that a comparison of ungated (Blanking Off) and gated (Blanking On) signals could easily be made. The blanking time (gate width) could be varied from 24 microseconds to 400 microseconds; for these measurements, the blanking time was approximately 250-350 microseconds.

The Rockwell Si:As detector was used exclusively throughout these measurements. Noise measurements were made at a background of  $5.6 \times 10^9$  p/s/cm<sup>2</sup>. Bias on the detector was 5 volts and the temperature was 4.5K. Three Cobalt-60 gamma sources, 0.1, 1.0, and 10 millicurie, were used to establish gamma flux levels of  $2 \times 10^5$ ,  $2 \times 10^6$ , and  $2 \times 10^7$  gamma/sec/cm<sup>2</sup>, respectively.

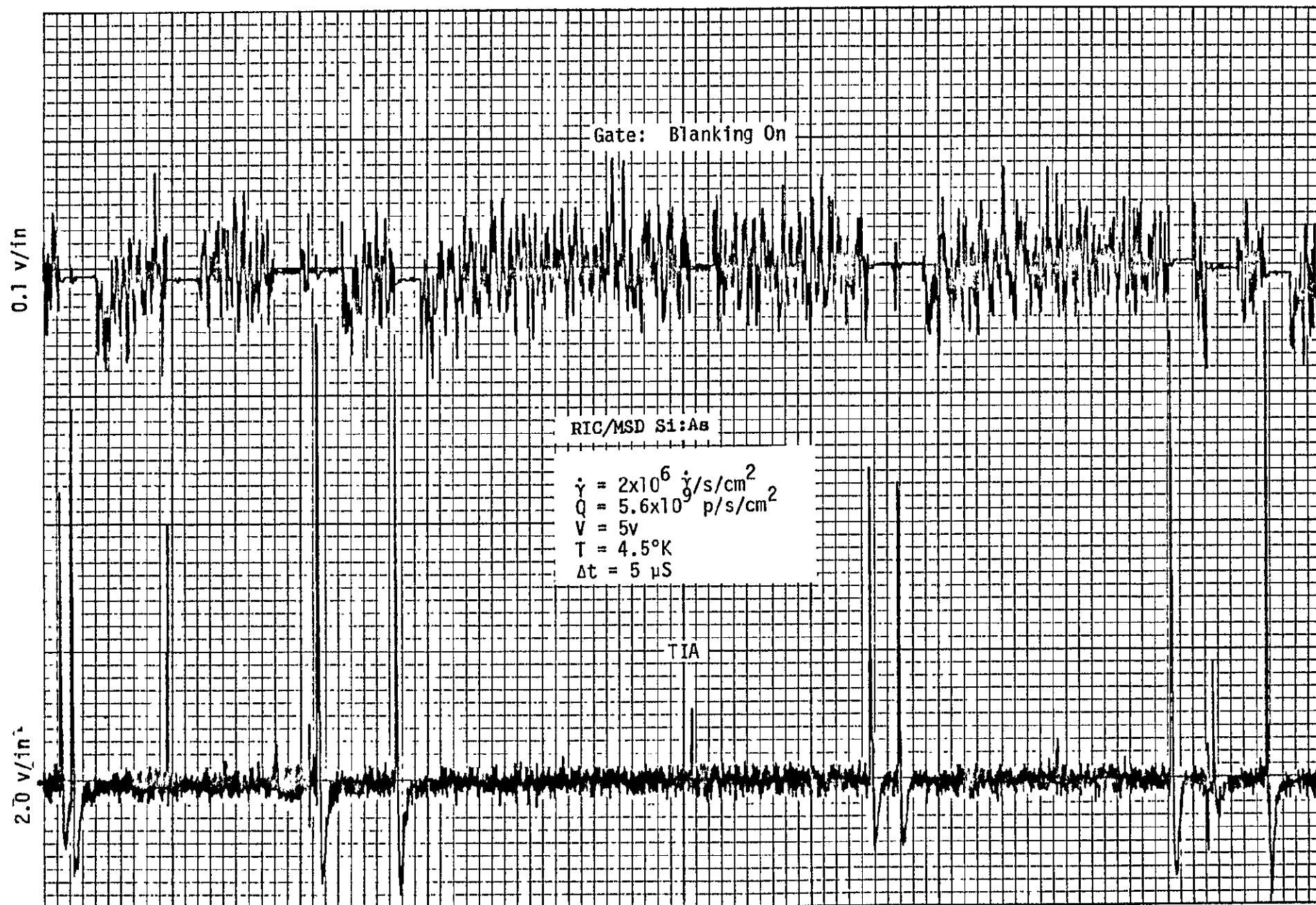
Figure 47 shows simultaneously-recorded data at the TIA output and the gate output with the blanking circuit operational. The effect of the blanking can be clearly seen. Figures 48 and 49 show the noise spectra at the TIA output for a clear environment and for the three gamma levels. Figure 50 shows the Noise spectra from the gate output but without blanking. These spectra are similar to those at the TIA output. Finally Fig. 51 shows the noise spectra from the gate output but with the blanking operational. The decrease in noise level is about a factor of 3 or 4.

---

1. C. M. Parry and J. B. Parkinson (AESC), Hardened Detector/Circuit Development (U), Volume I: AESC Final Report; DAHC 60-73-C-0059, September 1974 (SECRET).



It should be noted that the various adjustable parameters (peaking, lead compensation, pulse threshold, bandwidth, gate width, etc.) on the three circuit boards (preamplifier board, logic board, and gate board) in the AESC amplifier set, at the start of these measurements, to provide for the minimum distortion of the signal and noise output while using a minimum blanking time to suppress gamma pulses from the 1 millicurie gamma source. Once this optimum had been achieved, no further adjustments were made on the amplifier during the course of these measurements.



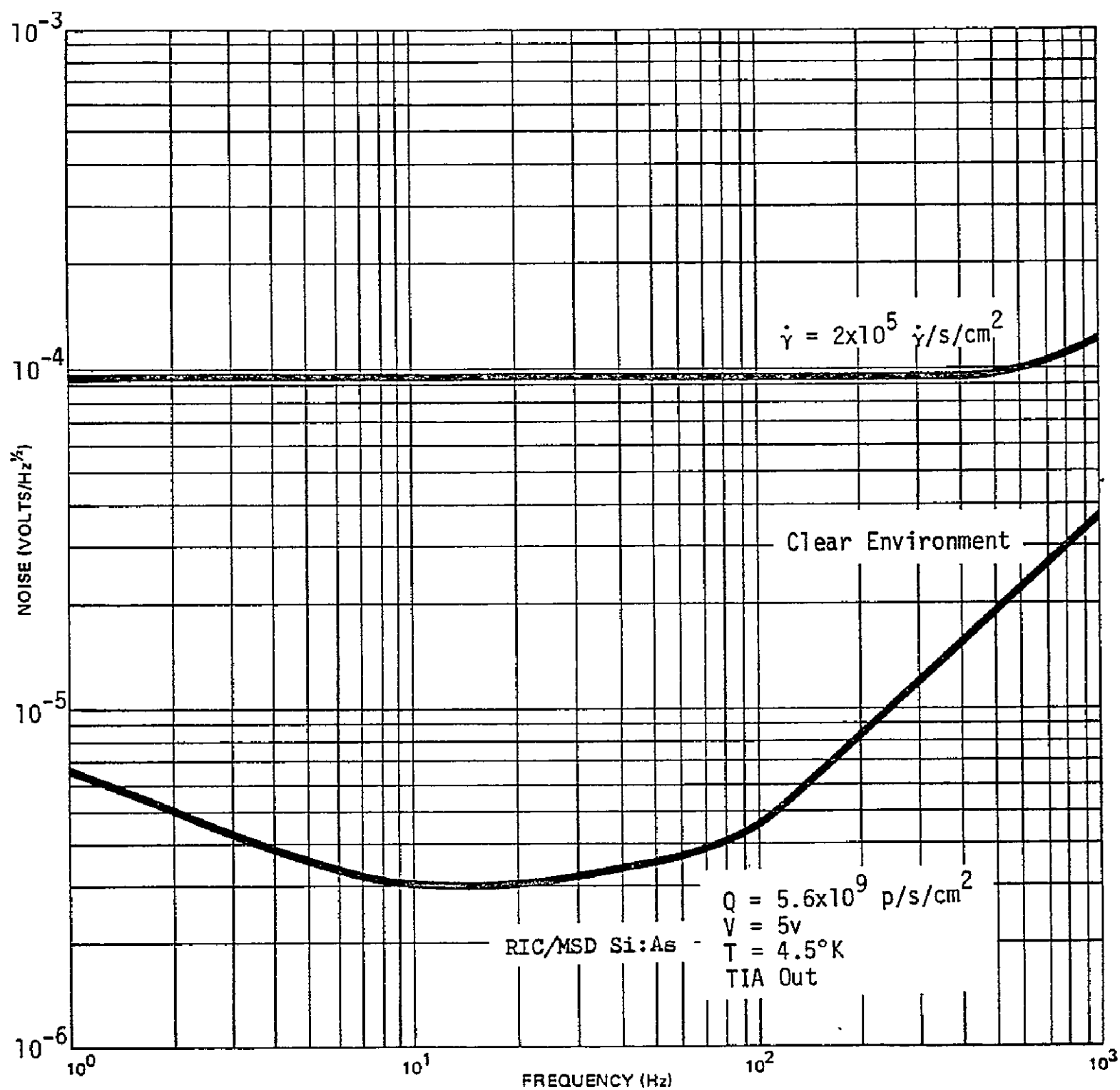


Figure 48

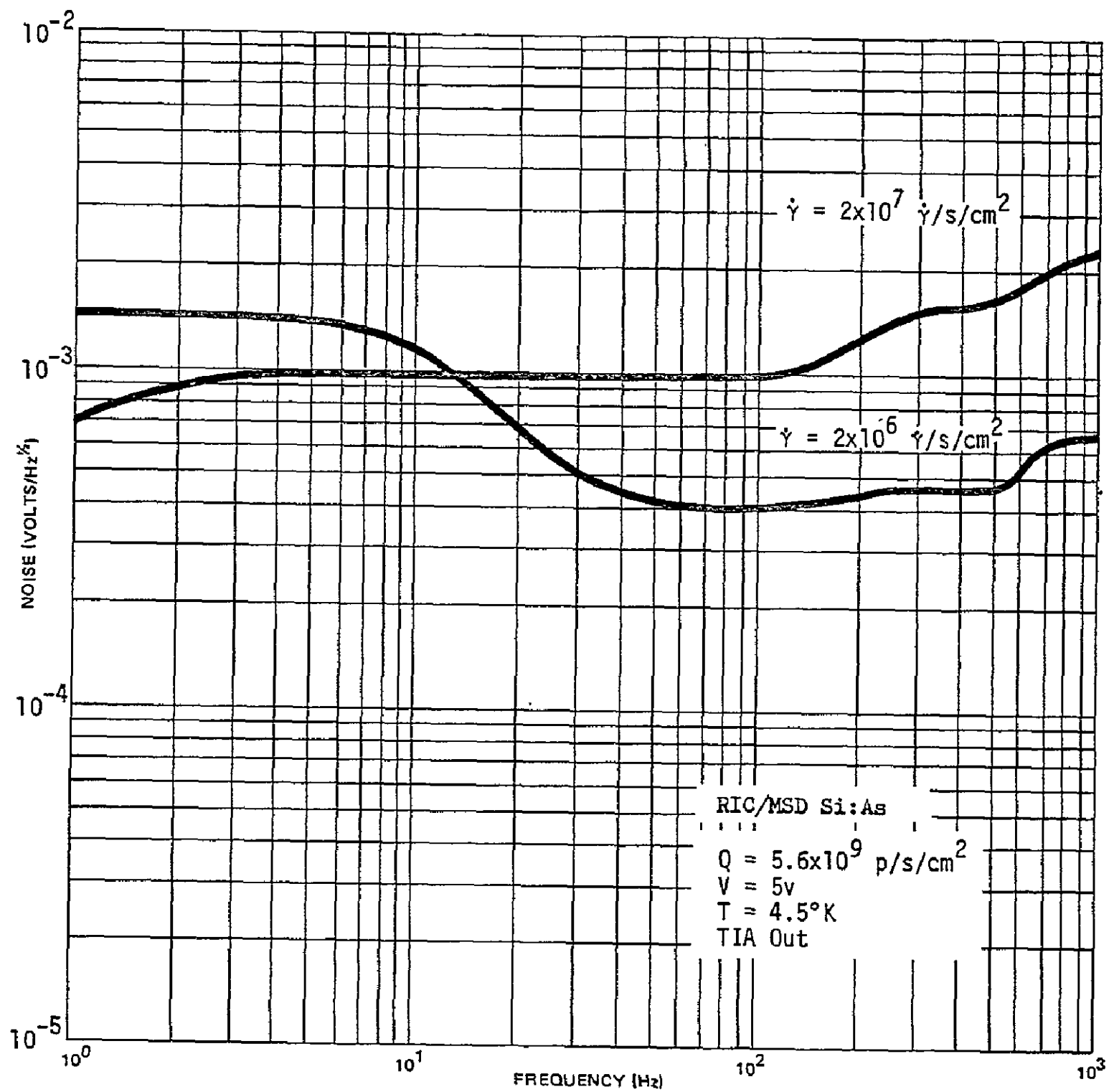


Figure 49

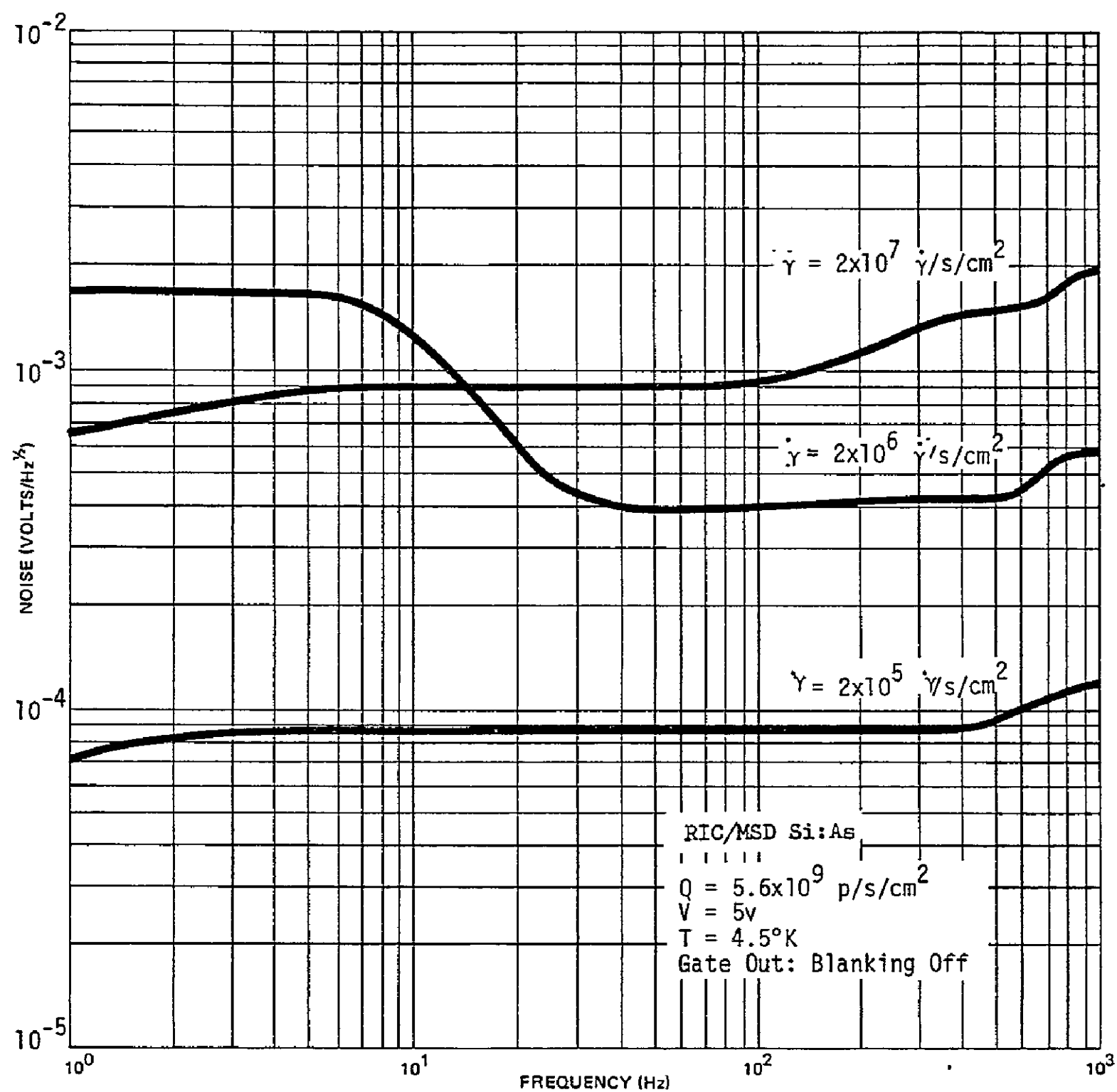


Figure 50

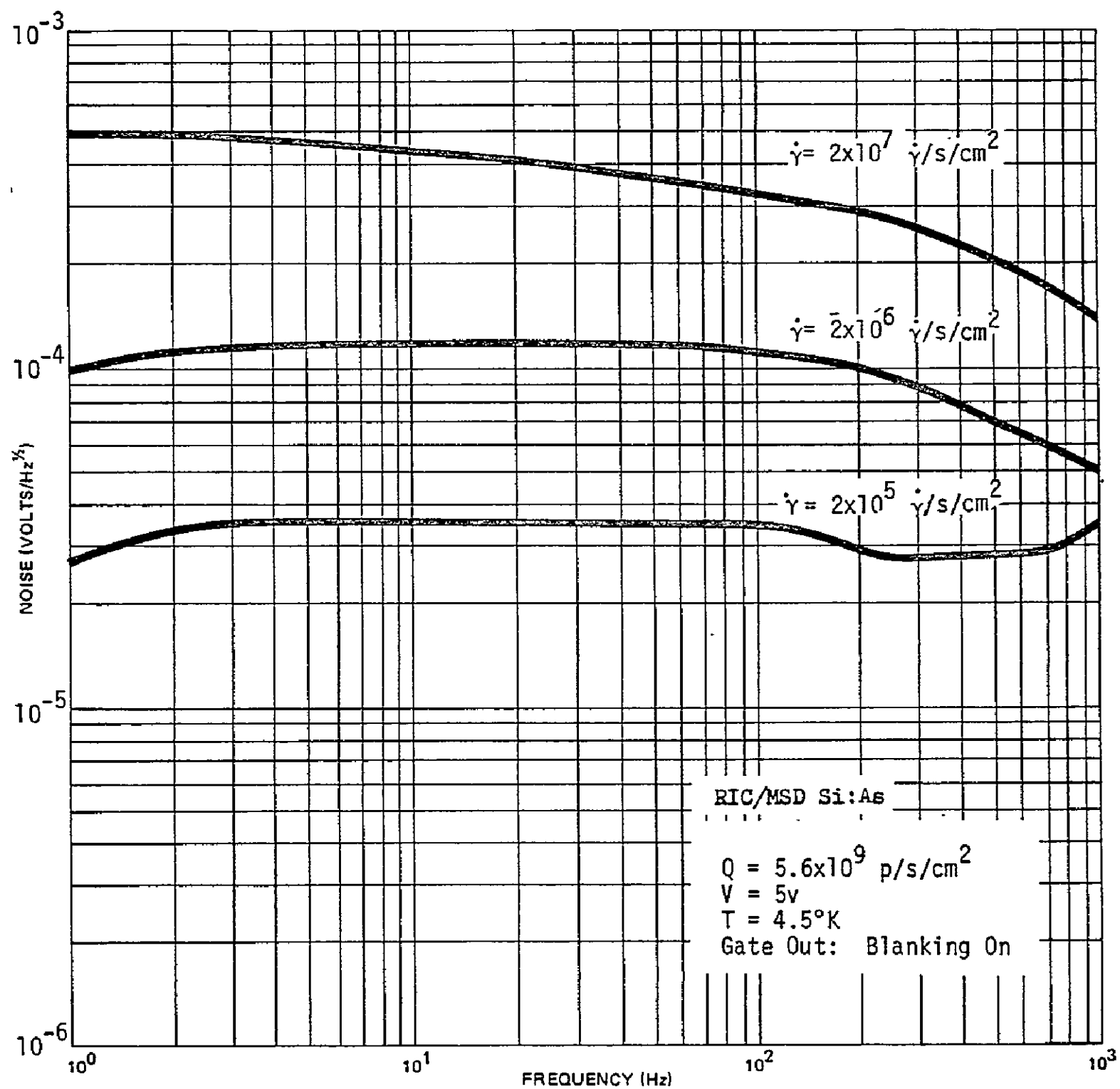


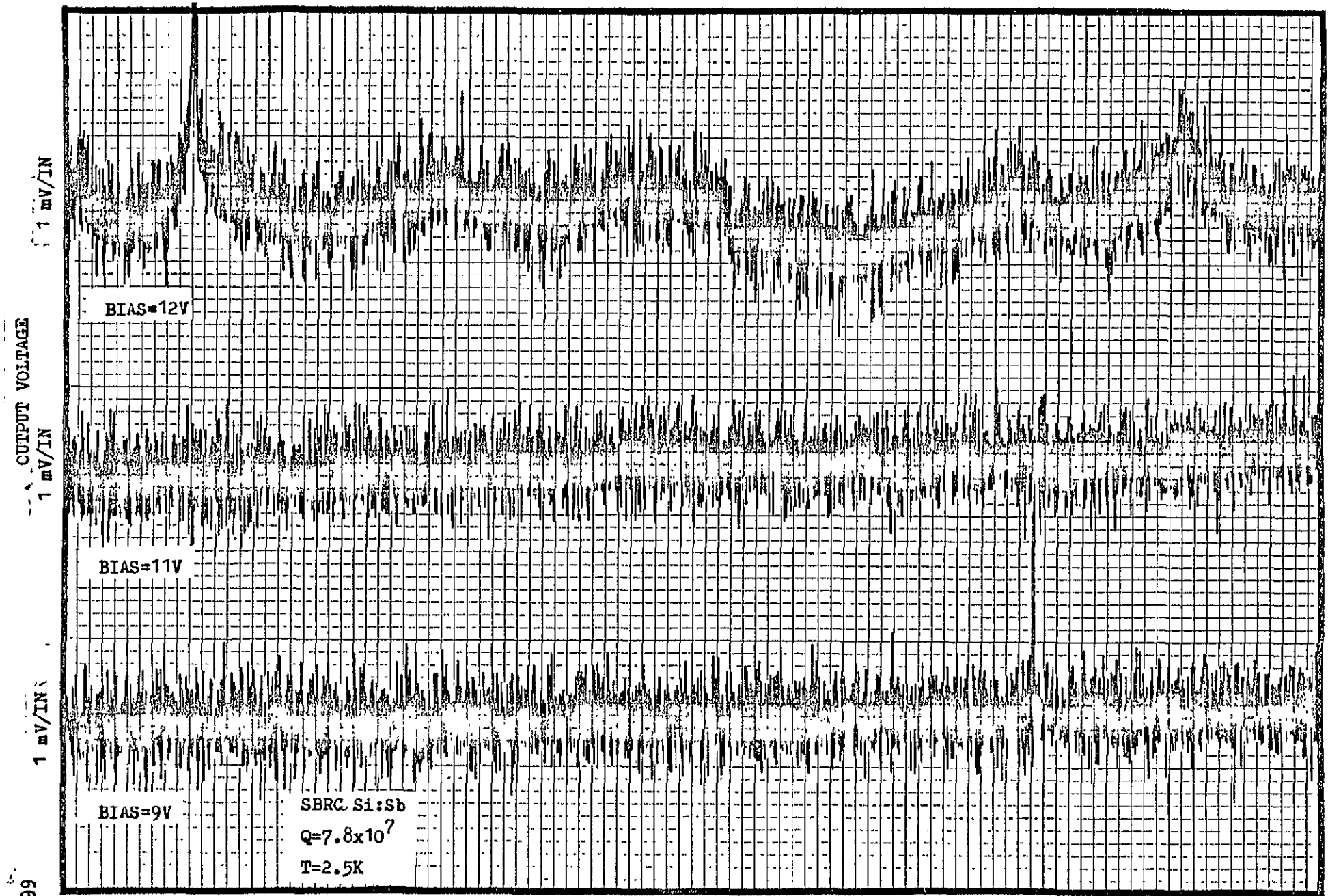
Figure 51

### 5.3 SBRC Si:Sb - Spontaneous Noise Spikes

An attempt was made to characterize the spontaneous noise spikes produced by the new Si:Sb detector (see Section 3.0). However, the output pulses did not have the time dependence usually associated with spontaneous noise spikes. The time shape is illustrated in Figs. 52-59 where detector outputs (using a TIA) are shown as functions of time at two temperatures, four backgrounds, and at biases between 9 and 12 volts.

While there are a few "normal" spikes in the data, most of the spikes at higher bias have a relatively slow rise time and, in some cases, appear to be almost symmetrical. Because of the slow rise times, it was not possible to use triggered-circuitry to obtain pulse rates or amplitude distribution data. However, it is apparent from the data that the conclusions made in Section 5.1.1 also hold for this detector. That is, the pulse rate increases with increasing bias, operating temperature, and photon background flux.

As was mentioned in Section 3.0, the optimum bias determined at 4.5K was 9 volts. If one looks at the 4.5K data presented here at biases greater than 9 volts, it is apparent that spikes will contribute to the rms noise. However, at 2.5K, the increase in rms noise due to spikes (at biases greater than 9 volts) appears to be somewhat smaller. This leads to the conclusion that biases greater than 9 volts may be optimum at the lower temperature.



TIME : 10 SEC/IN

Figure 52



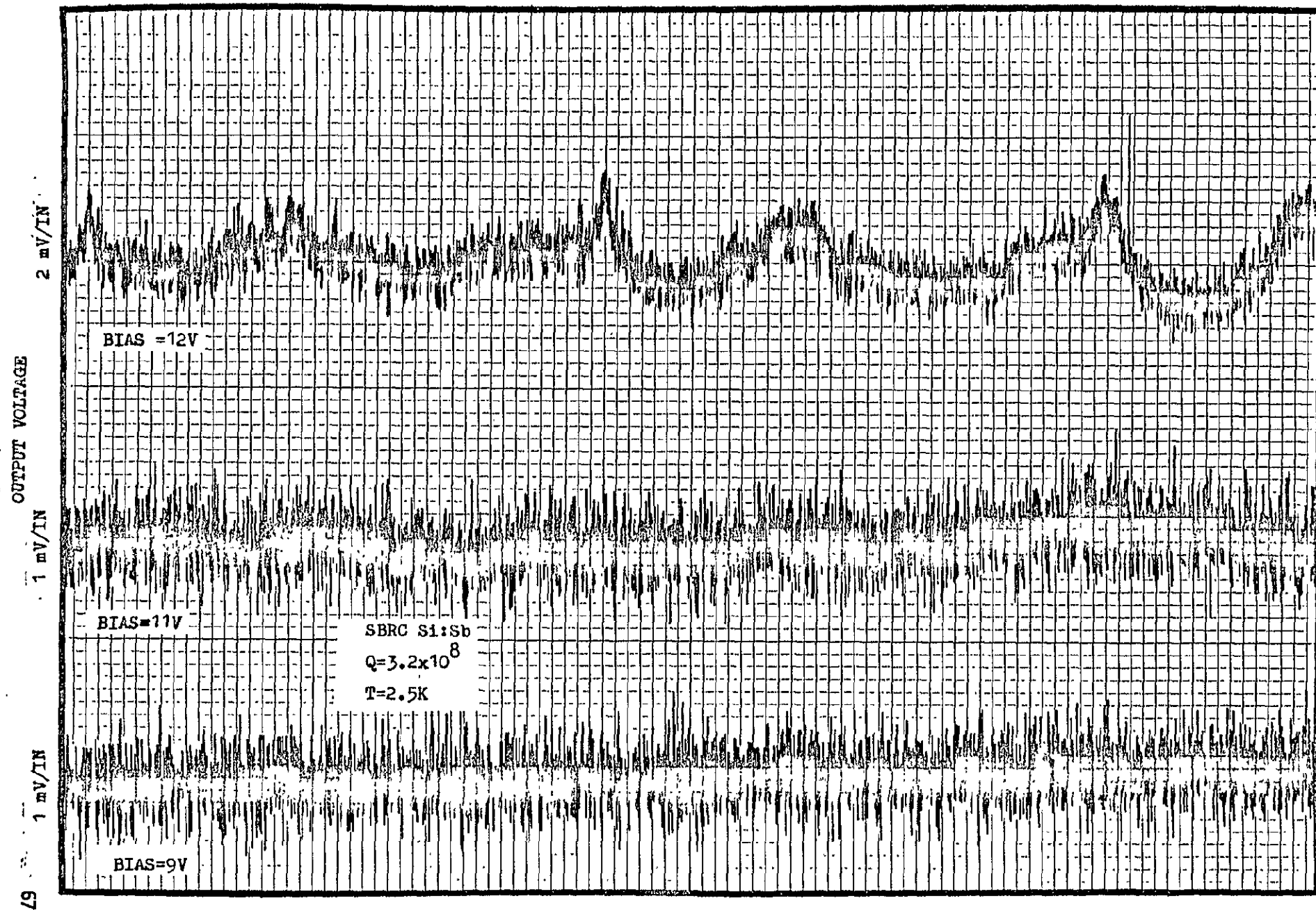
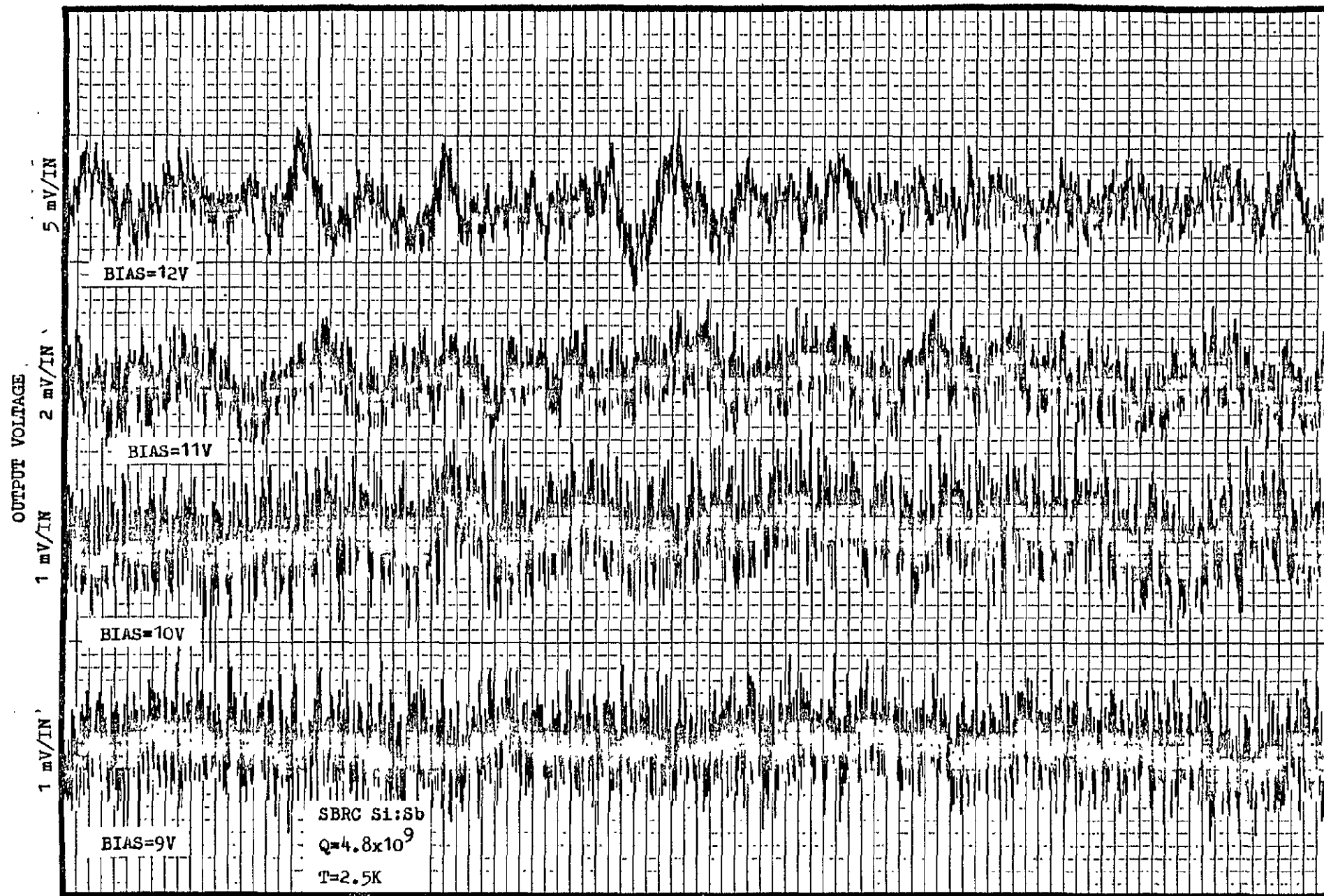


Figure 53



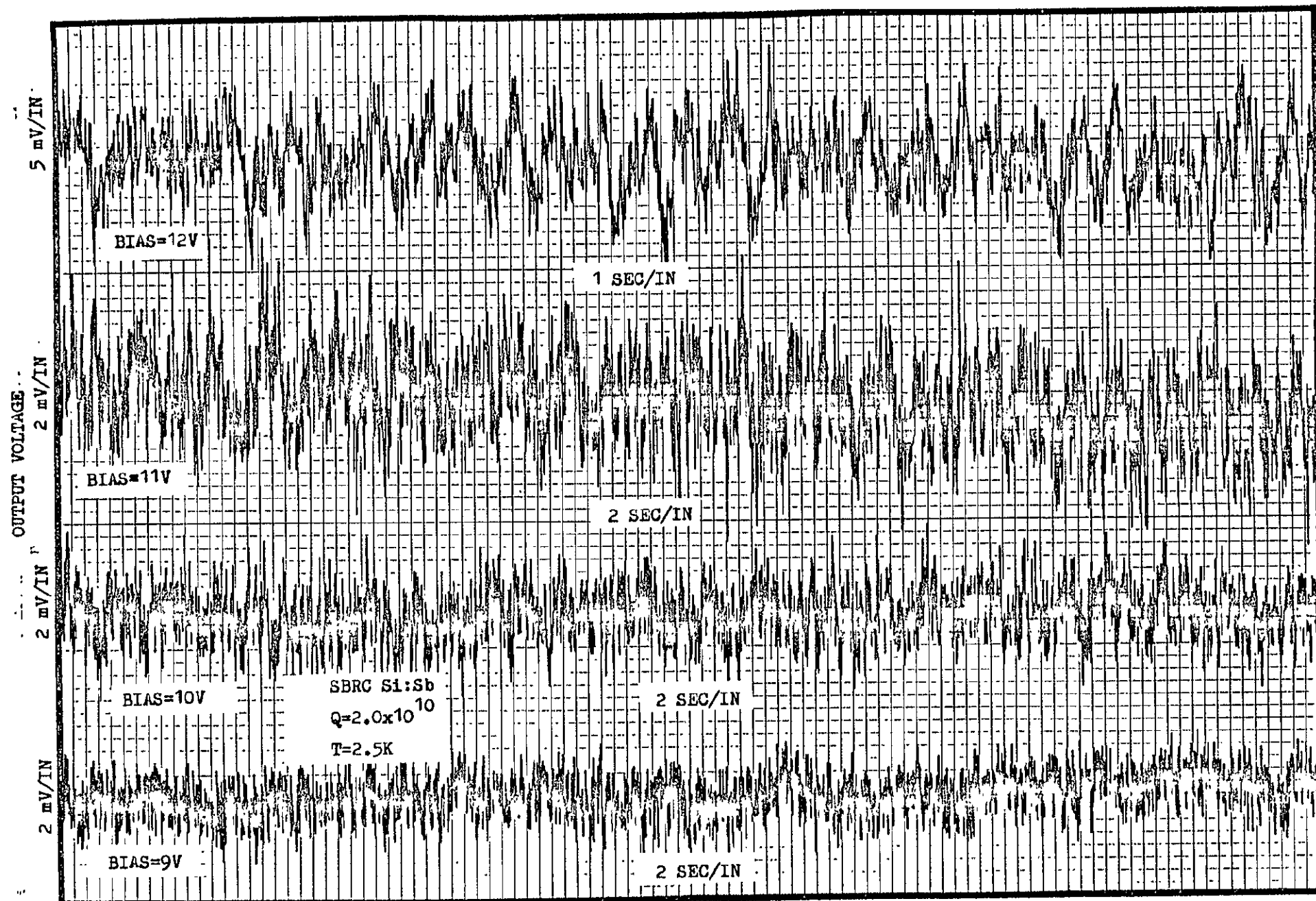
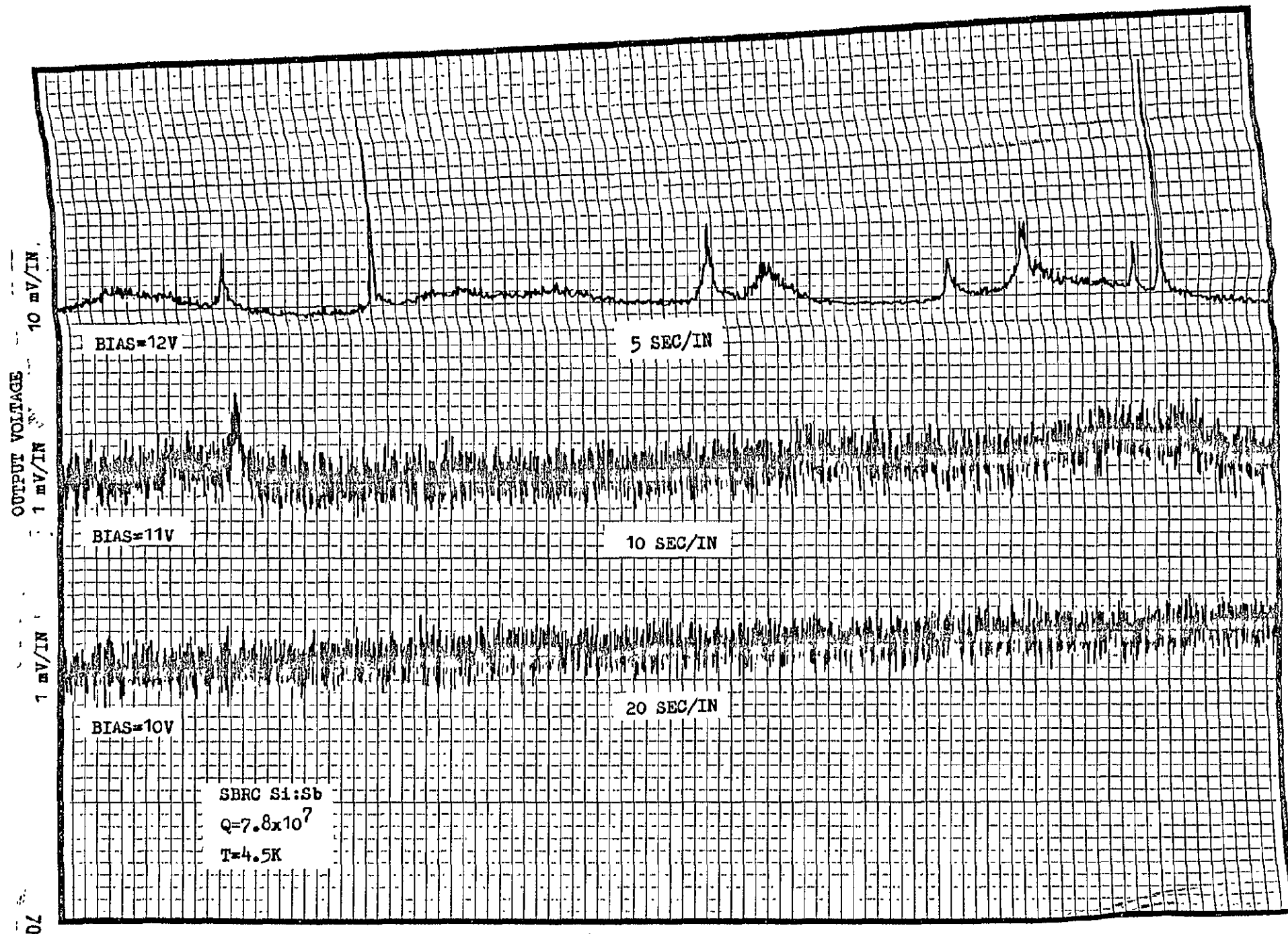


Figure 55



TIME

Figure 56

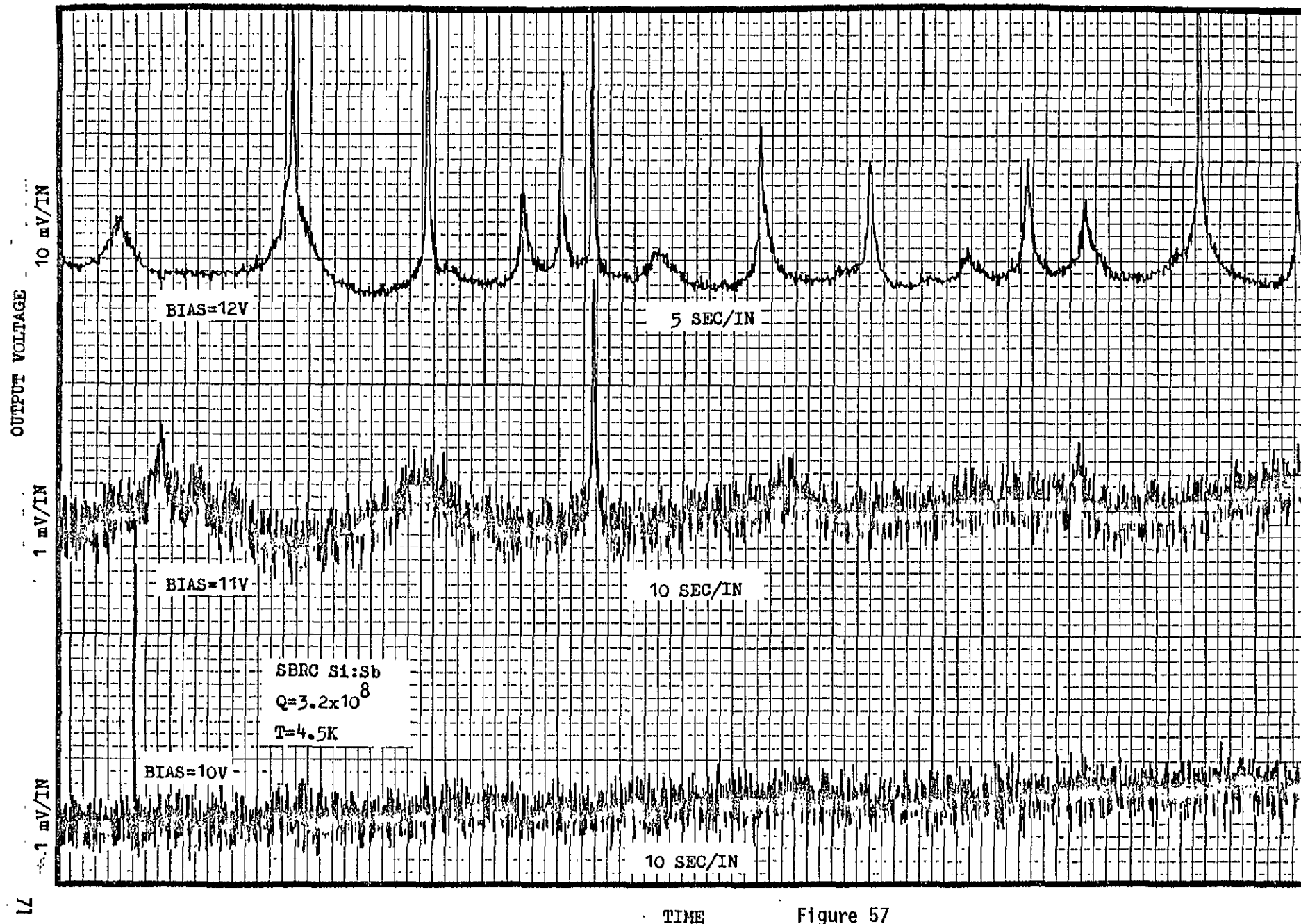
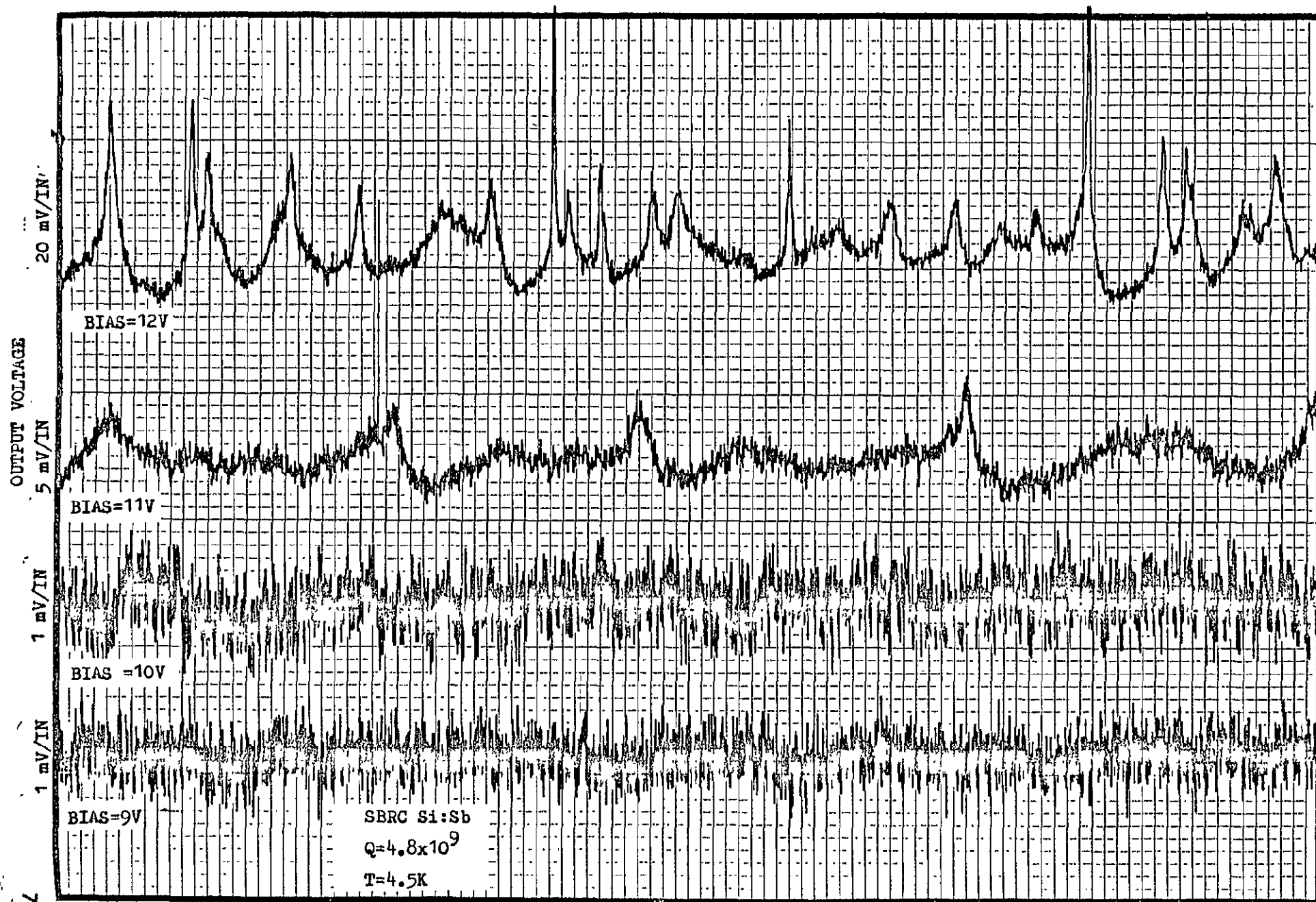


Figure 57



TIME 1 SEC/IN

Figure 58



TIME 1 SEC/IN

Figure 59

## 6.0 DC-COUPLED OUTPUT MEASUREMENTS

A number of measurements were made to characterize the response of two detectors to step function changes in background photon flux. The detectors used were the SBRC Si:As (previously reported) and the new SBRC Si:Sb (Section 3.0). For these measurements a TIA was used and the electronics were dc-coupled from the detector to the recording device. The data for the Si:As detector are given in Figs. 60-106. Figures 107-130 show the data for the Si:Sb detector.

The background levels shown on the graphs are equivalent photon flux densities at the peak wavelength of each detector. That is, the relative spectral response of each detector and the spectral distribution of the photons from the source were taken into account in each case. Data are presented at two operating temperatures and four backgrounds for each detector. Two bias values (6 volts and 12 volts) were used for the Si:As detector. Because batteries were used in a number of places in the circuit, a long term dc-drift appears in some of the data. This drift is particularly noticeable where the output sensitivity is high. For instance, in Fig. 82 there is a drift of about 600 $\mu$ V in 500 sec.

It is very difficult to make any general conclusions from these data. The output wave shape appears to be a function of every possible variable (i.e., initial background, final background, bias, temperature, etc.). Figures 101-106 show the output of the Si:As detector at biases ranging from +4 V to +12 V and from -4 V to -12 V. It is apparent from these data that the shape of the signal pulse also depends on the polarity of the bias. It should be pointed out that the data in this Section was quite reproducible. For example, the rather complicated output shown in Fig. 87 could be duplicated (the amplitude of the pulses varied somewhat) time after time.



OUTPUT (1 mV/IN)

SBRC S1:AS

BIAS = 6V  
TEMP = 2.5K

$Q=3.0 \times 10^8$

$Q=3.0 \times 10^8$

$Q=7.7 \times 10^7$

$Q=7.7 \times 10^7$

Q=ZILCH

Q=ZILCH

Q=ZILCH

Figure 60

TIME (10 SEC/IN)

OUTPUT (1 mV/IN)

SBRC S1:As

BIAS = 6V

TEMP = 2.5K

$Q=7.7 \times 10^7$

Q= ZILCH

Q=ZILCH

$Q=7.7 \times 10^7$

Q=ZILCH

Q= ZILCH

Figure 61

TIME (10 SEC/IN)

OUTPUT (1 mV/IN)

SBRC Si:As

BIAS = 6V

TMEP = 2.5K

$Q=3.0 \times 10^8$

Q=ZILCH

Q=ZILCH

TIME ( 10 SEC/IN)

Figure 62

OUTPUT (1 mV/IN)

SBRC Si:As

BIAS = 6V

TEMP = 2.5K

$Q=3.0 \times 10^8$

$Q=7.7 \times 10^7$

$Q=7.7 \times 10^7$

TIME (10 SEC/IN)

Figure 63

OUTPUT (1 mV/IN)

SBRC Si:As

BIAS = 6V

TEMP = 2.5K

$Q=3.0 \times 10^8$

$Q=7.7 \times 10^7$

TIME (10 SEC/IN)

Figure 64

OUTPUT (5mV/IN)

SBRC Si:As

BIAS = 12V  
TEMP = 2.5K

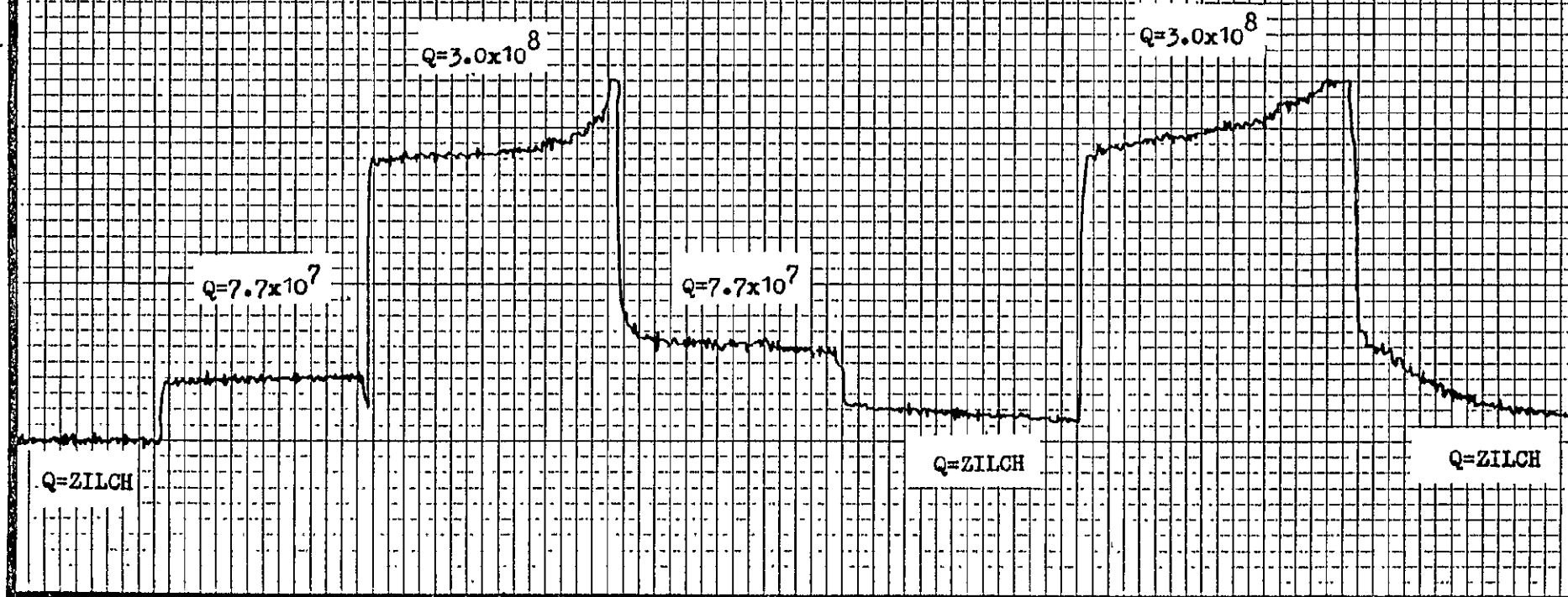


Figure 65

TIME (10 SEC/IN)

OUTPUT (1 mV/IN)

SBRC Si:As

BIAS = 12V  
TEMP = 2.5K

$Q=7.7 \times 10^7$

Q=ZILCH

Q=ZILCH

Figure 66

TIME (10 SEC/IN)

OUTPUT (5 mV/IN)

SBRC Si:As

BIAS = 12V

TEMP = 2.5K

$Q=3.0 \times 10^8$

Q=ZILCH

Q=ZILCH

TIME (10 SEC/IN)

Figure 67



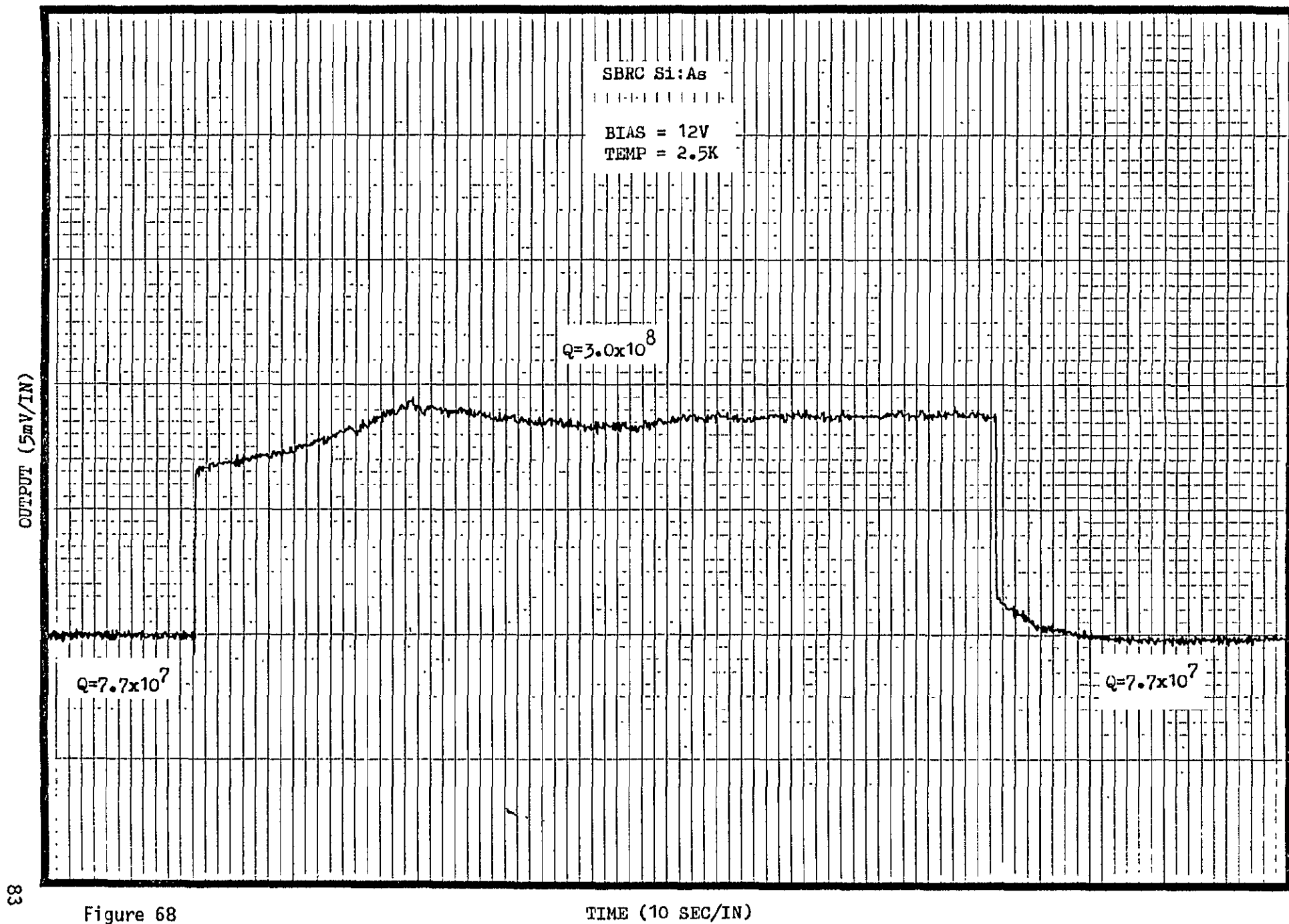


Figure 68

OUTPUT (2 mV/IN)

SBRC Si:As

BIAS = 12V

TEMP = 2.5K

$Q=3.0 \times 10^8$

$Q=7.7 \times 10^7$

TIME (10 SEC/IN)

Figure 69

OUTPUT (50 mV/IN)

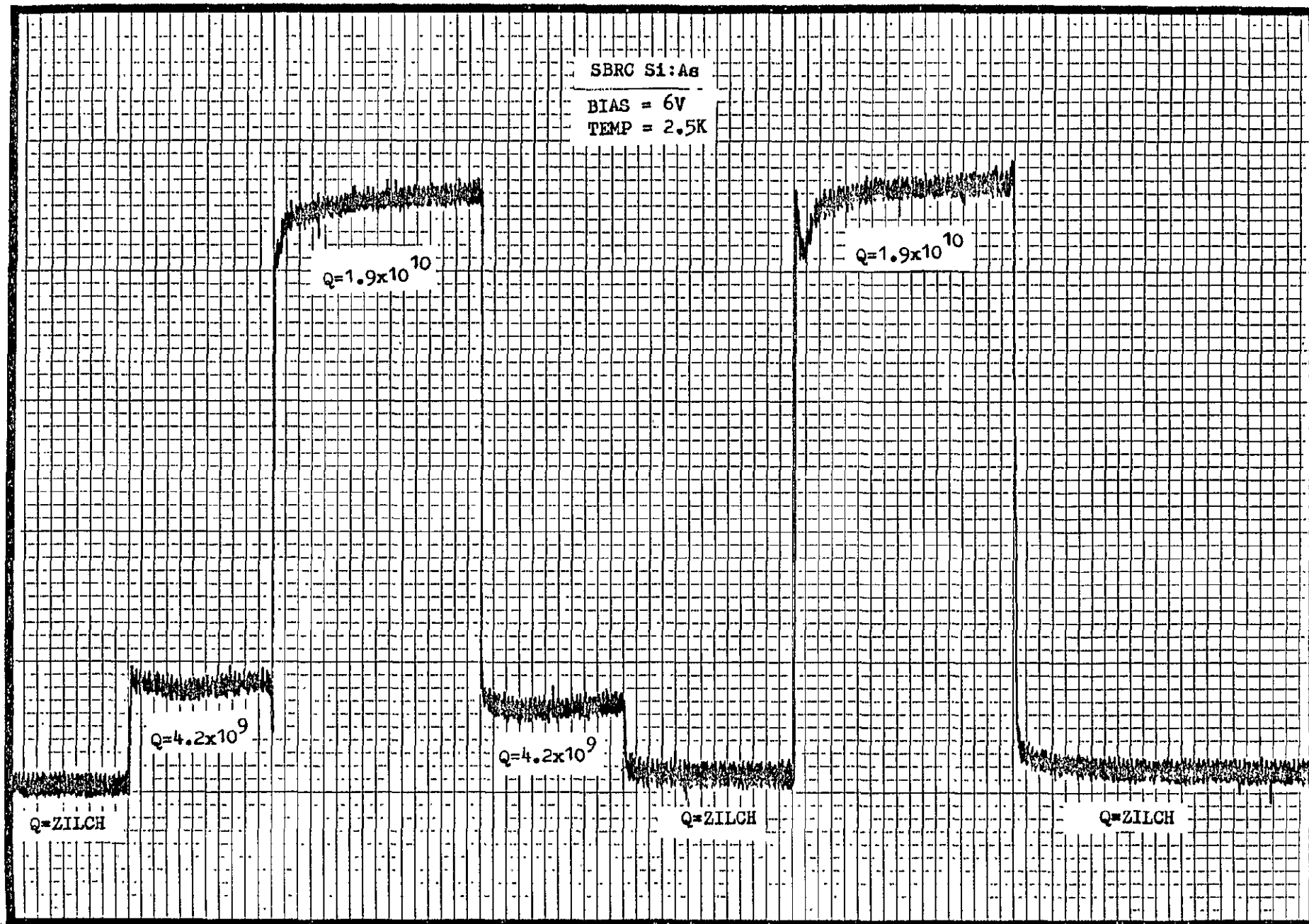


Figure 70

TIME (10 SEC/IN)

OUTPUT (20 mV/IN)

SBRC Si:As

BIAS = 6V

TEMP = 2.5K

$Q = 4.2 \times 10^9$

Q=ZILCH

Q=ZILCH

TIME (10 SEC/IN)

Figure 71

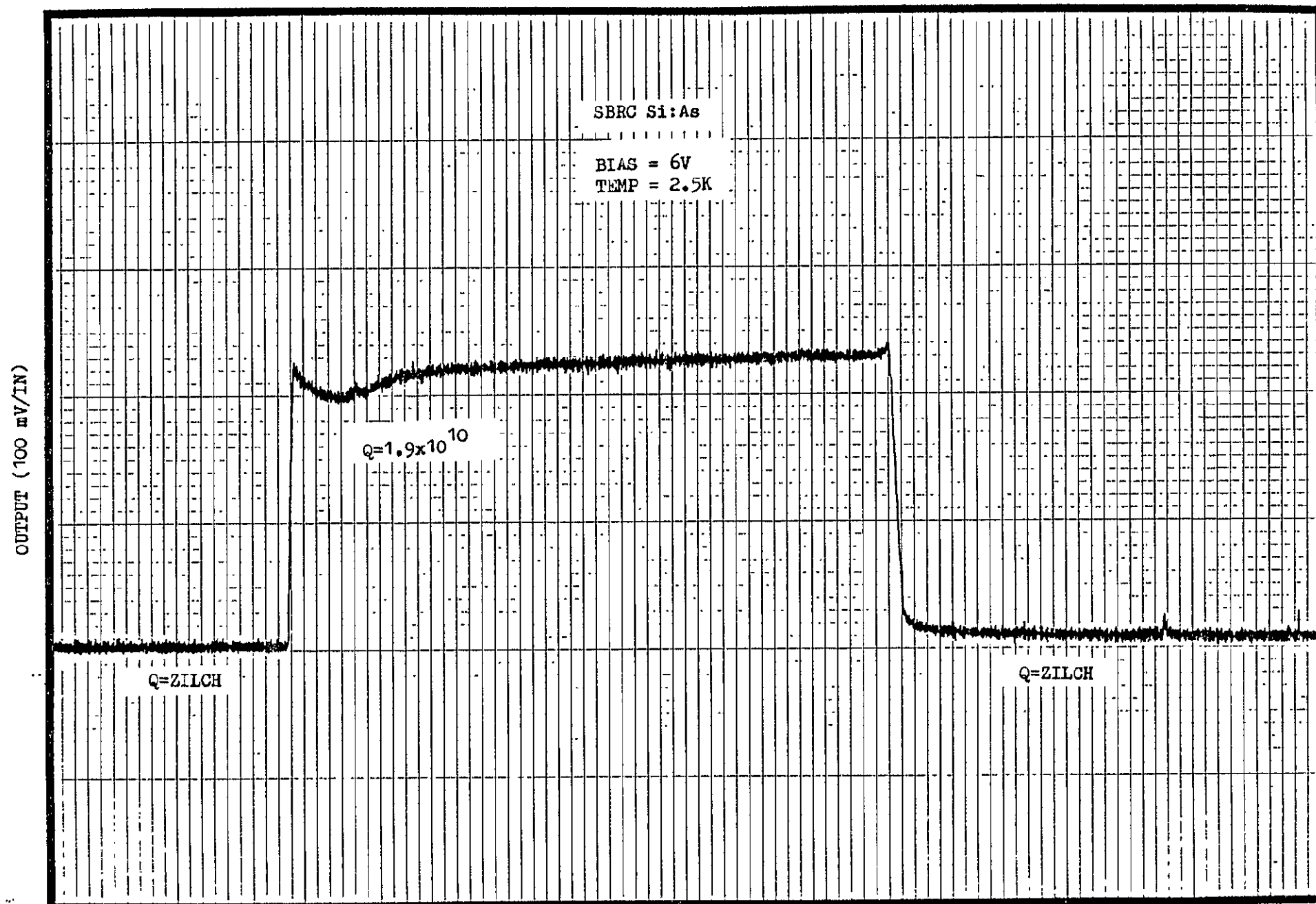


Figure 72

TIME (2 SEC/IN)

OUTPUT (50 mV/IN)

SBRC Si:As

BIAS = 6V

TEMP = 2.5K

$Q=1.9 \times 10^{10}$

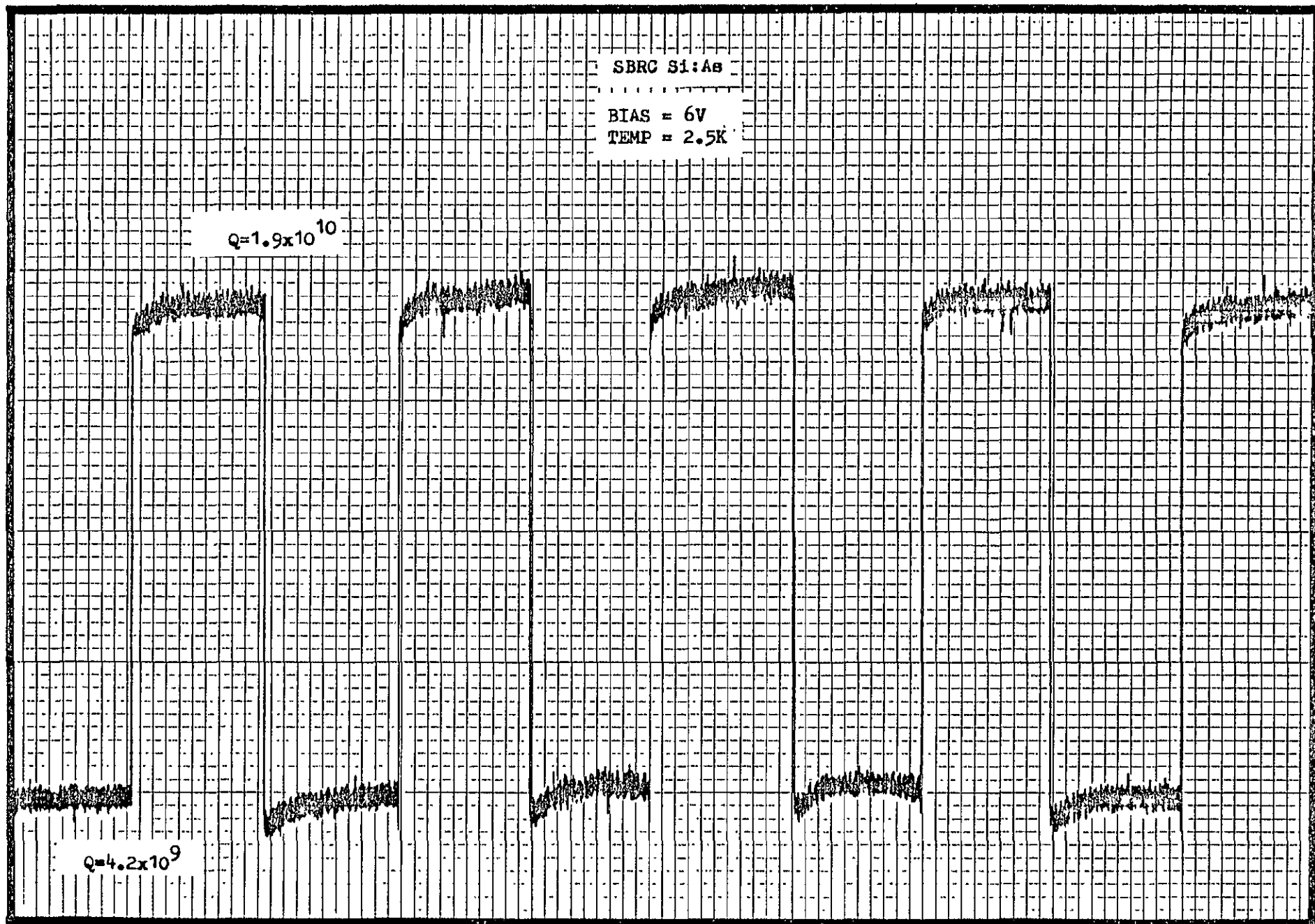
$Q=4.2 \times 10^9$

$Q=4.2 \times 10^9$

Figure 73

TIME (0.5 SEC/IN)

OUTPUT (50 mV/IN)



OUTPUT (100 mV/IN)

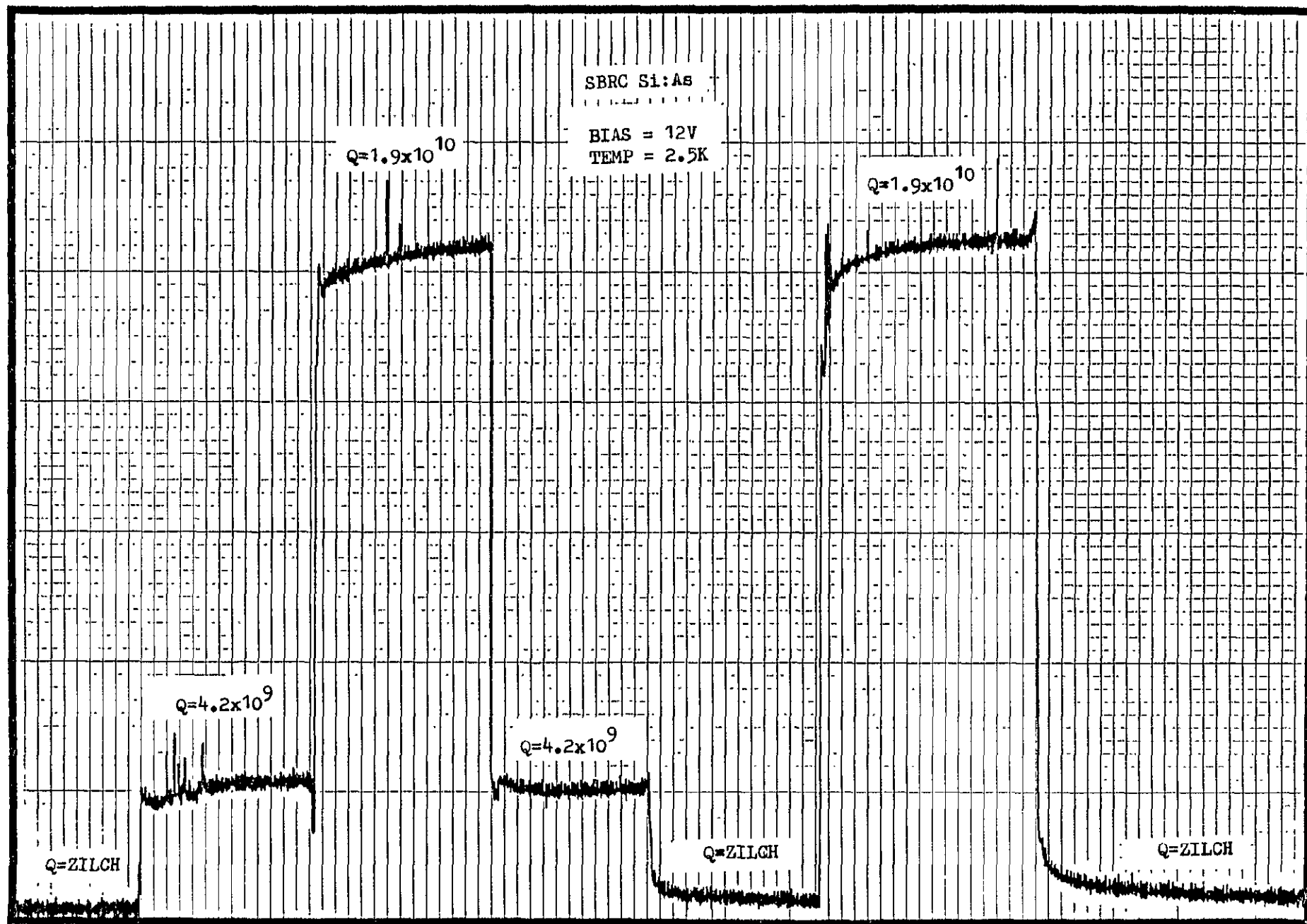


Figure 75

TIME (10 SEC/IN)



OUTPUT (50 mV/IN)

SBRC Si:As

BIAS = 12V

TEMP = 2.5K

$Q=4.2 \times 10^9$

Q-ZILCH

Q-ZILCH

Figure 76

TIME (10 SEC/IN)

4L

OUTPUT (100 mV/IN)

92

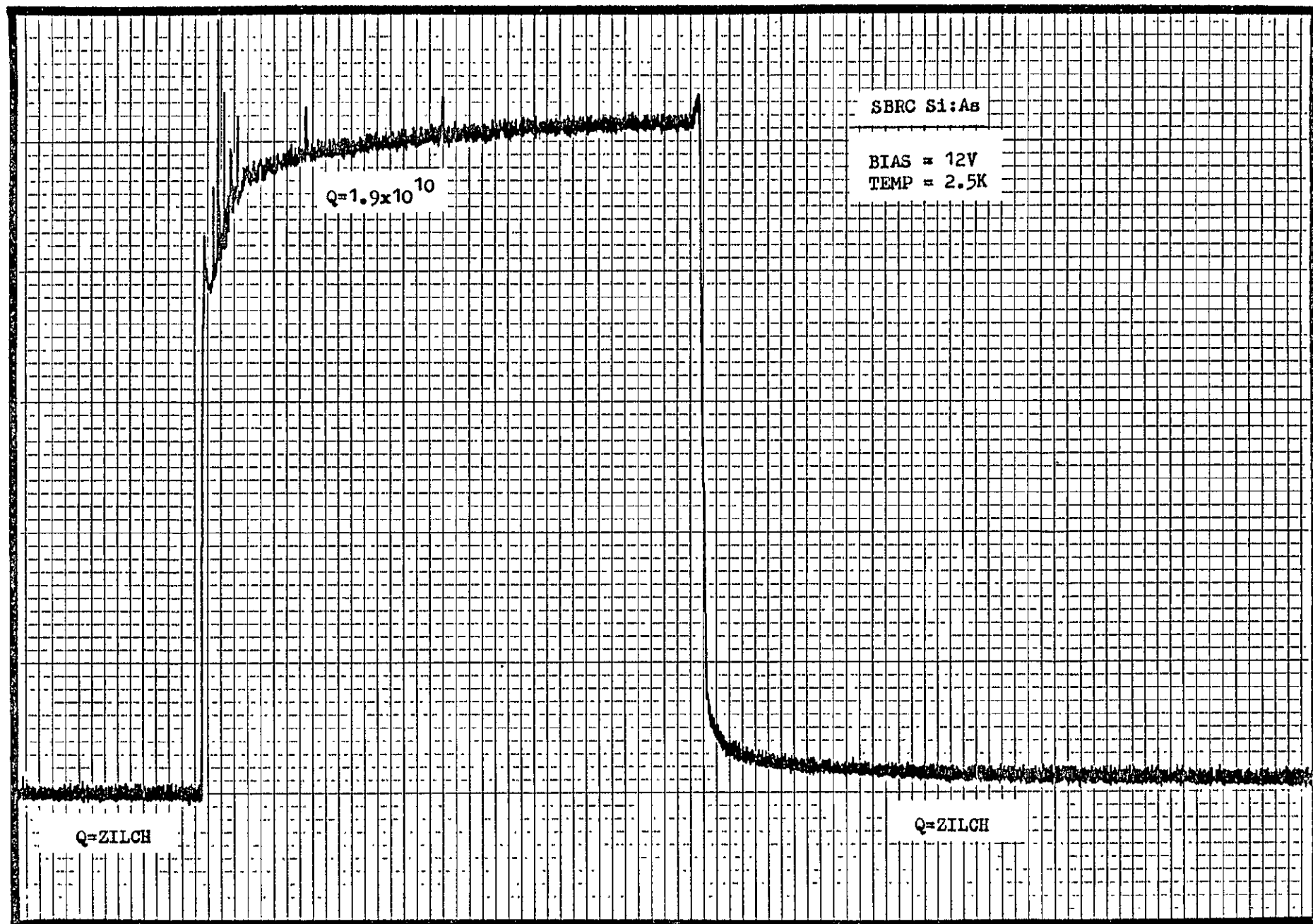
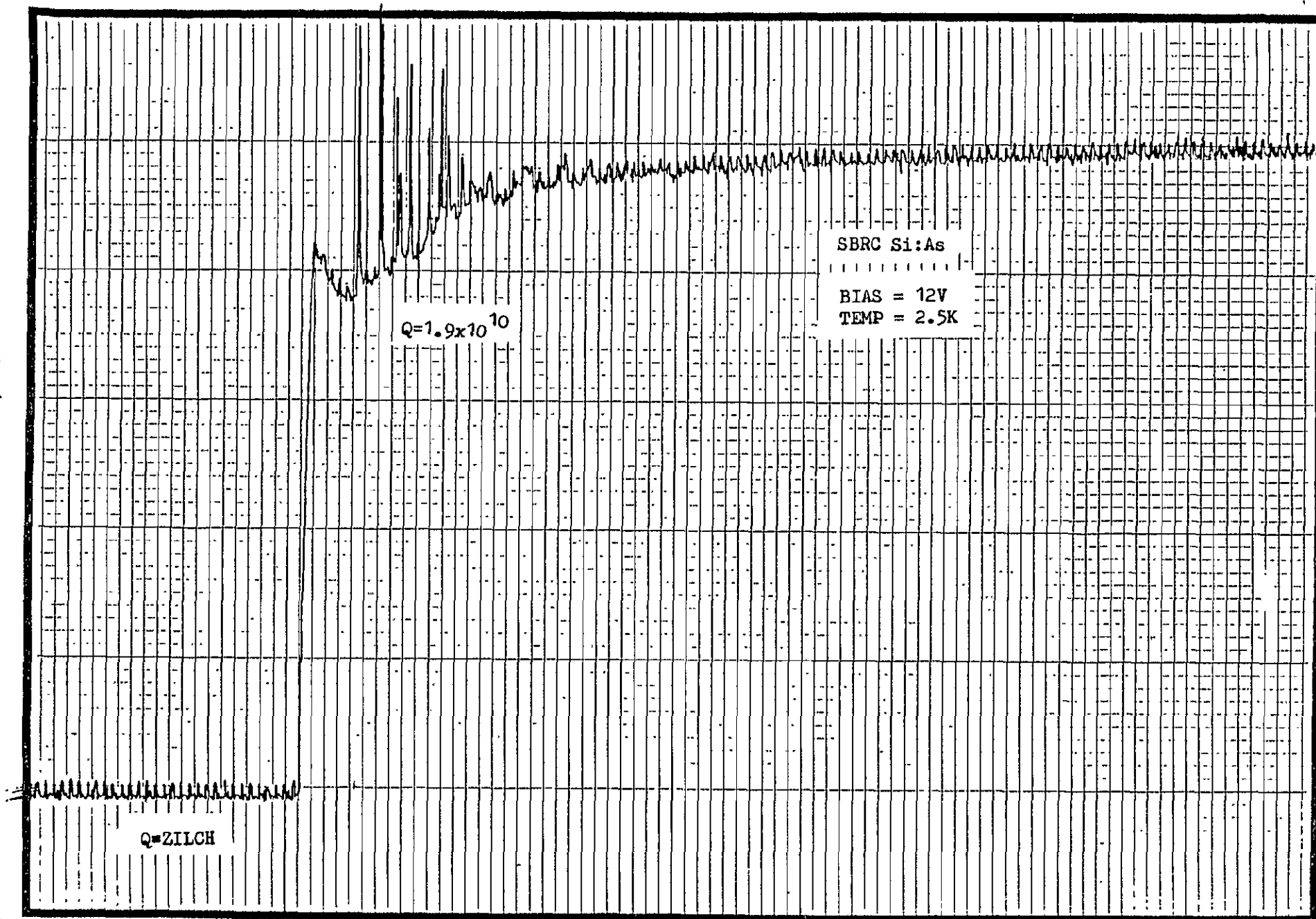


Figure 77

TIME (5 SEC/IN)

OUTPUT (100 mV/IN)



93

Figure 78

TIME (1.0 SEC/IN)

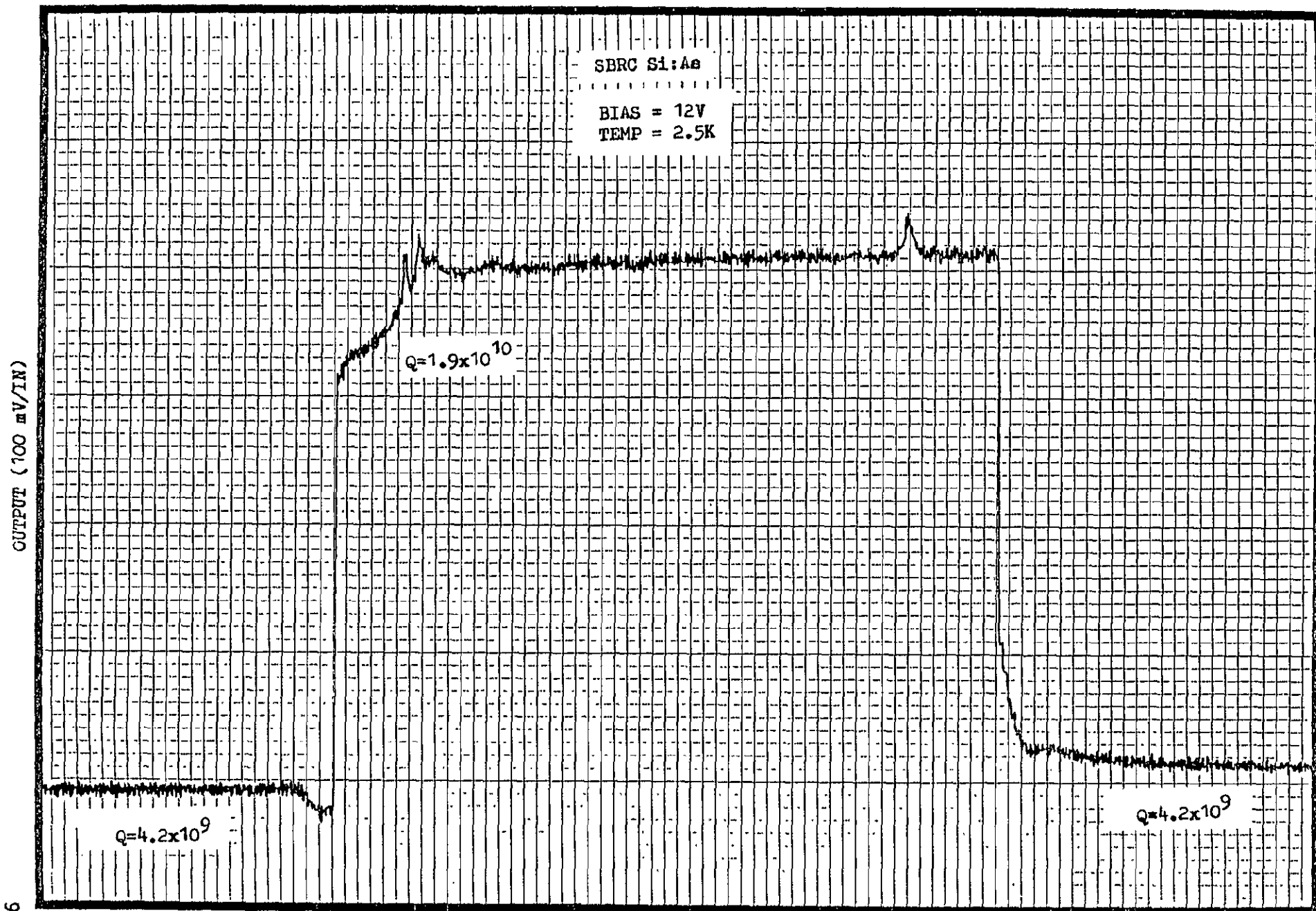


Figure 79

TIME (0.5 SEC/IN)

OUTPUT (100 mV/IN)

SBRC Si:As

BIAS = 12V

TEMP = 2.5K

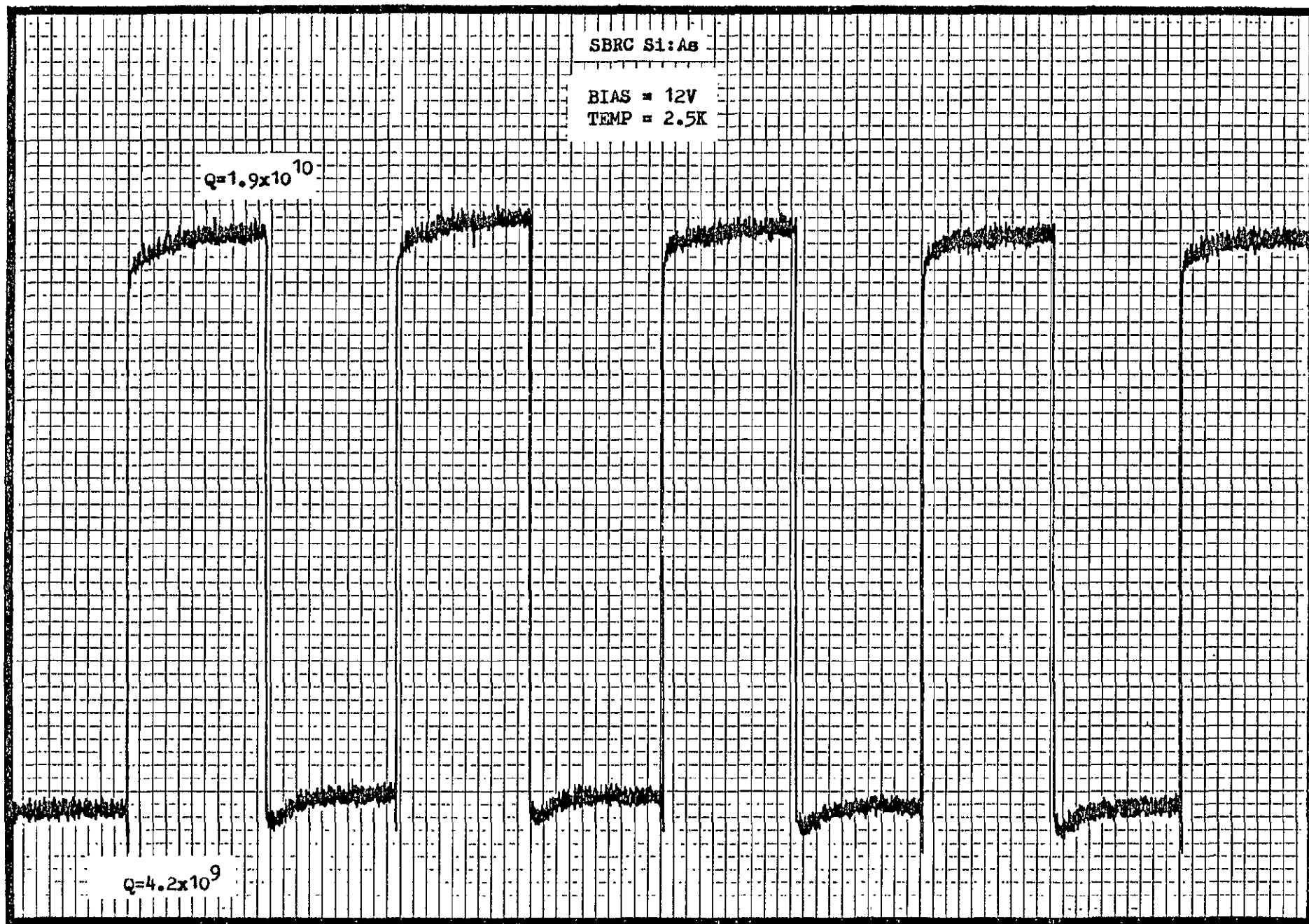
$Q=1.9 \times 10^{10}$

$Q=4.2 \times 10^9$

56

TIME (100 SEC/IN)

Figure 80



C-2

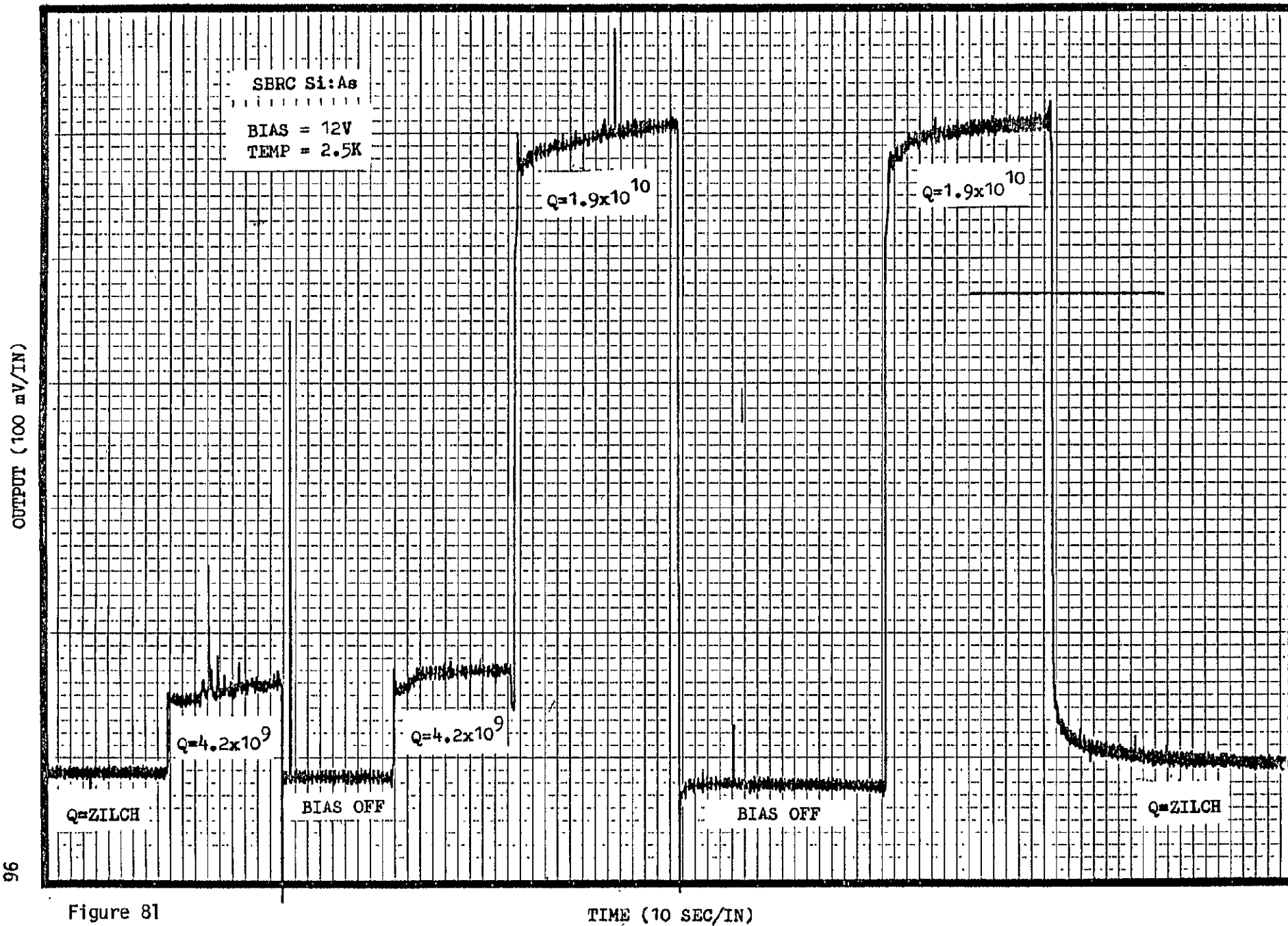


Figure 81

TIME (10 SEC/IN)

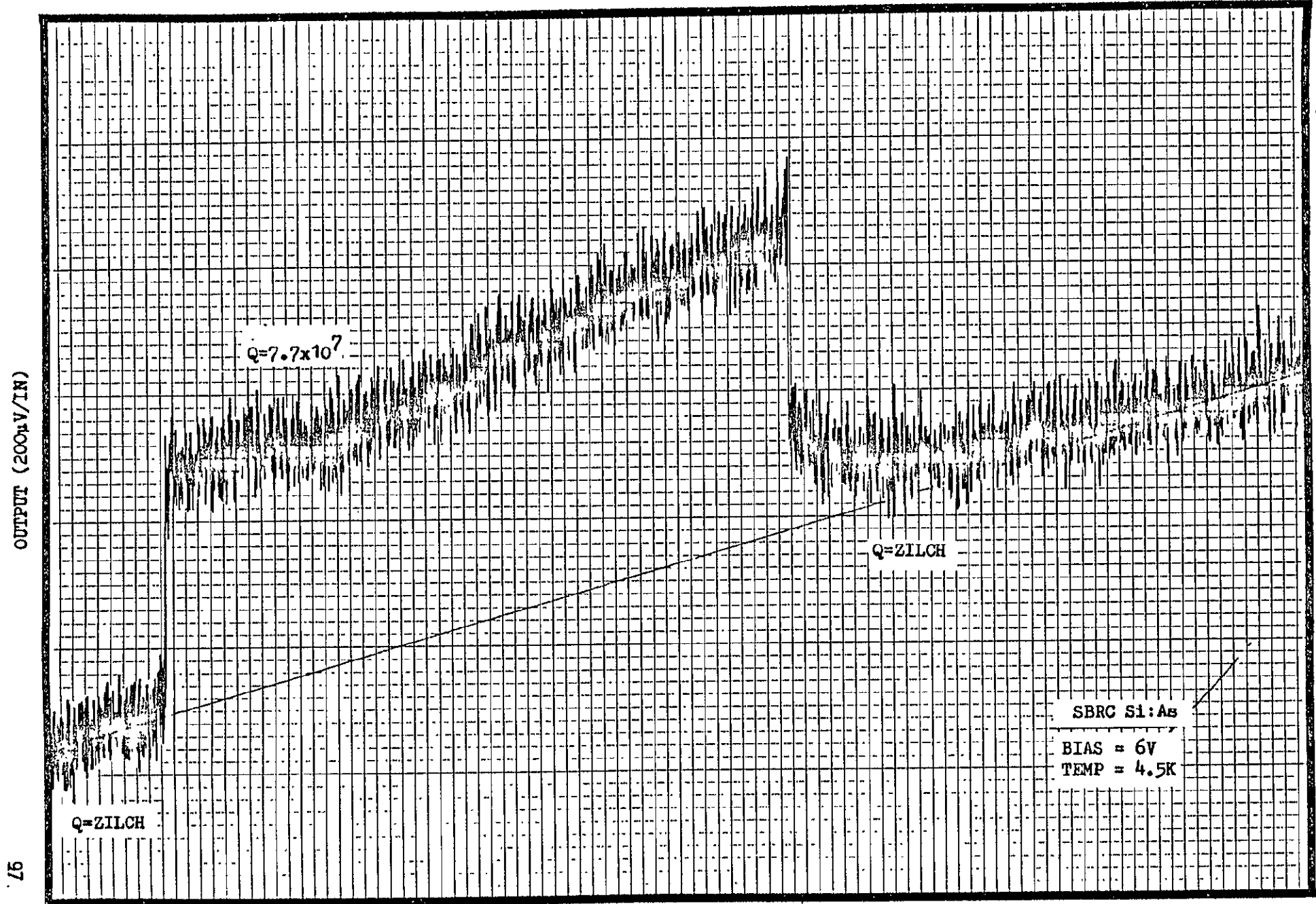
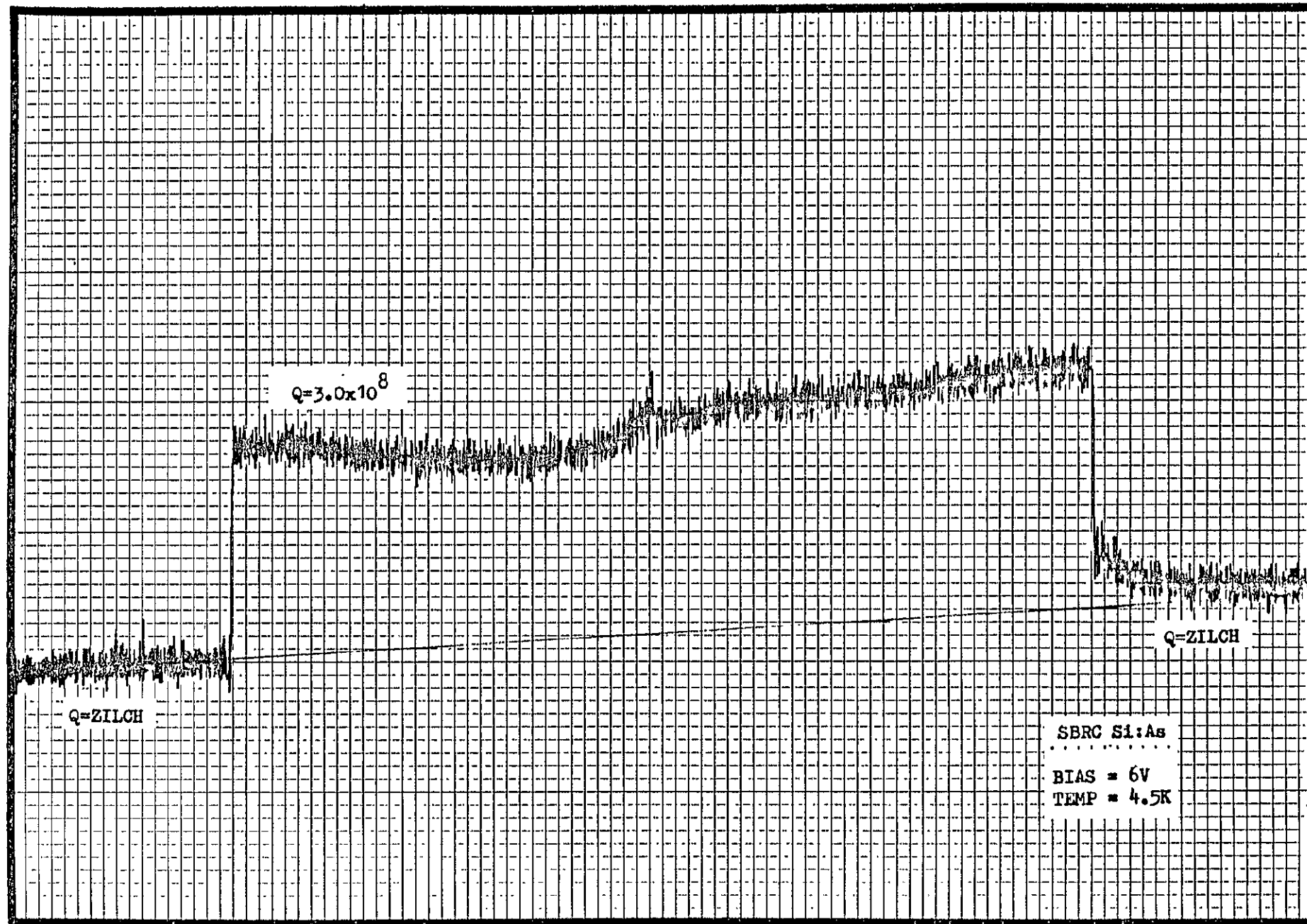


Figure 82

TIME (50 SEC/IN)

OUTPUT (500μV/IN)



86

Figure 83

TIME (20 SEC/IN)



OUTPUT (200mV/IN)

66

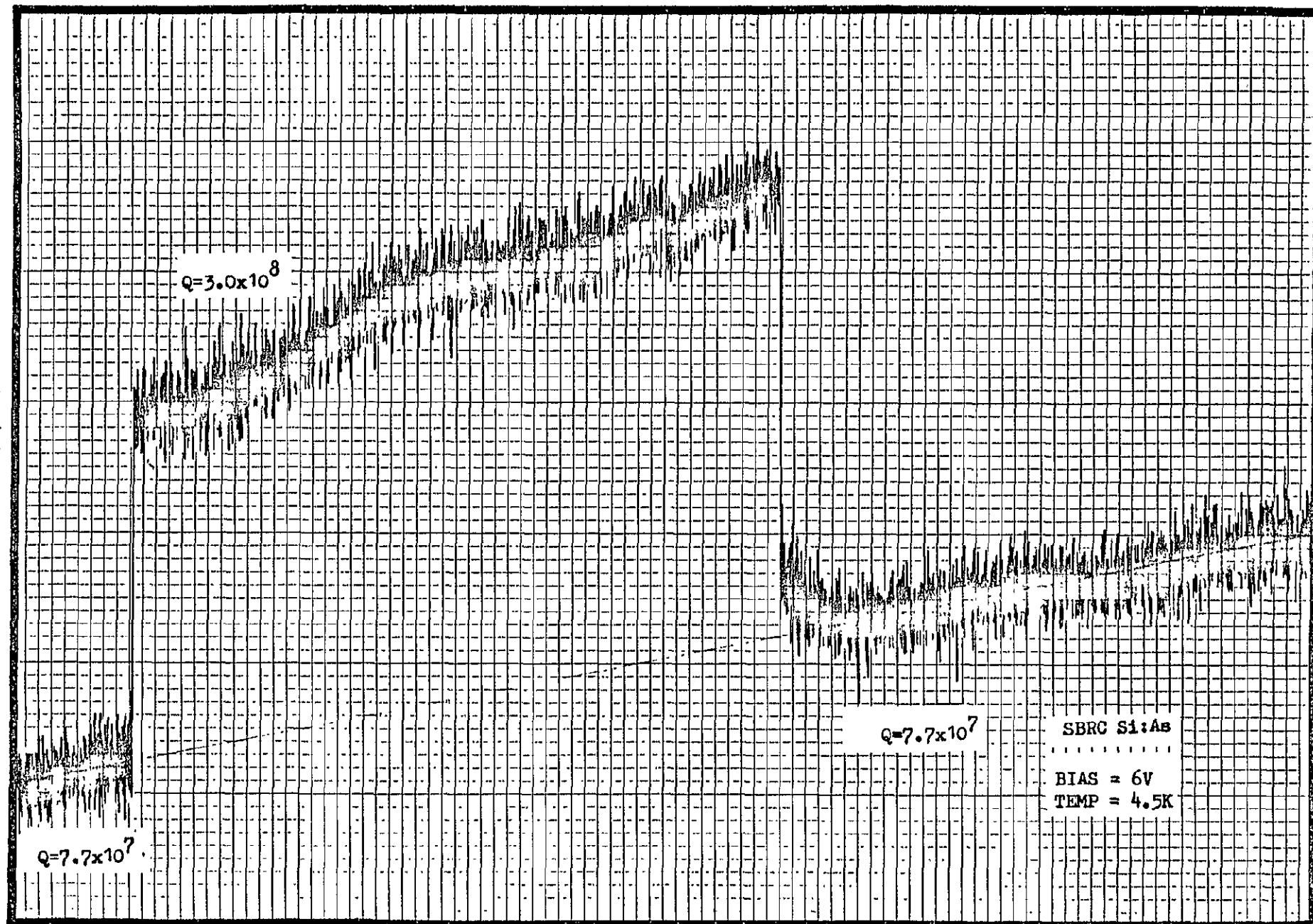


Figure 84

TIME (20 SEC/IN)

OUTPUT ( 1 mV/IN )

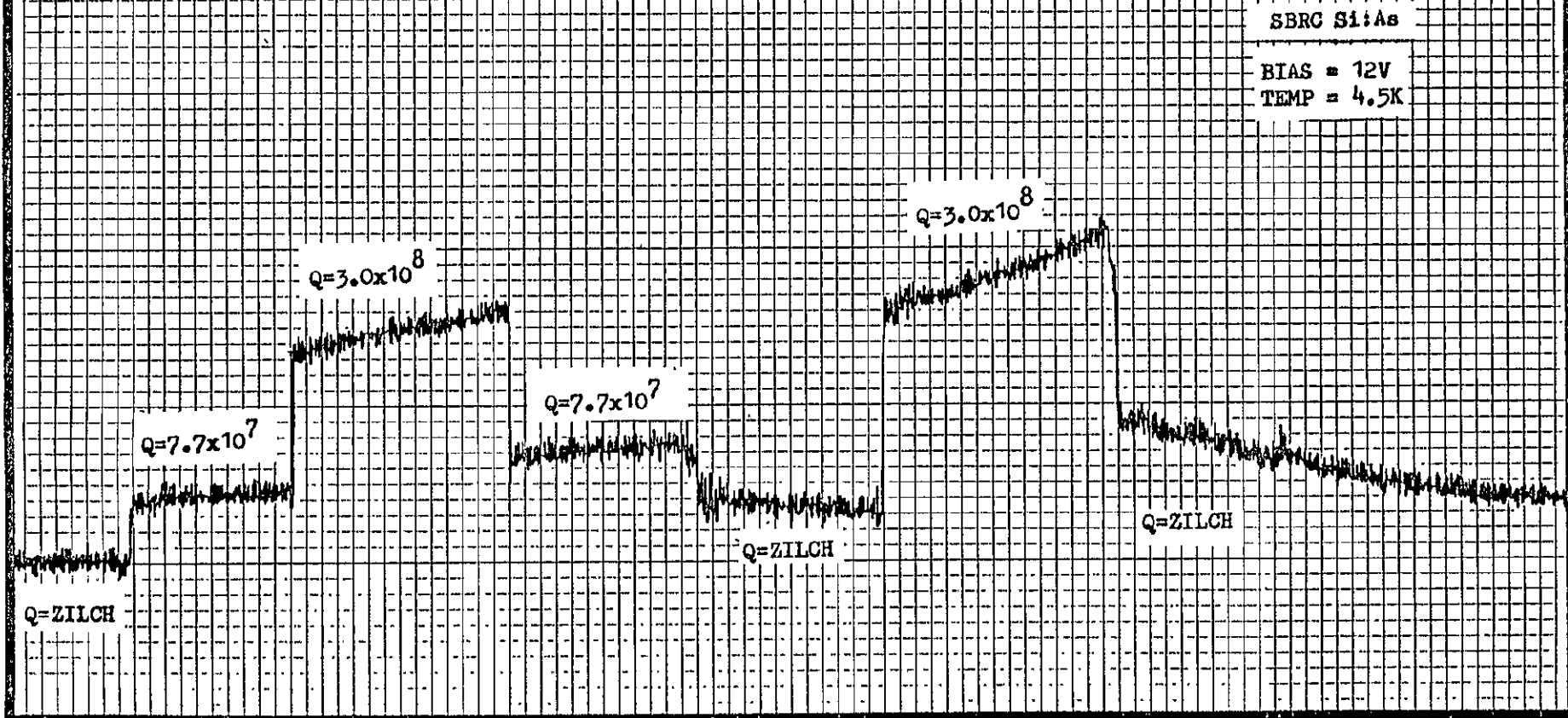


Figure 85

TIME (10 SEC/IN)

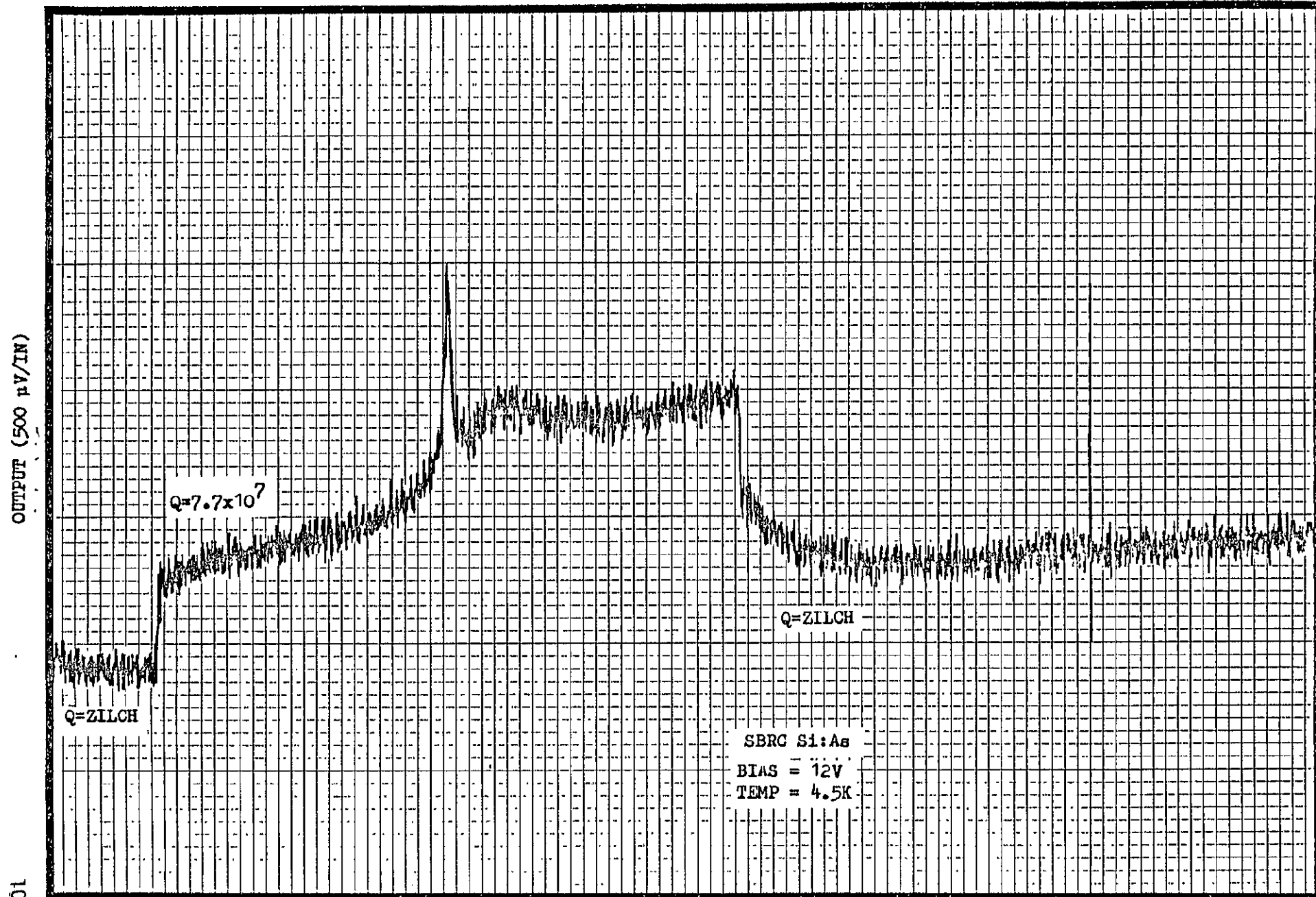


Figure 86

TIME (50 SEC/IN)

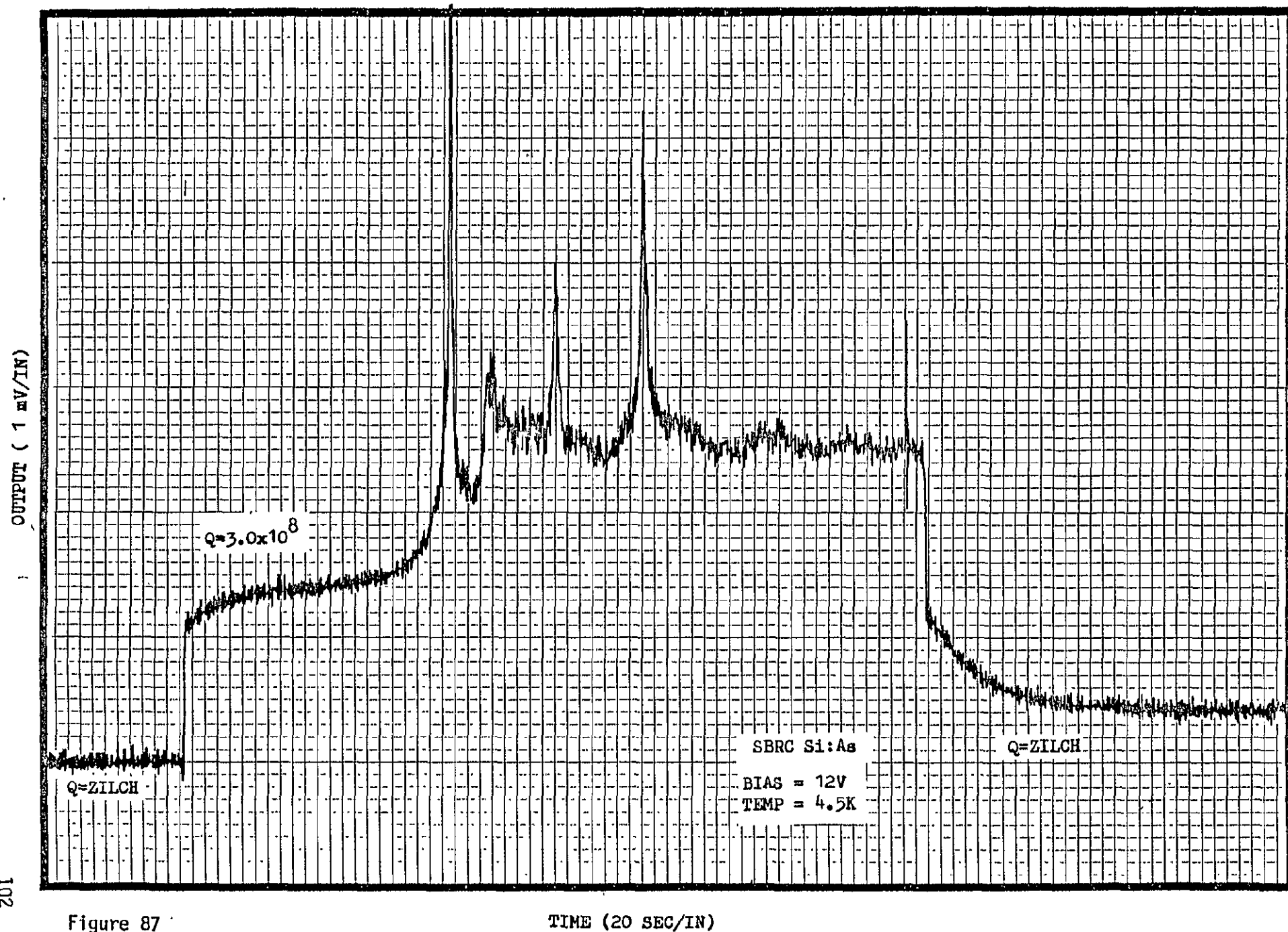


Figure 87

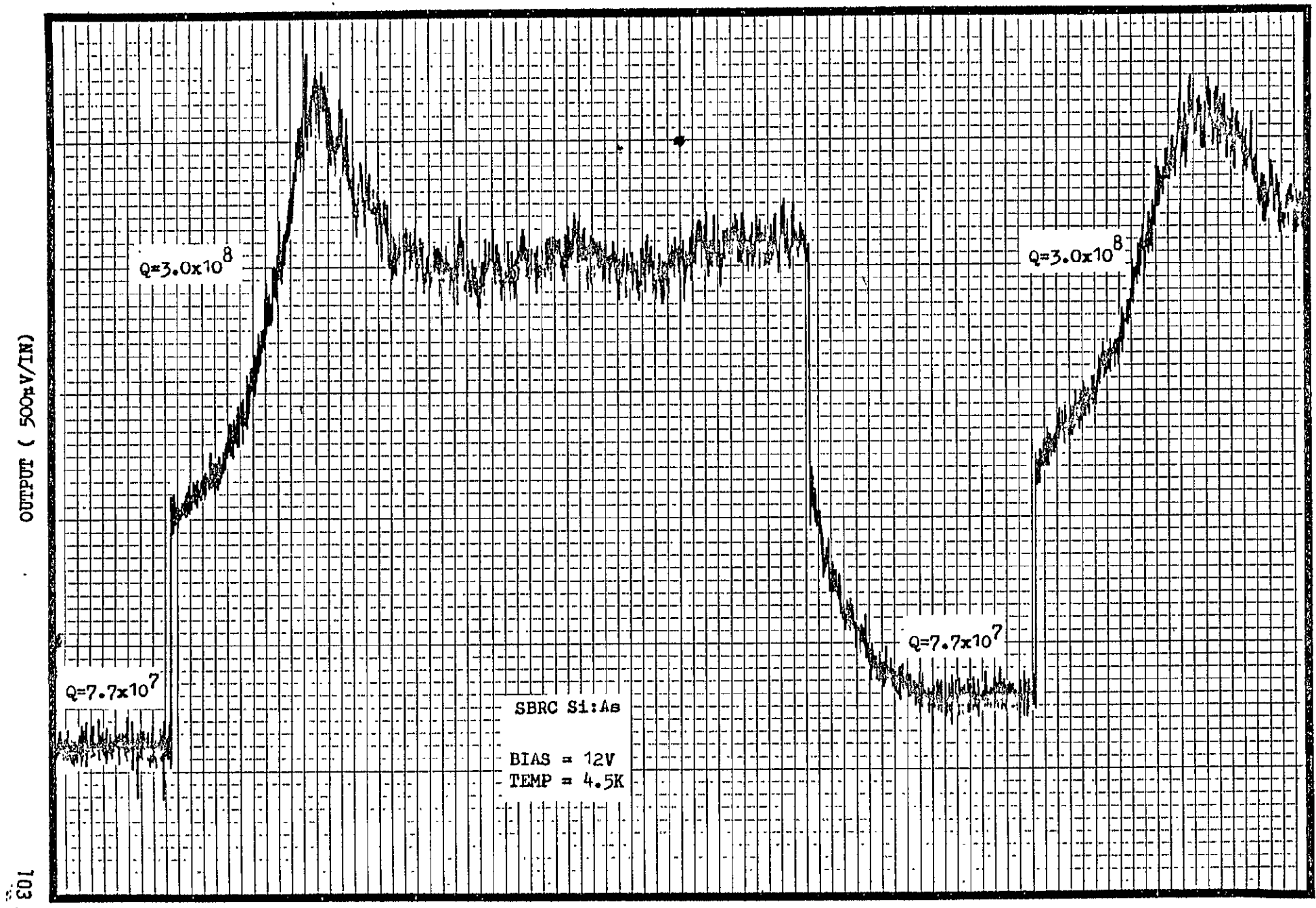


Figure 88

TIME (20 SEC/IN)

OUTPUT (20 mV/IN)

SBRC S1:As

BIAS = 6V

TEMP = 4.5K

$Q=1.9 \times 10^{10}$

$Q=1.9 \times 10^{10}$

$Q=4.2 \times 10^9$

$Q=4.2 \times 10^9$

Q-ZILCH

Q-ZILCH

Q-ZILCH

Figure 89.

TIME (10 SEC/IN)

OUTPUT (10 mV/IN)

SBRC Si:As

BIAS = 6V  
TEMP = 4.5K

$Q = 4.2 \times 10^9$

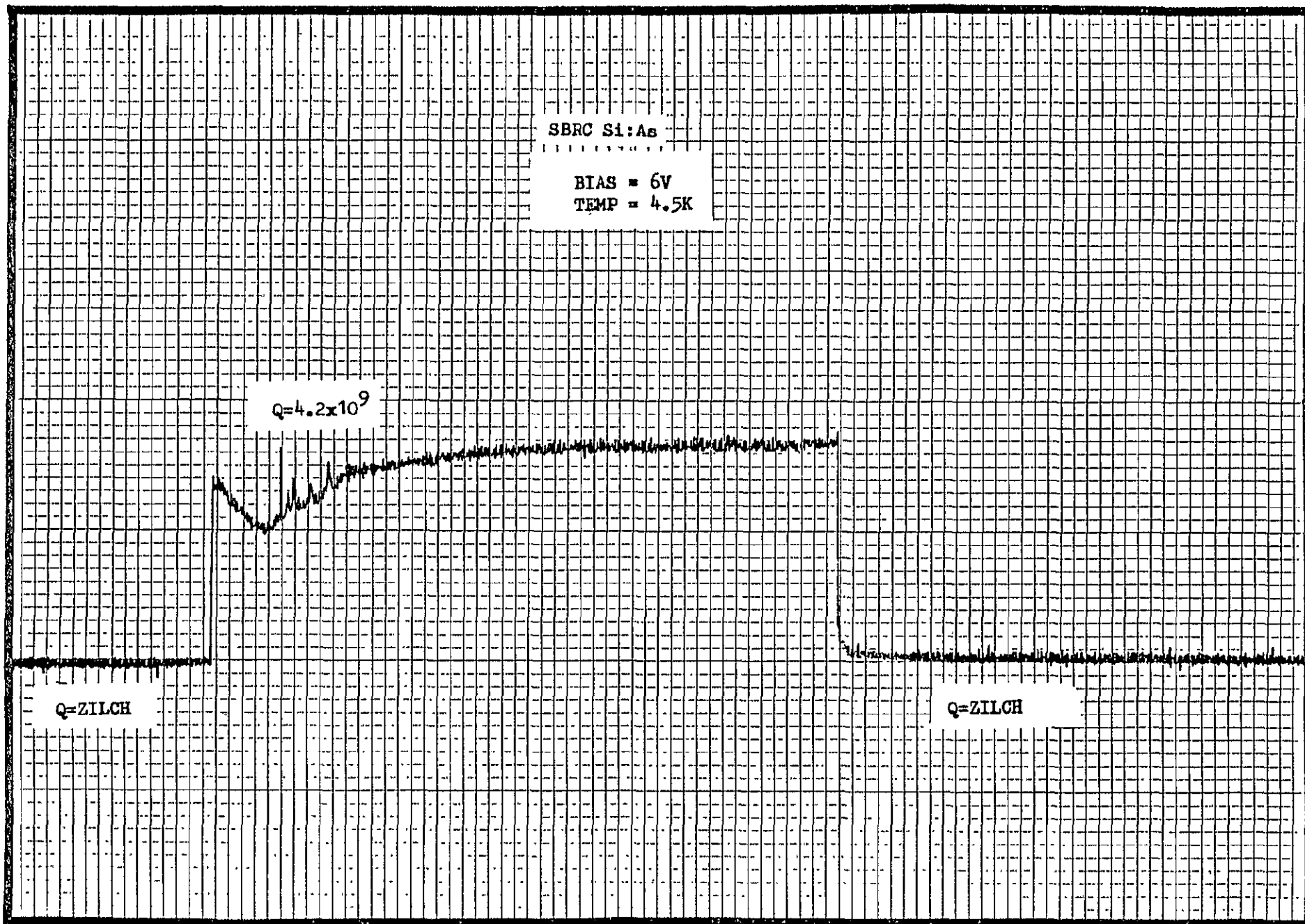
Q-ZILCH

Q-ZILCH

105

Figure 90

TIME (10 SEC/IN)



OUTPUT (20 mV/IN)

SBRC S1:As

BIAS = 6V  
TEMP = 4.5K

$Q=1.9 \times 10^{10}$

Q=ZILCH

Q=ZILCH

TIME (10 SEC/IN)

Figure 91



OUTPUT (20 mV/IN)

SBRC Si:As

BIAS = 6V

TEMP = 4.5K

$Q=1.9 \times 10^{10}$

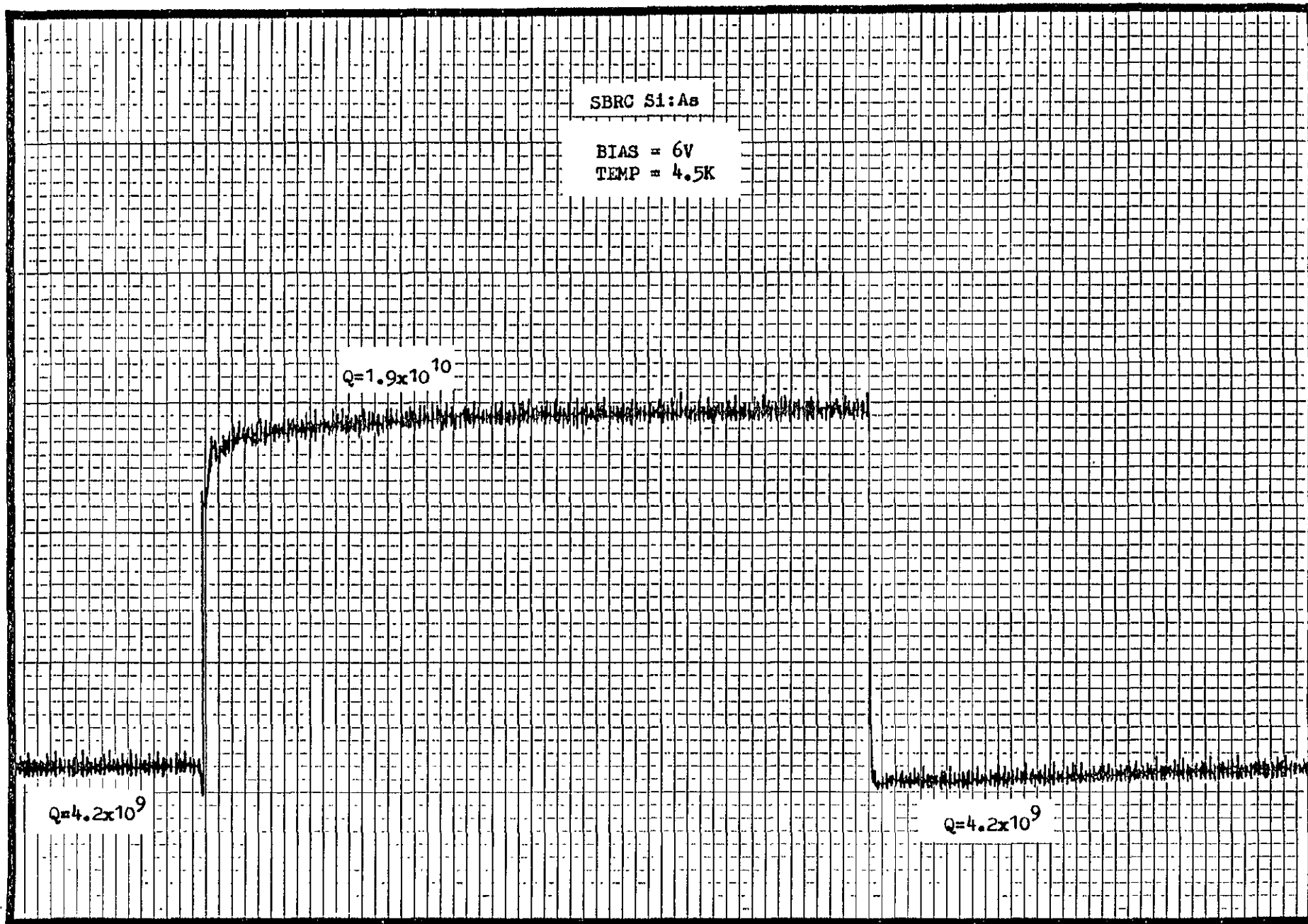
$Q=4.2 \times 10^9$

$Q=4.2 \times 10^9$

107

Figure 92

TIME (10 SEC/IN)



OUTPUT (20 mV/IN)

SBRC S1:AS

BIAS = 6V

TEMP = 4.5K

$Q=1.9 \times 10^{10}$

$Q=4.2 \times 10^9$

$Q=4.2 \times 10^9$

TIME (0.5 SEC/IN)

Figure 93

OUTPUT (20 mV/IN)

109

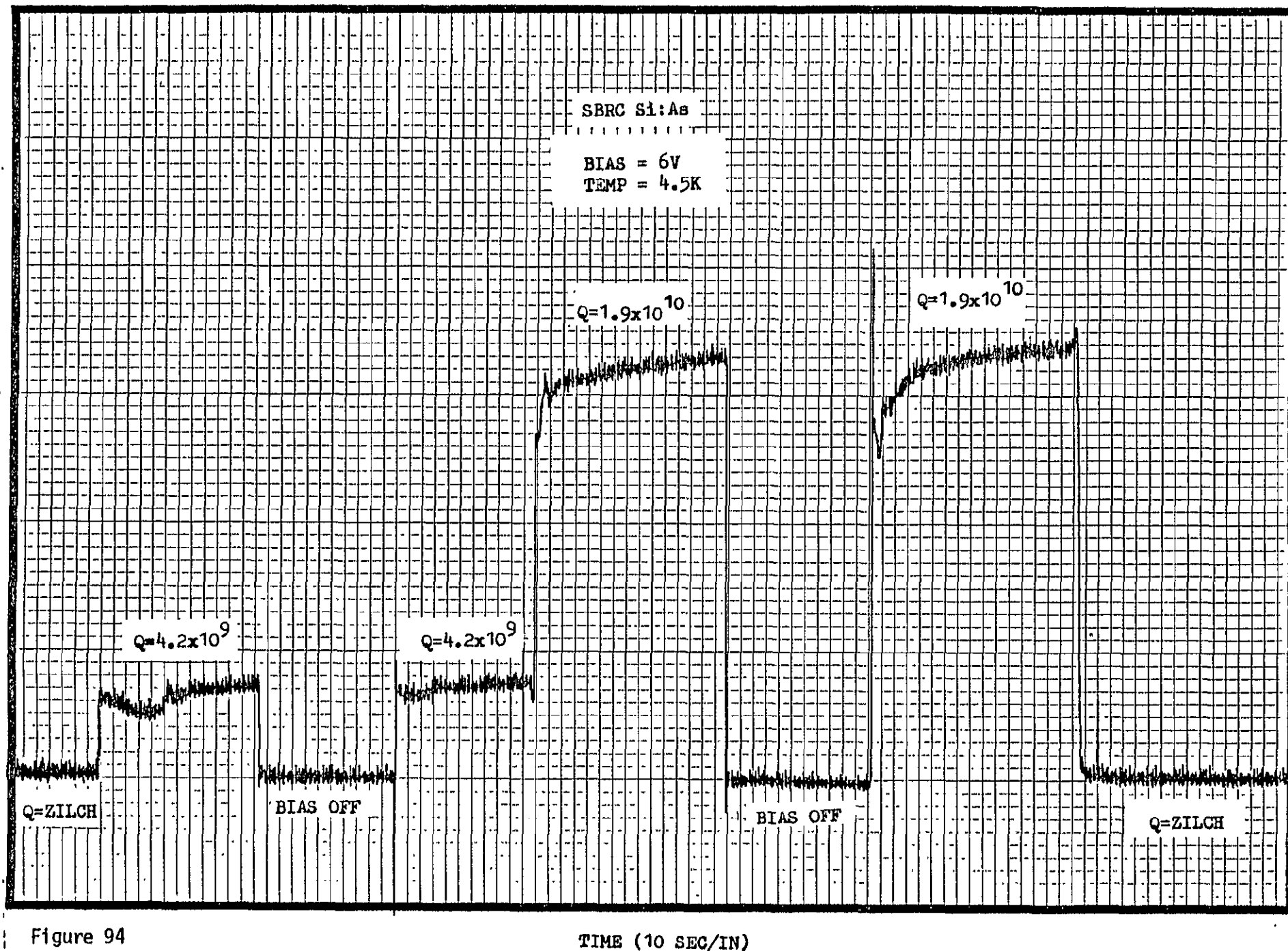


Figure 94

TIME (10 SEC/IN)

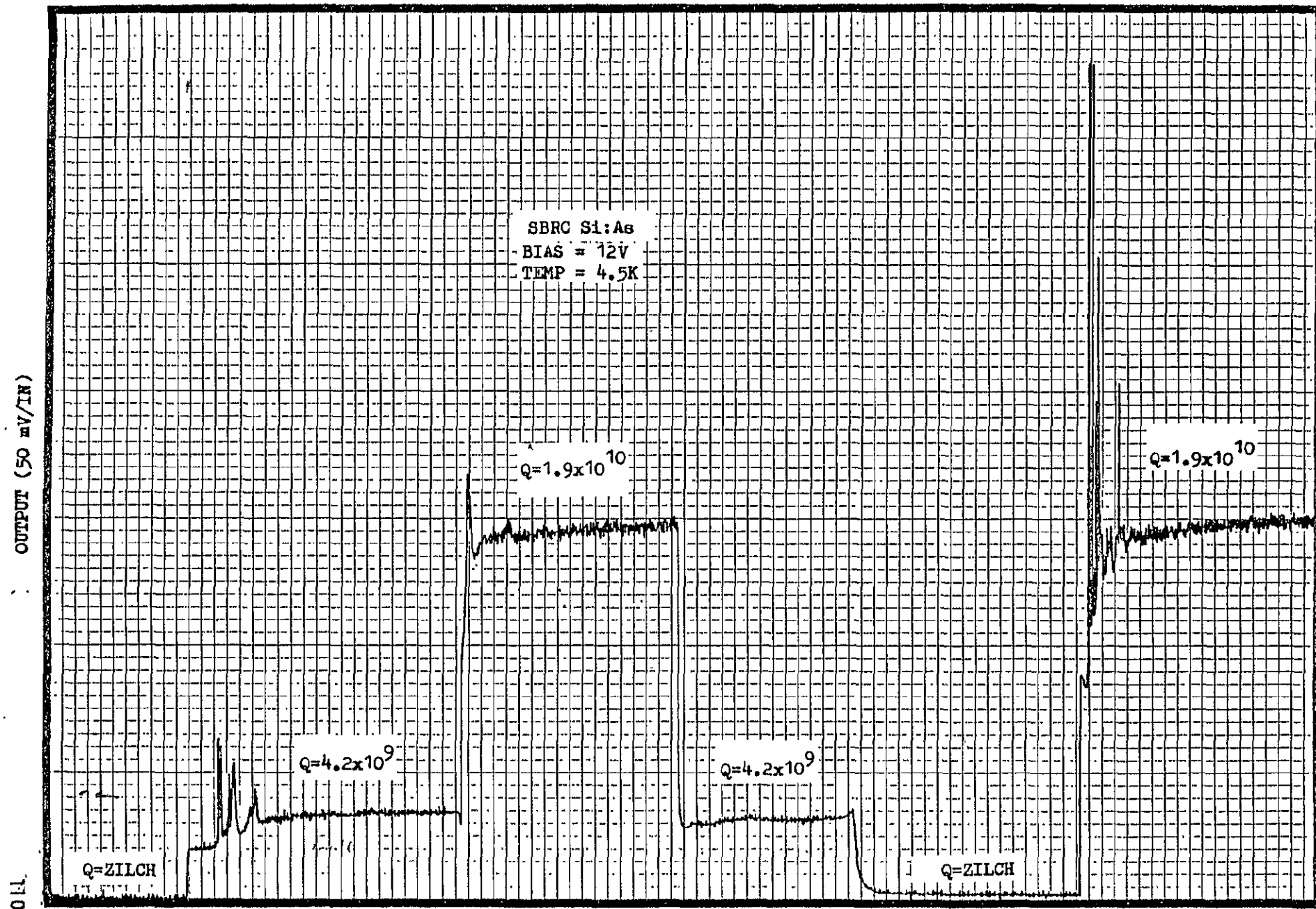


Figure 95

TIME (10 SEC/IN)

OUTPUT (100mV/IN)

SBRC Si:As

BIAS = 12V

TEMP = 4.5K

$Q=1.9 \times 10^{10}$

Q=ZILCH

TIME (2 SEC/IN)

Figure 96

OUTPUT (50 mV/IN)

112

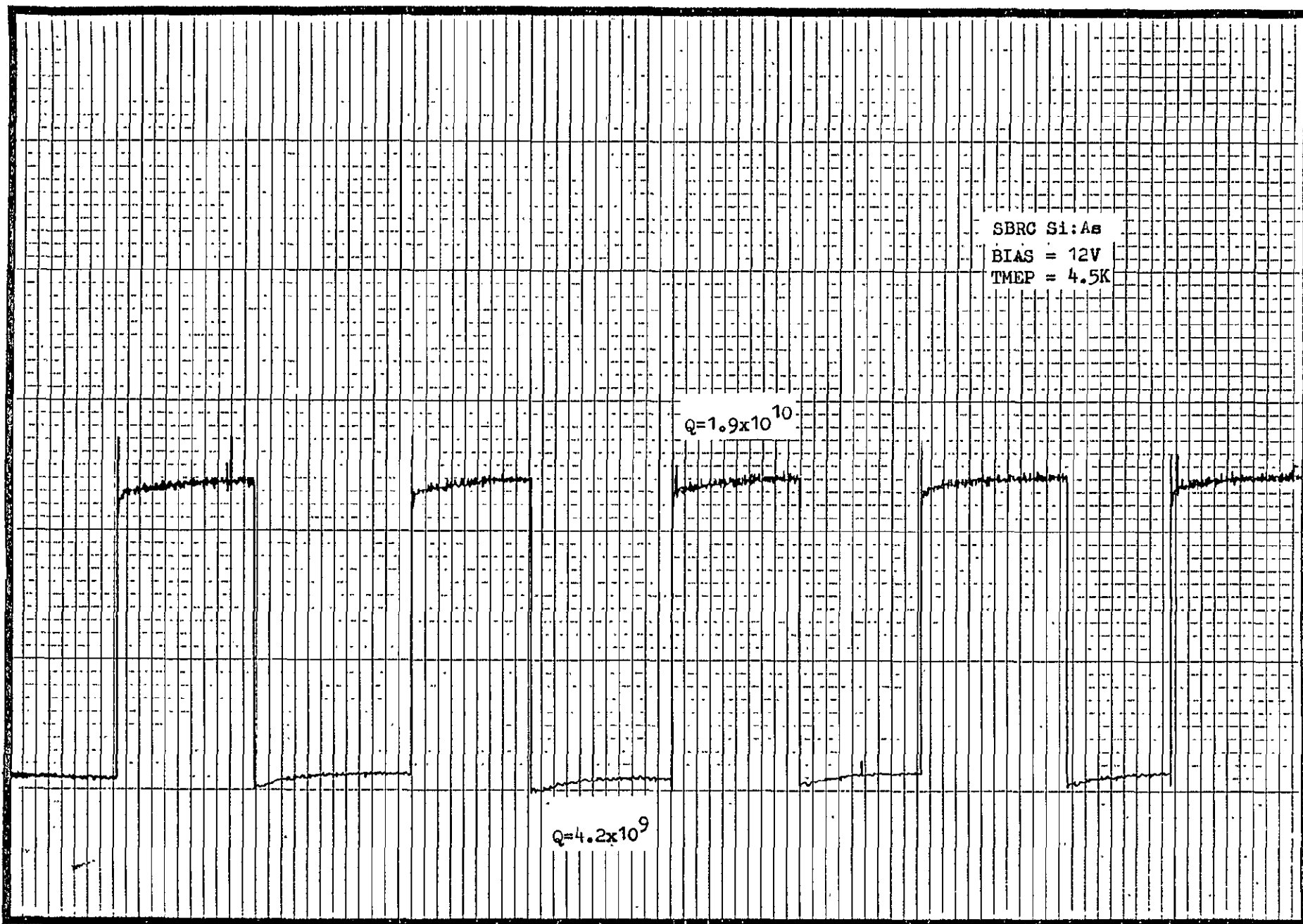
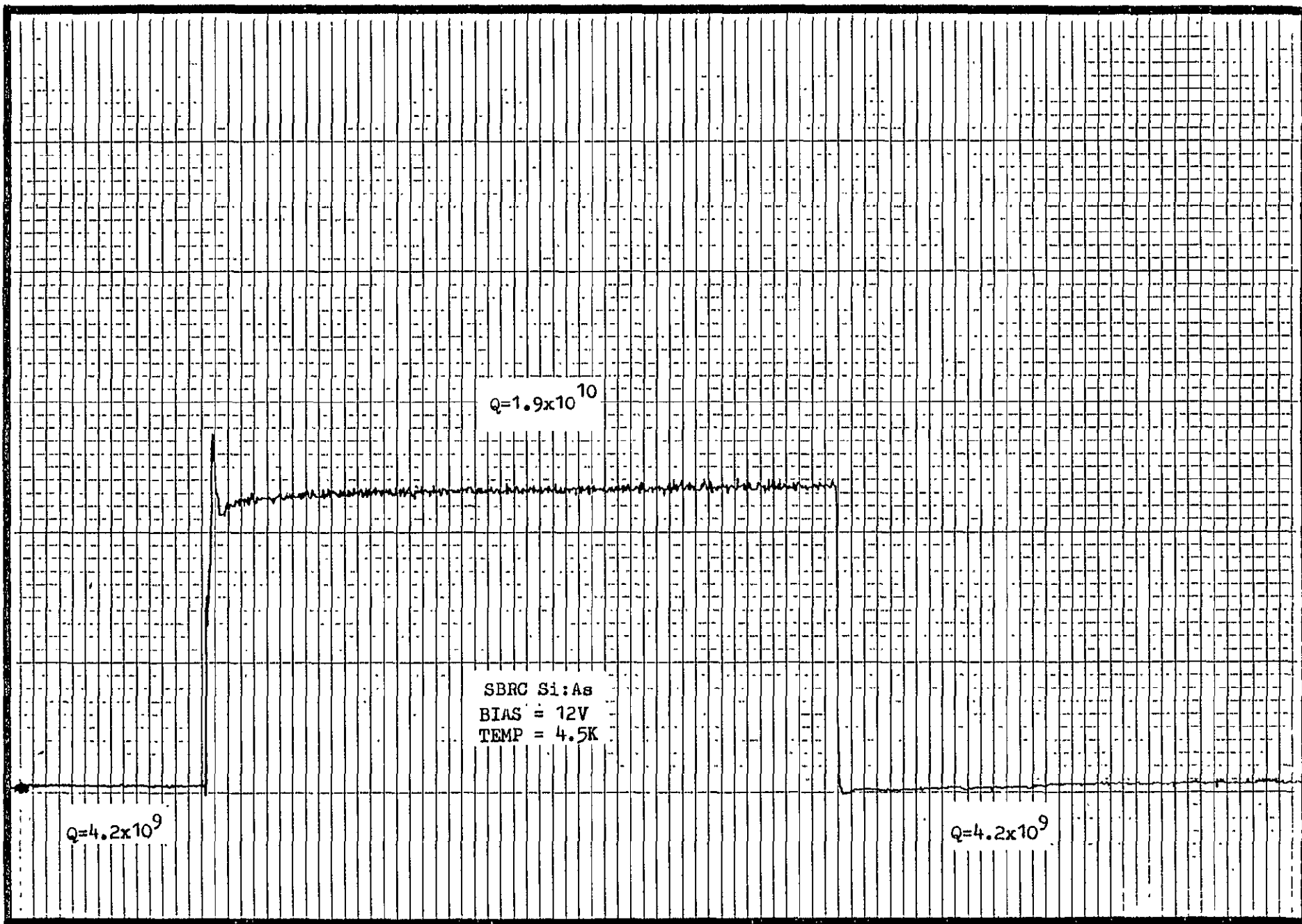


Figure 97

TIME (100 SEC/IN)

OUTPUT (50 mV/IN)



113

Figure 98

TIME (10/SEC/IN)

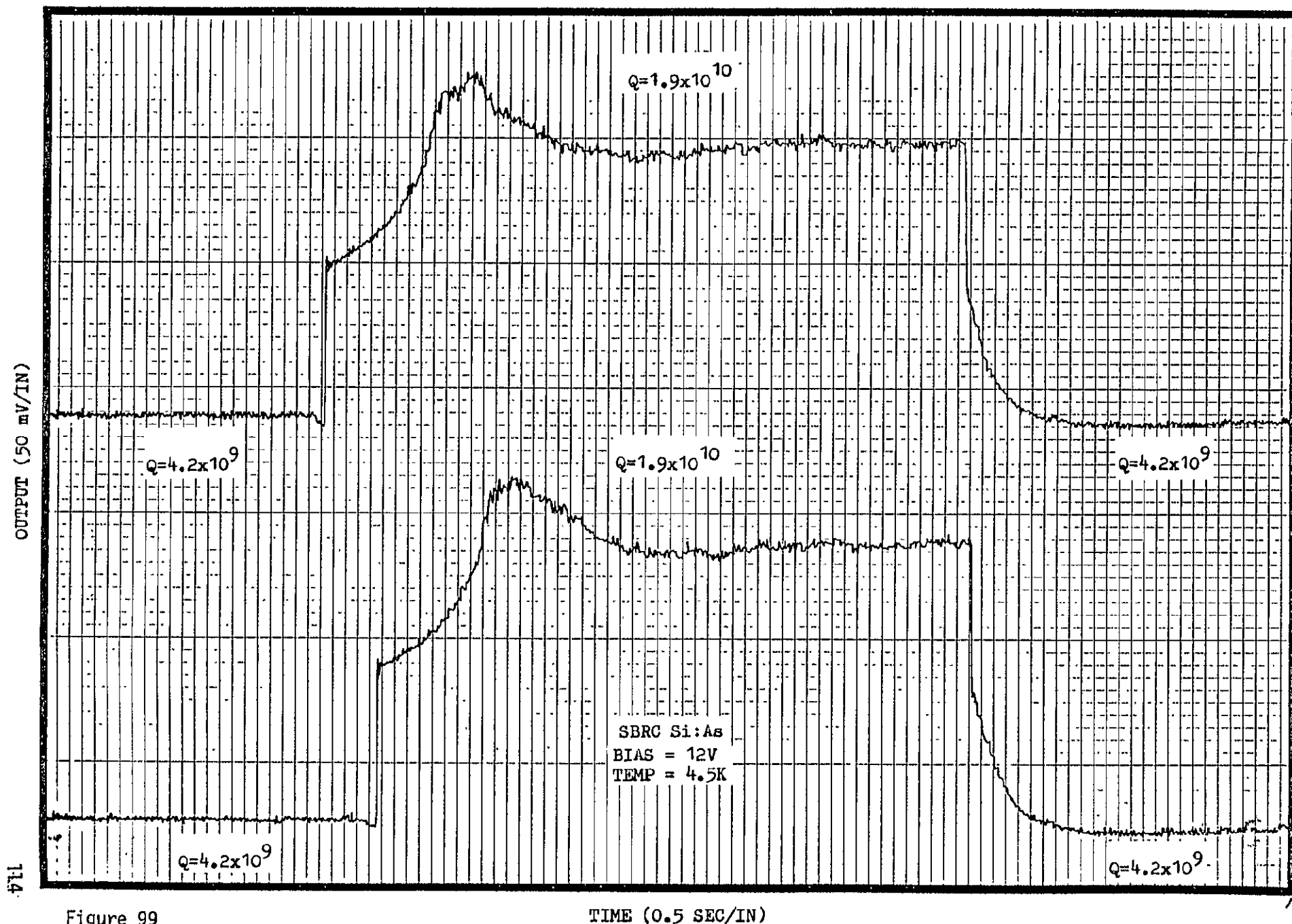


Figure 99

TIME (0.5 SEC/IN)



OUTPUT (50 mV/IN)

SBRC Si:As

BIAS = 12V

TEMP = 4.5K

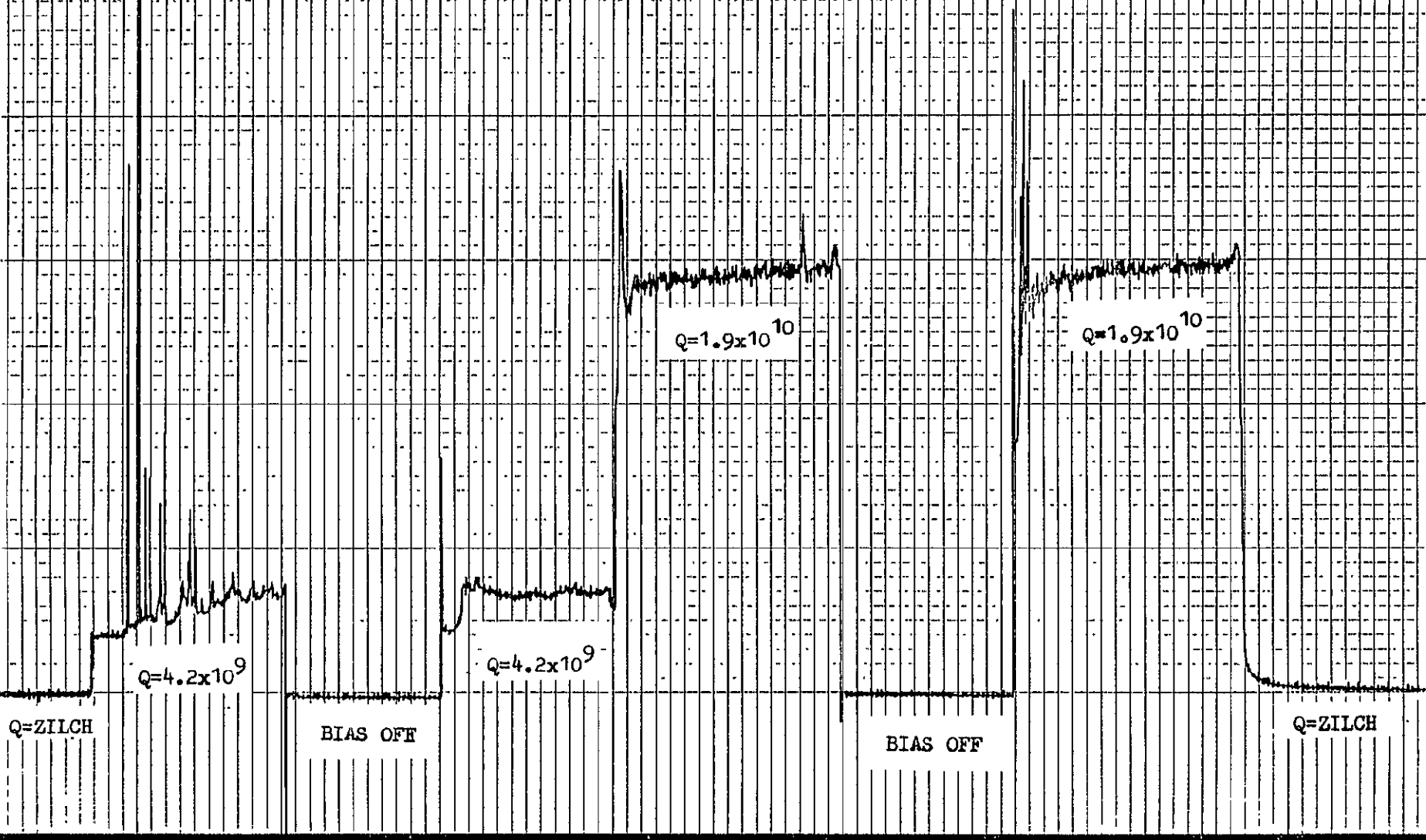


Figure 100

TIME (10 SEC/IN)

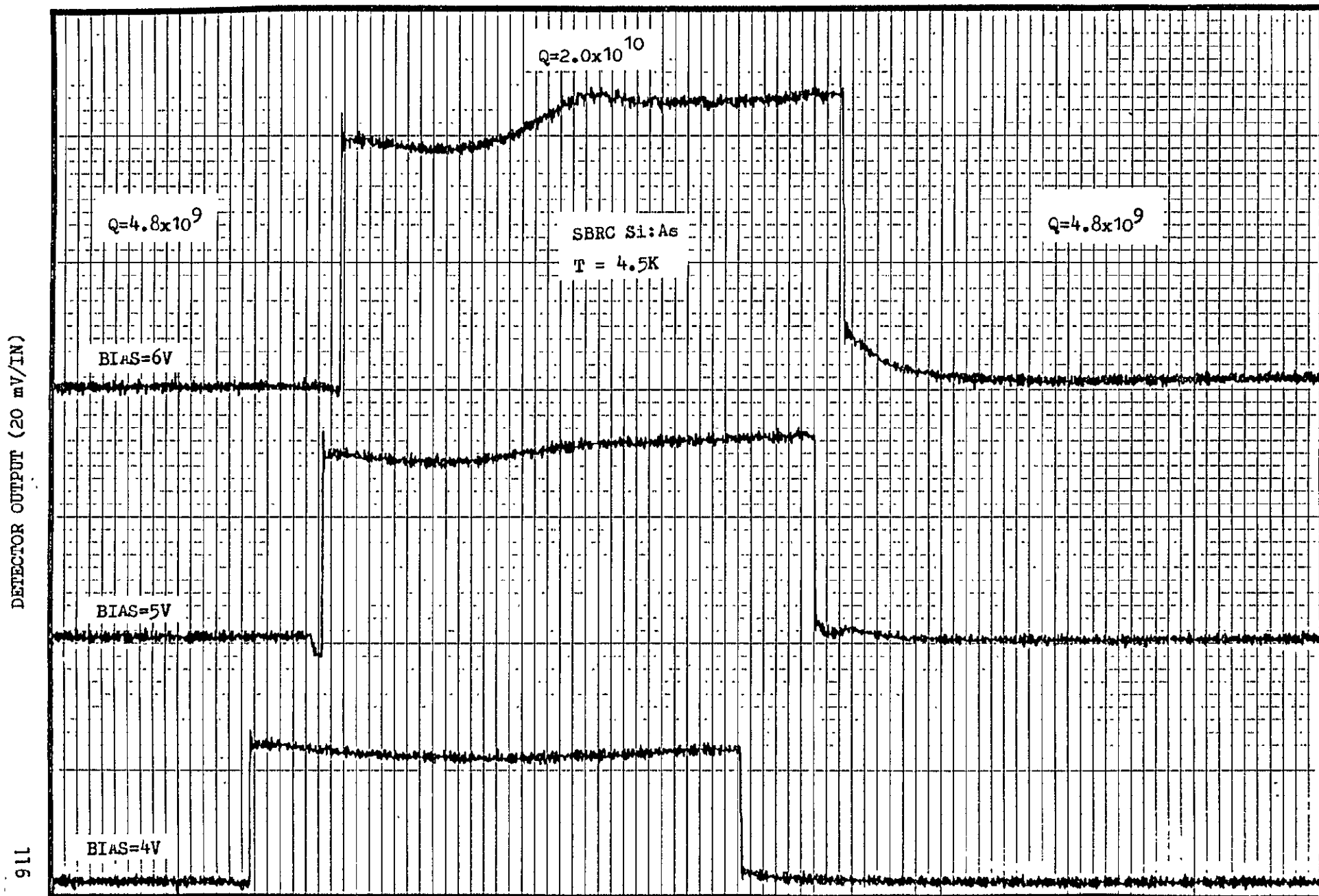


Figure 101

TIME (0.5 SEC/IN)

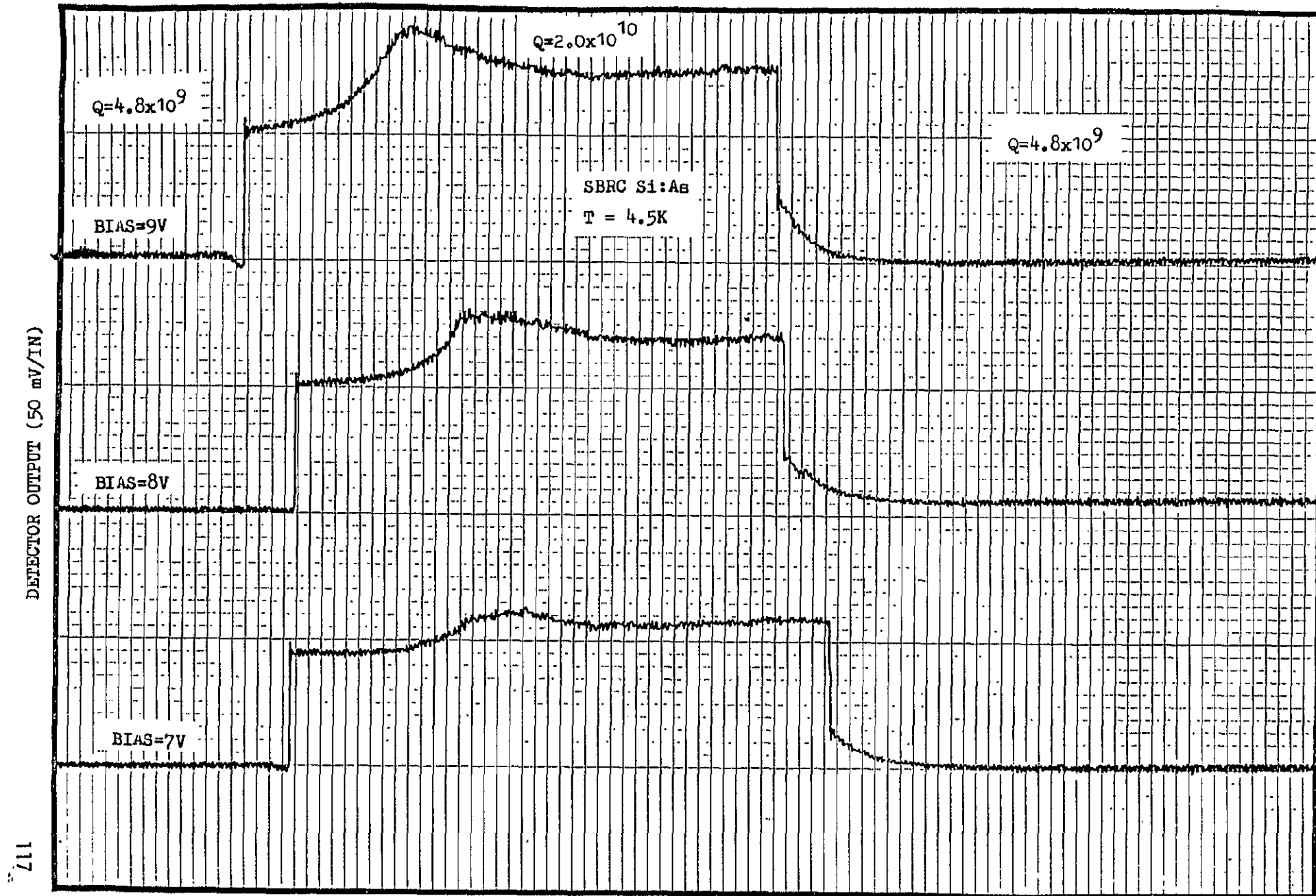


Figure 102

TIME (0.5 SEC/IN)

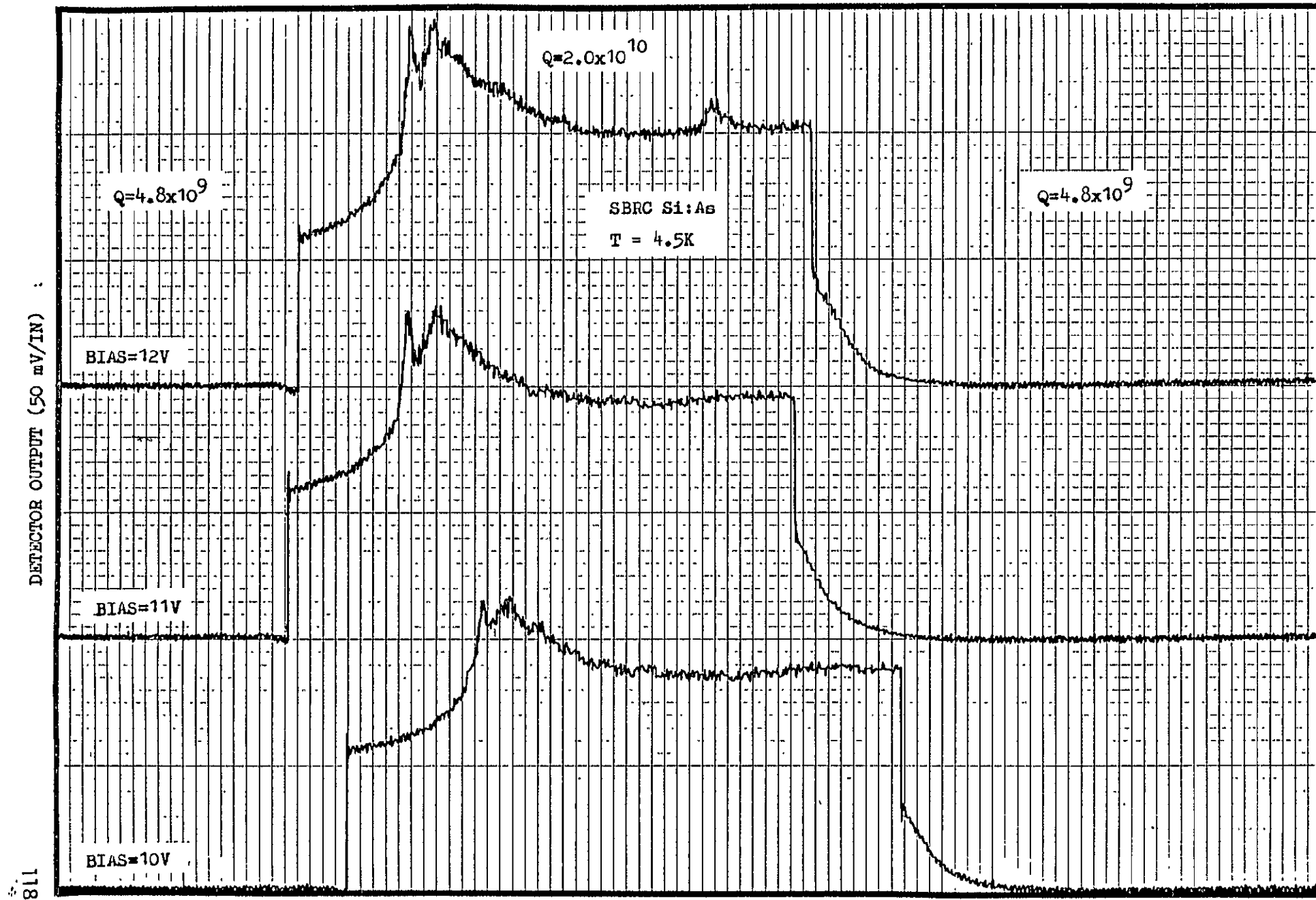


Figure 103

TIME (0.5 SEC/IN)

5Sec.

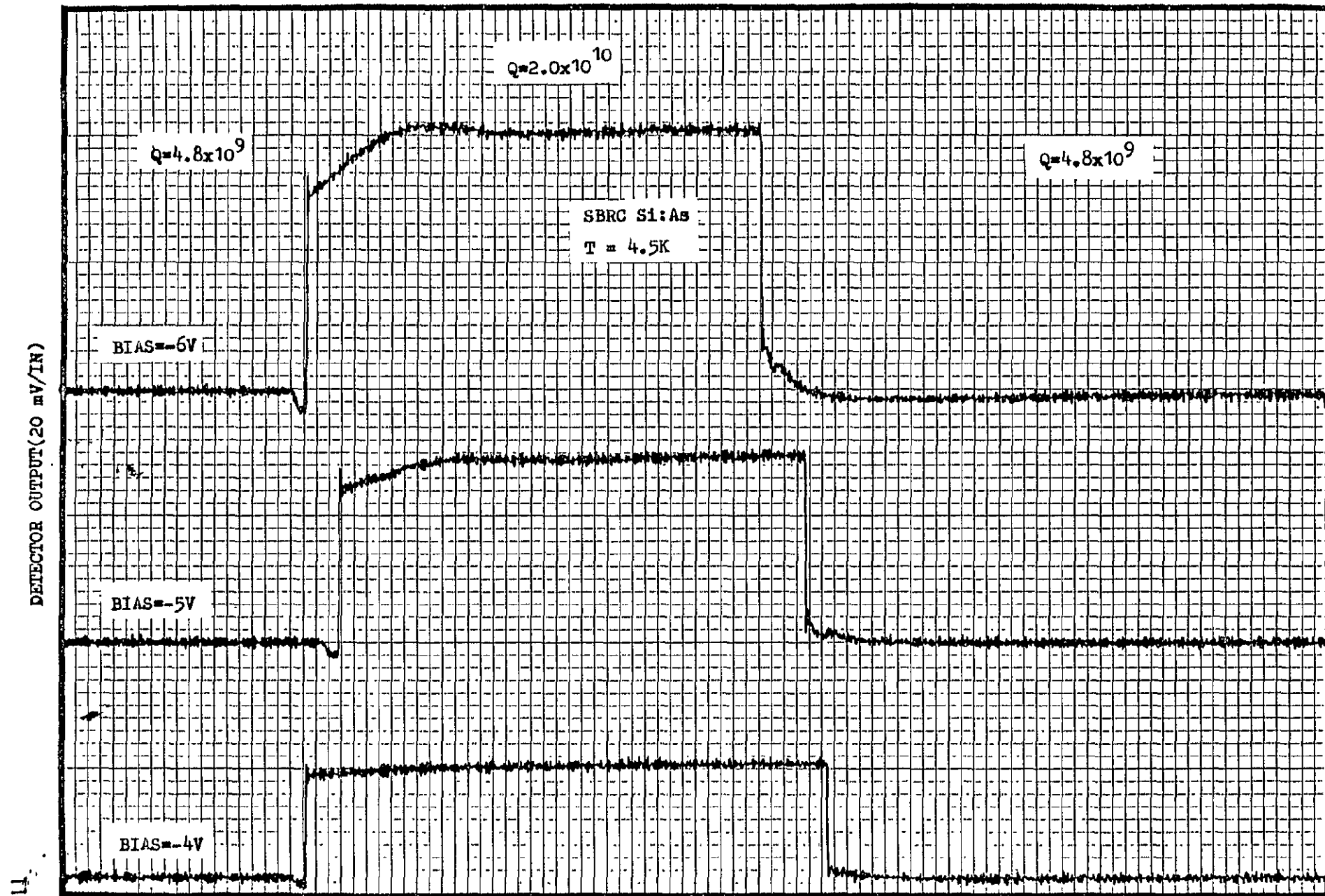
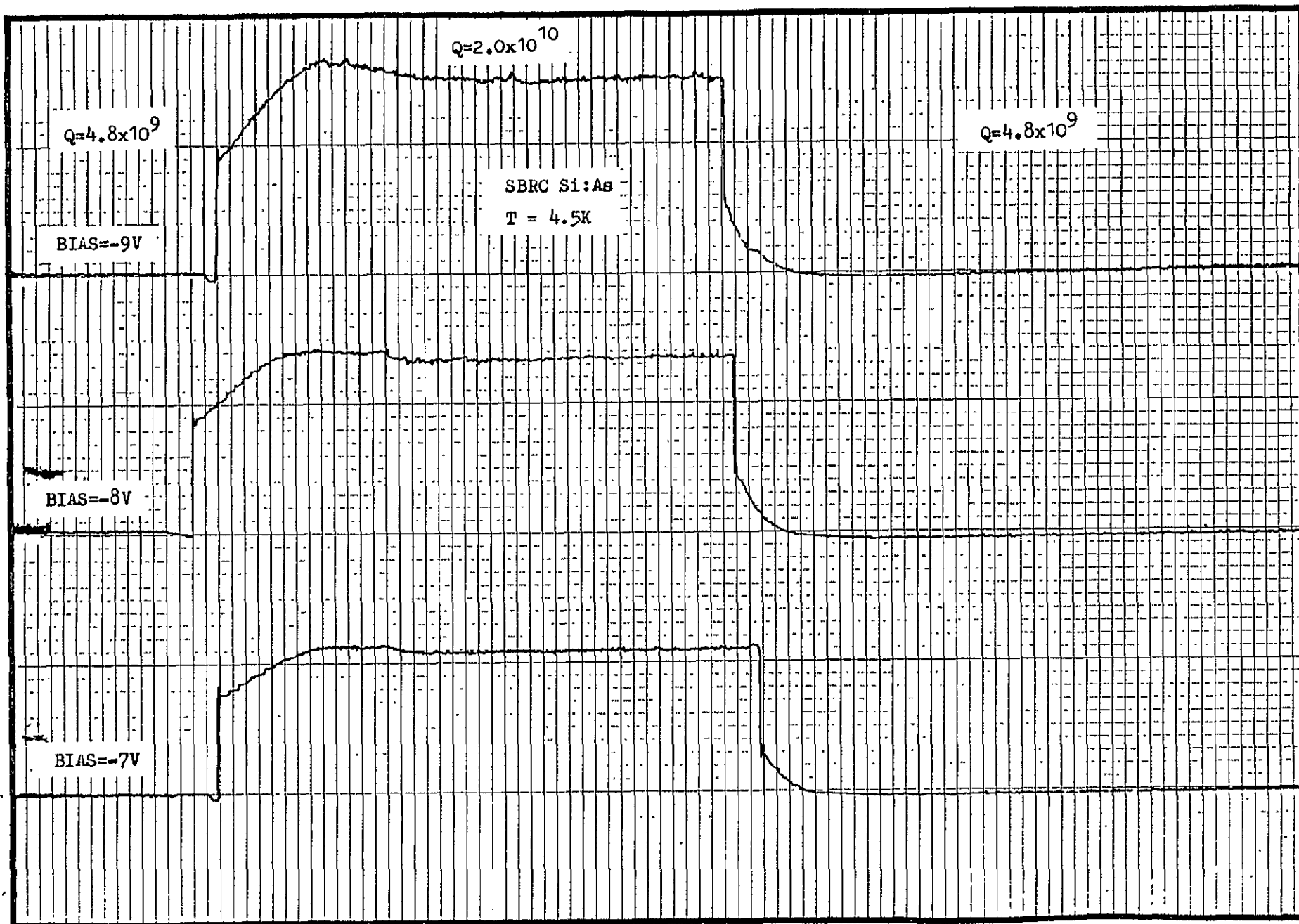


Figure 104

TIME (0.5 SEC/IN)

DETECTOR OUTPUT (50 mV/IN)



120

Figure 105

TIME (0.5 SEC/IN)

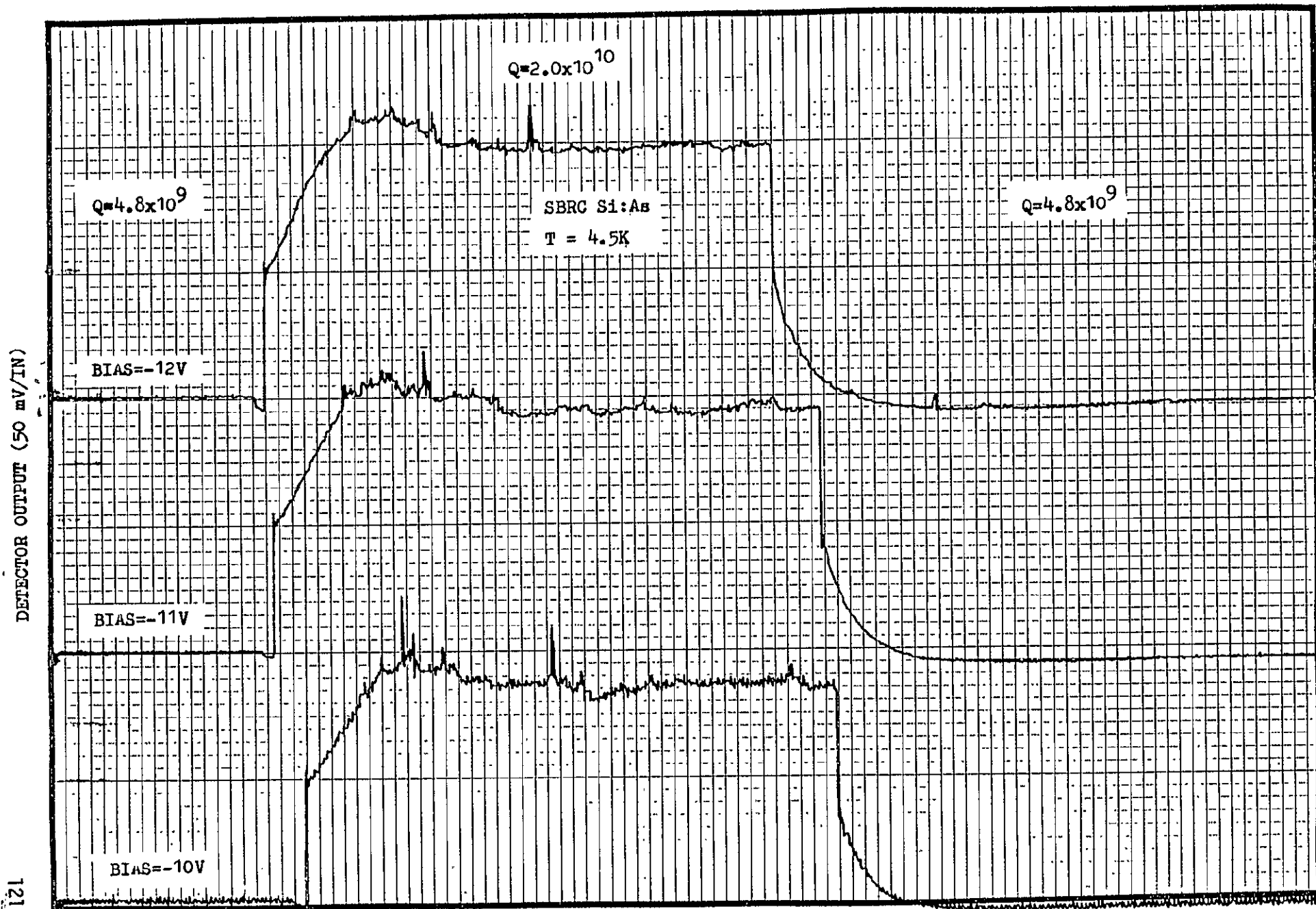


Figure 106

TIME (0.5 SEC/IN)

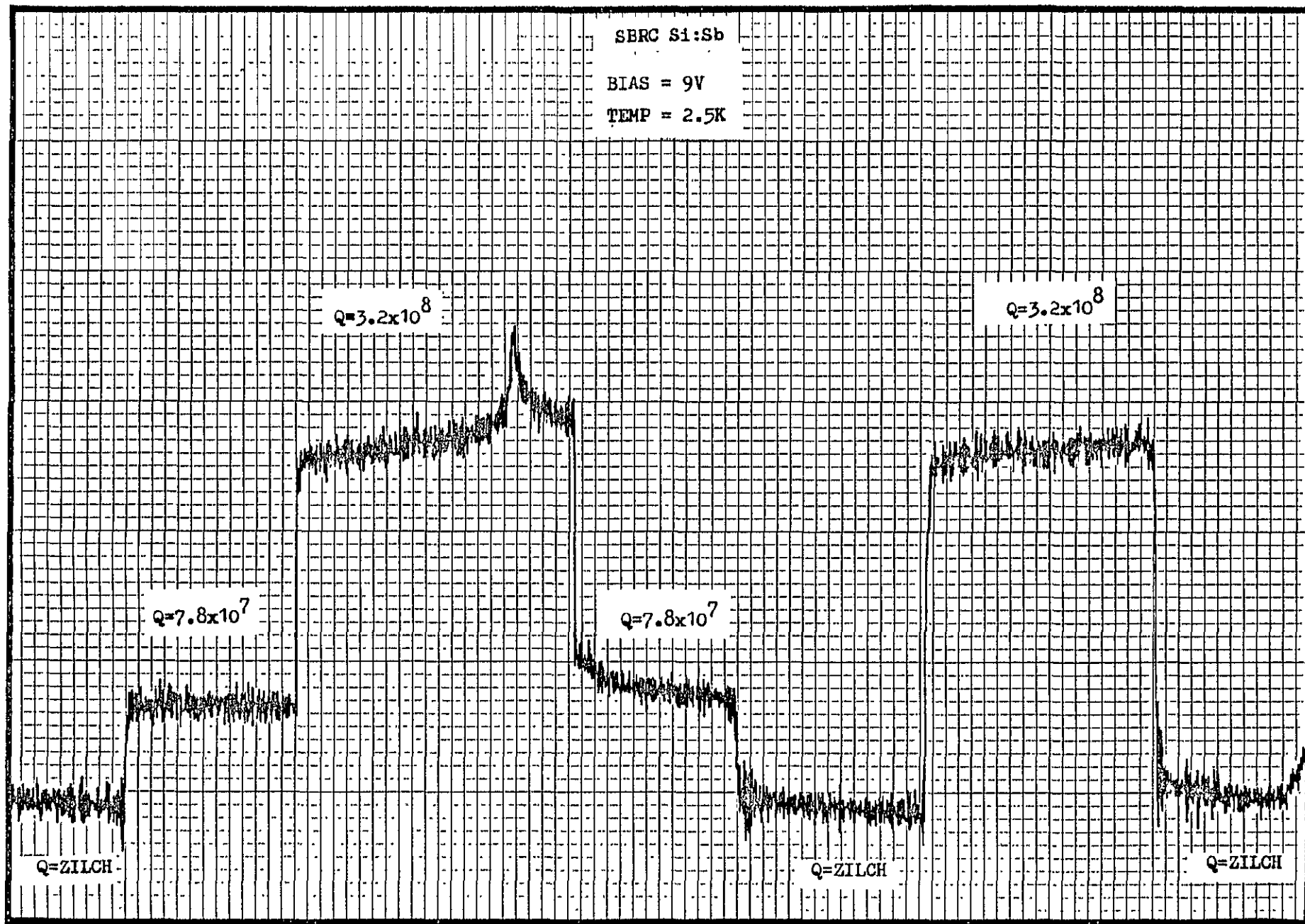


Figure 107

TIME (10 SEC/IN)



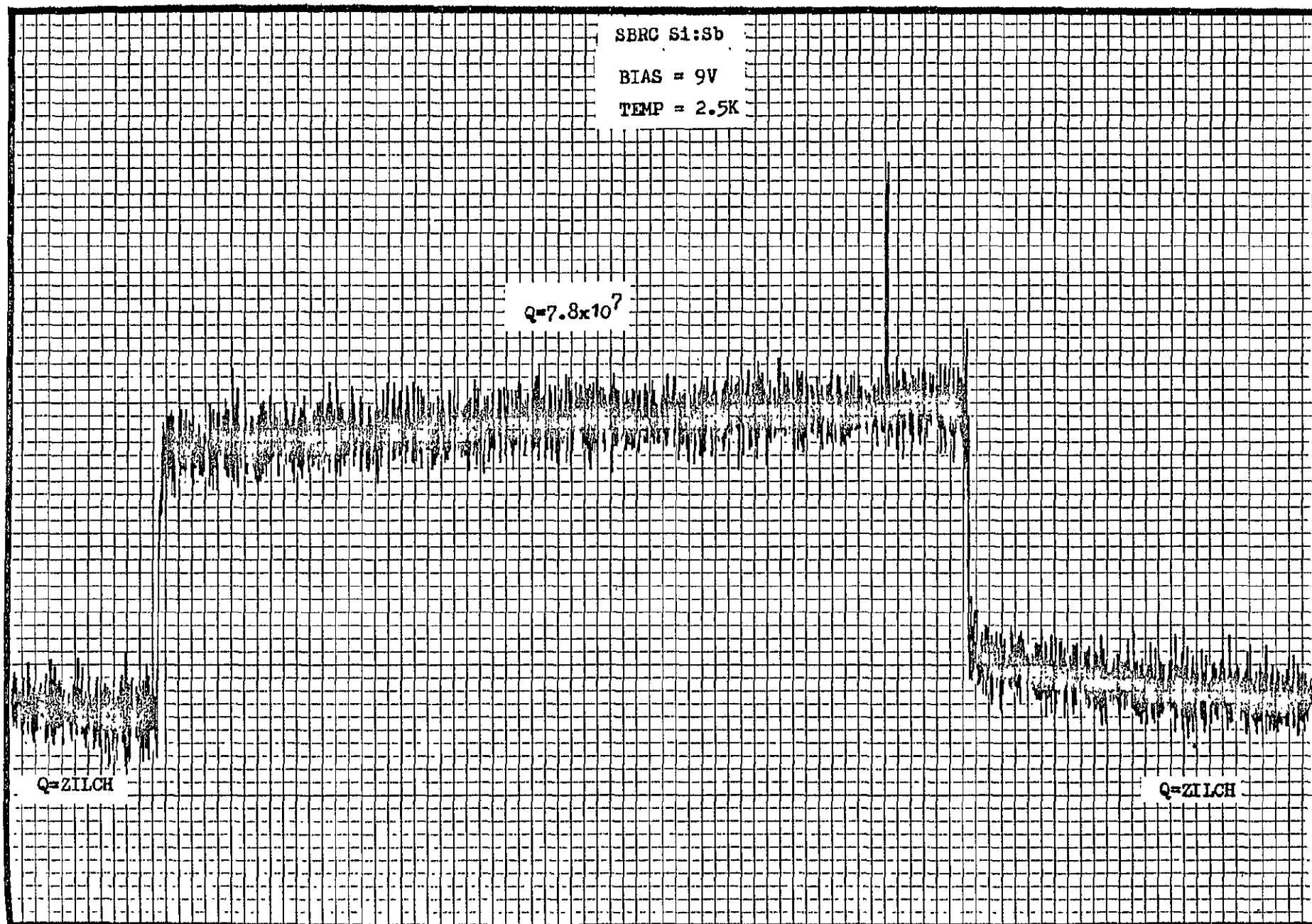


Figure 108

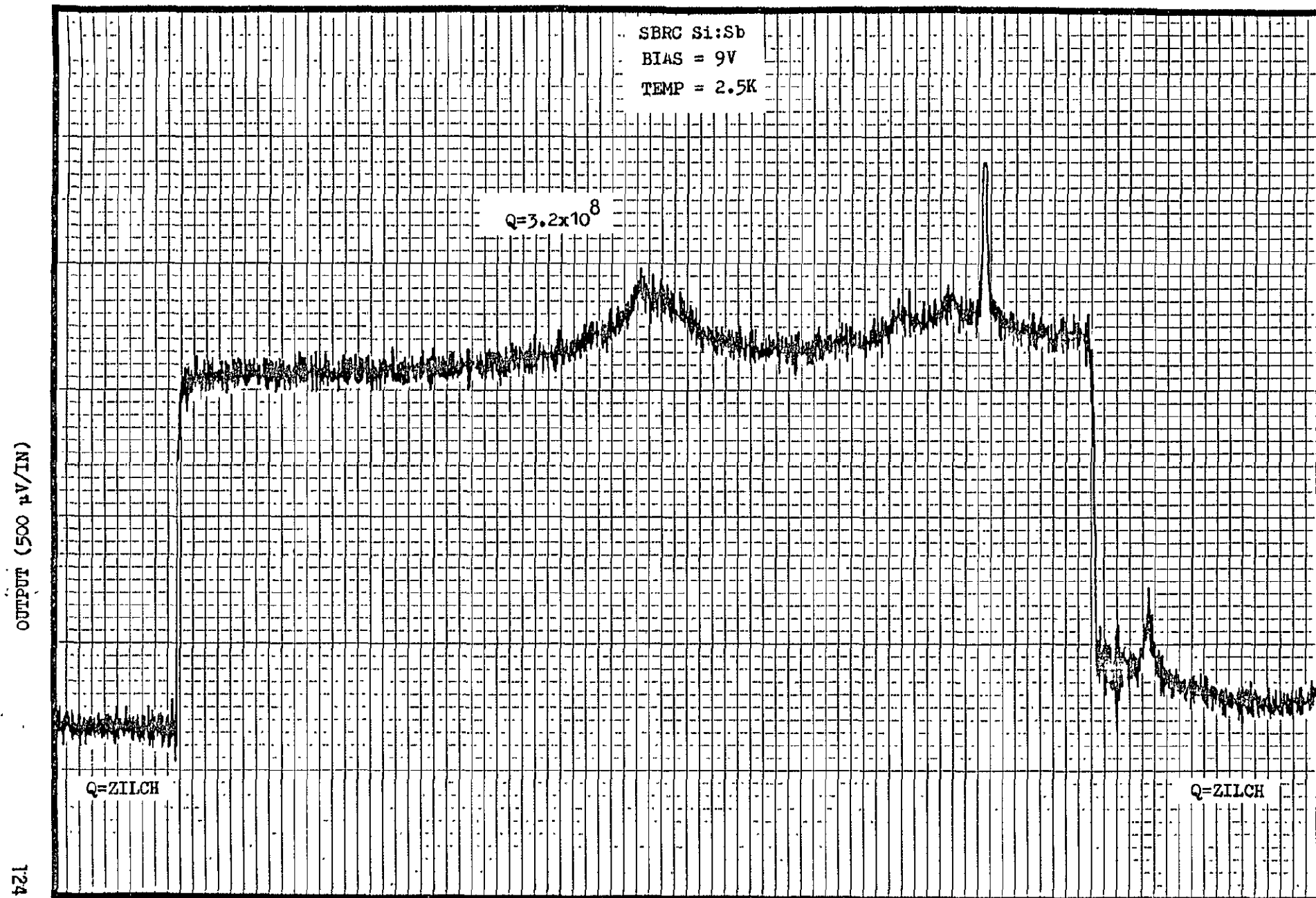


Figure 109

TIME (10 SEC/IN)

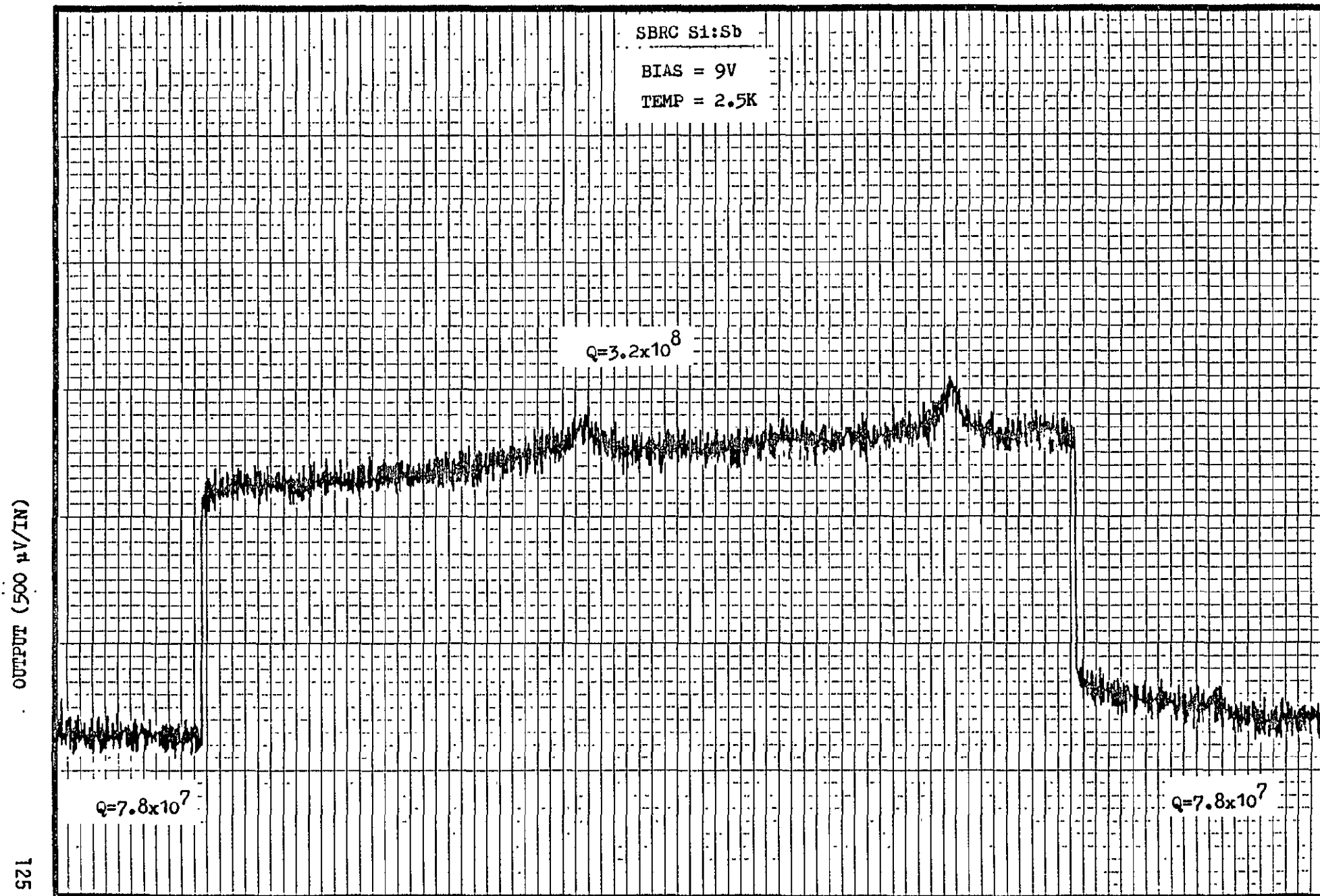


Figure 110

TIME (10 SEC/IN)

OUTPUT (500 μV/IN)

SBRC Si:Sb  
BIAS = 9V  
TEMP = 2.5K

$Q = 3.2 \times 10^8$

$Q = 7.8 \times 10^7$

Figure 111

TIME (10 SEC/IN)

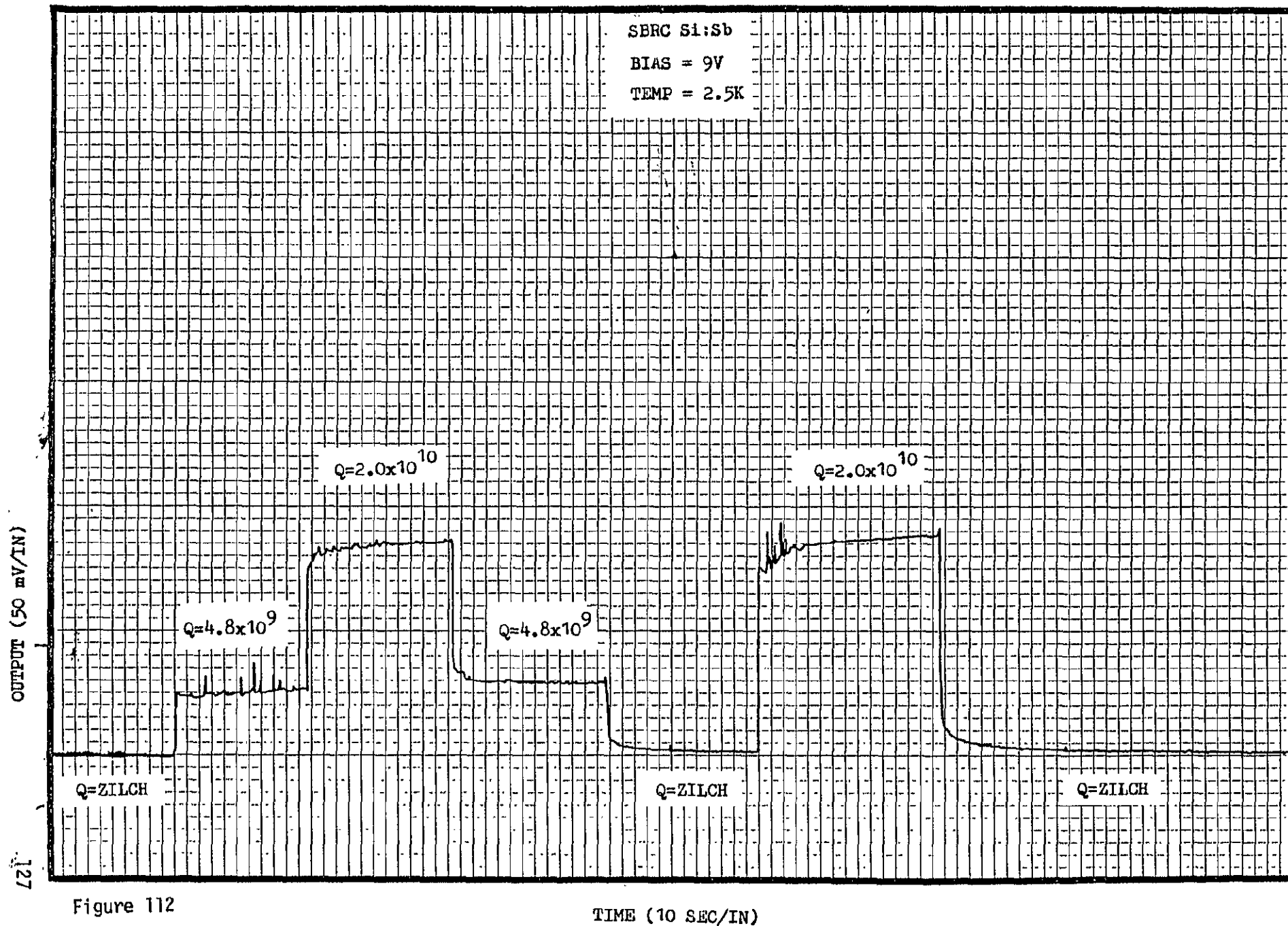
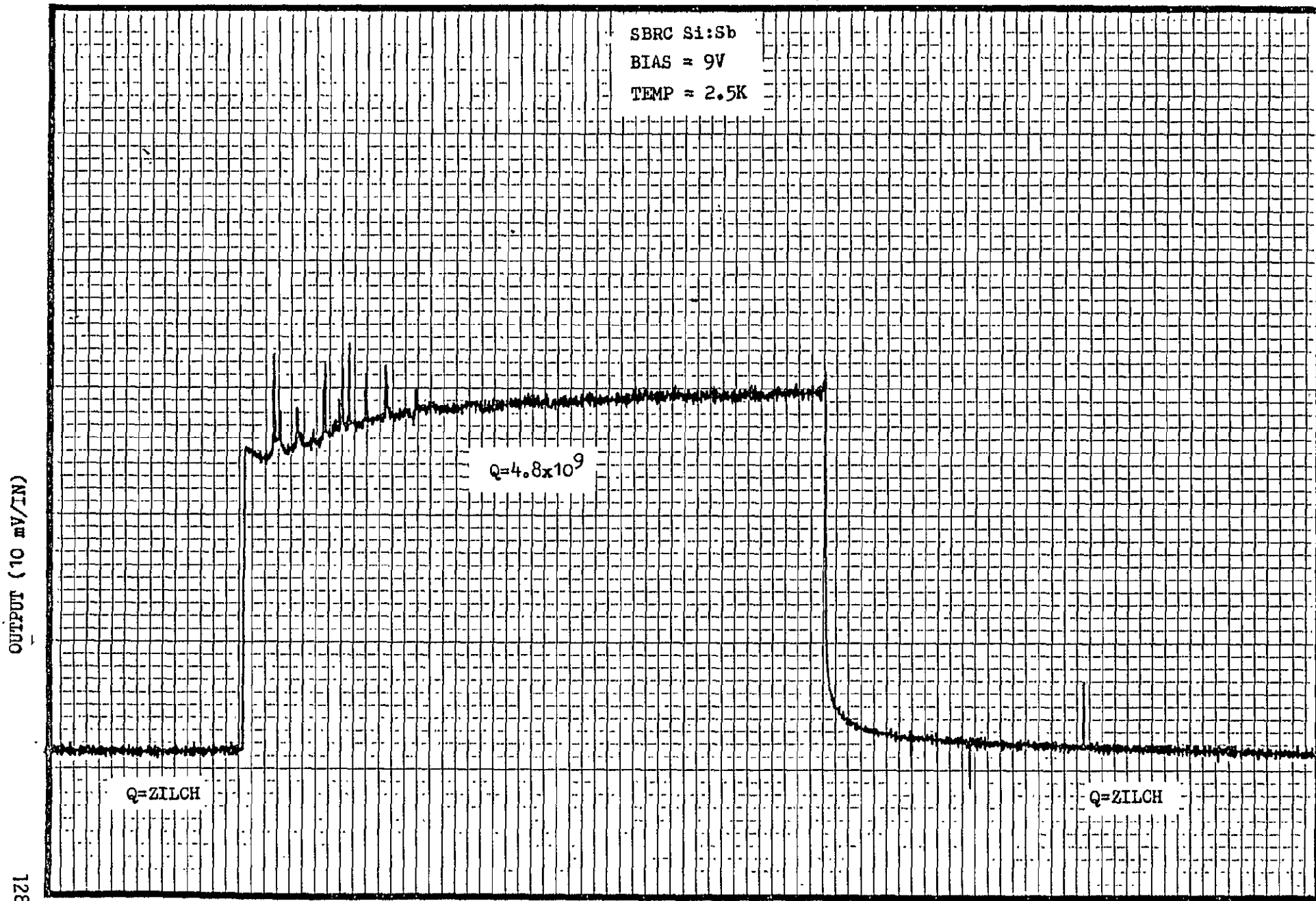


Figure 112

TIME (10 SEC/IN)



128

Figure 113

TIME (10 SEC/IN)

(NI/A 05) TUPUO

129

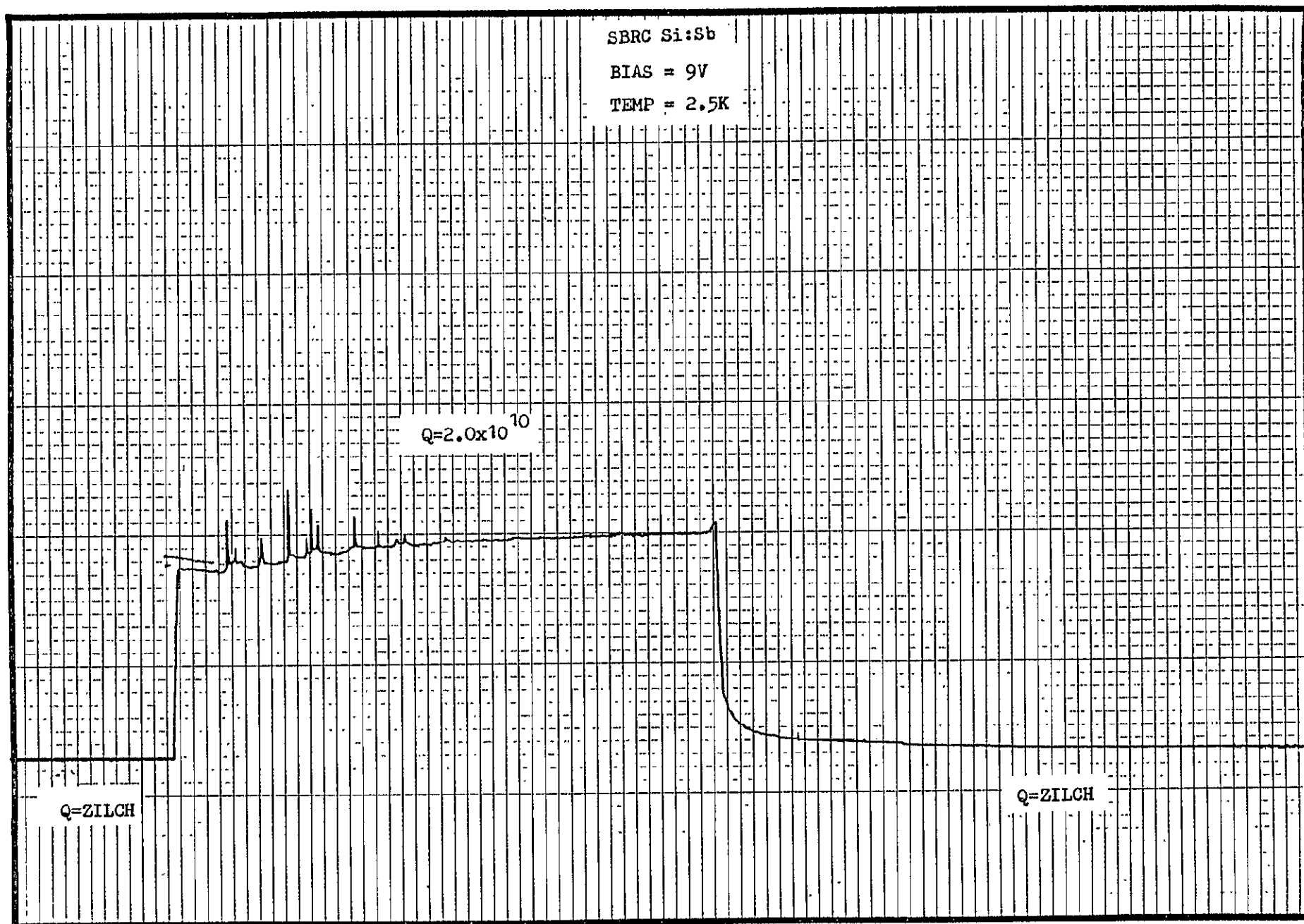


Figure 114

TIME (2 SEC/IN)

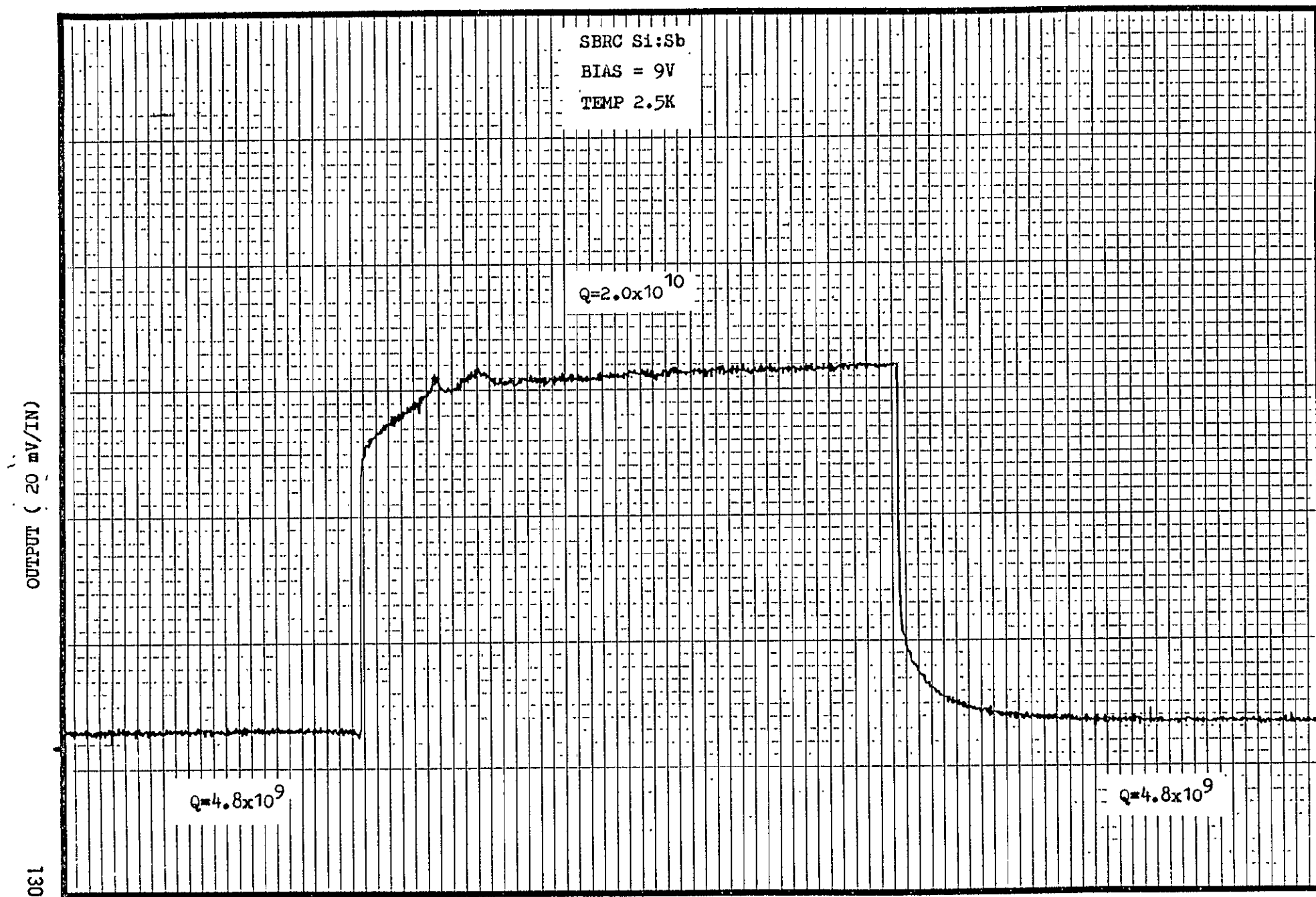


Figure 115

TIME (1 SEC/IN)



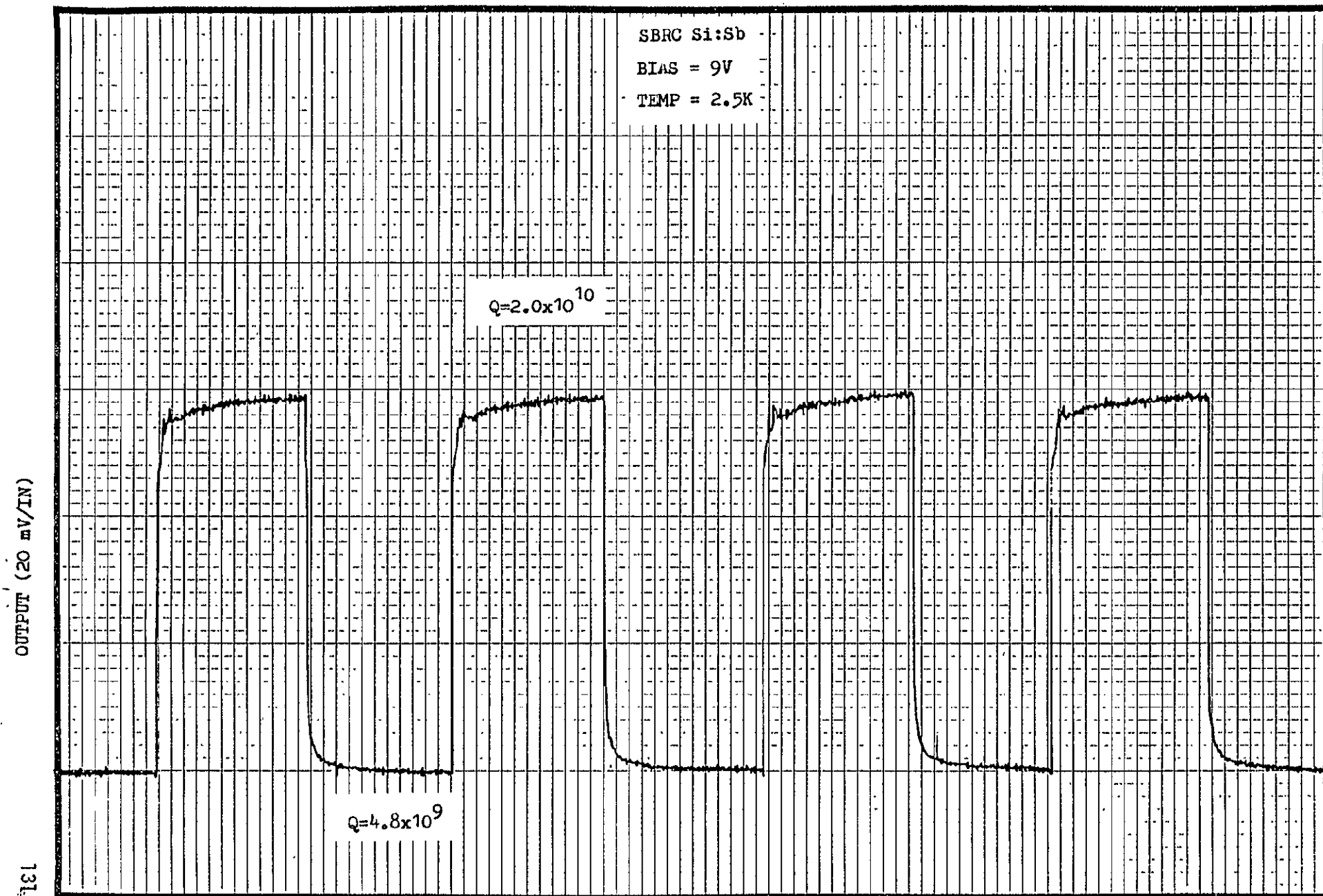


Figure 116

TIME (10 SEC/IN)

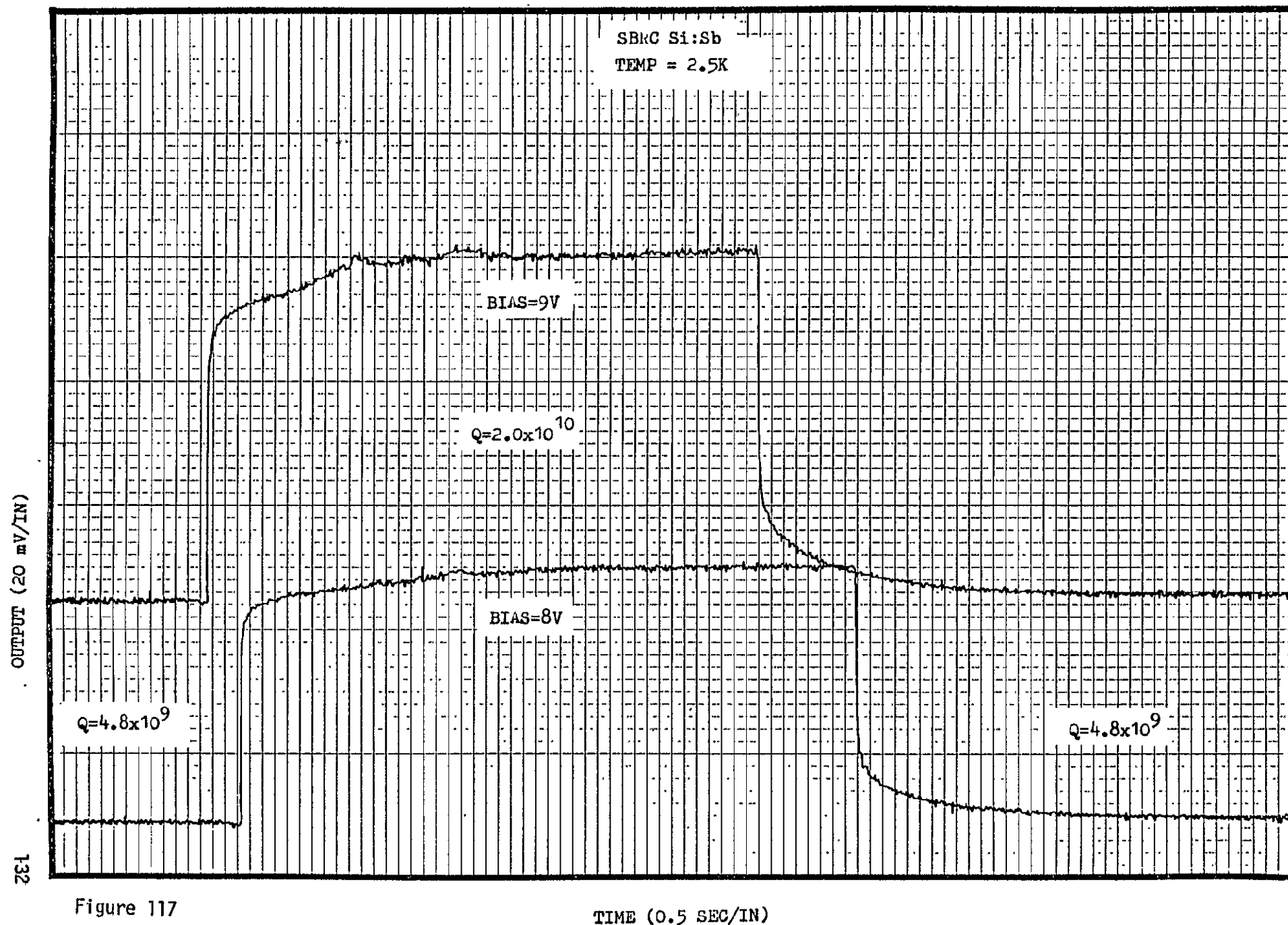


Figure 117

TIME (0.5 SEC/IN)

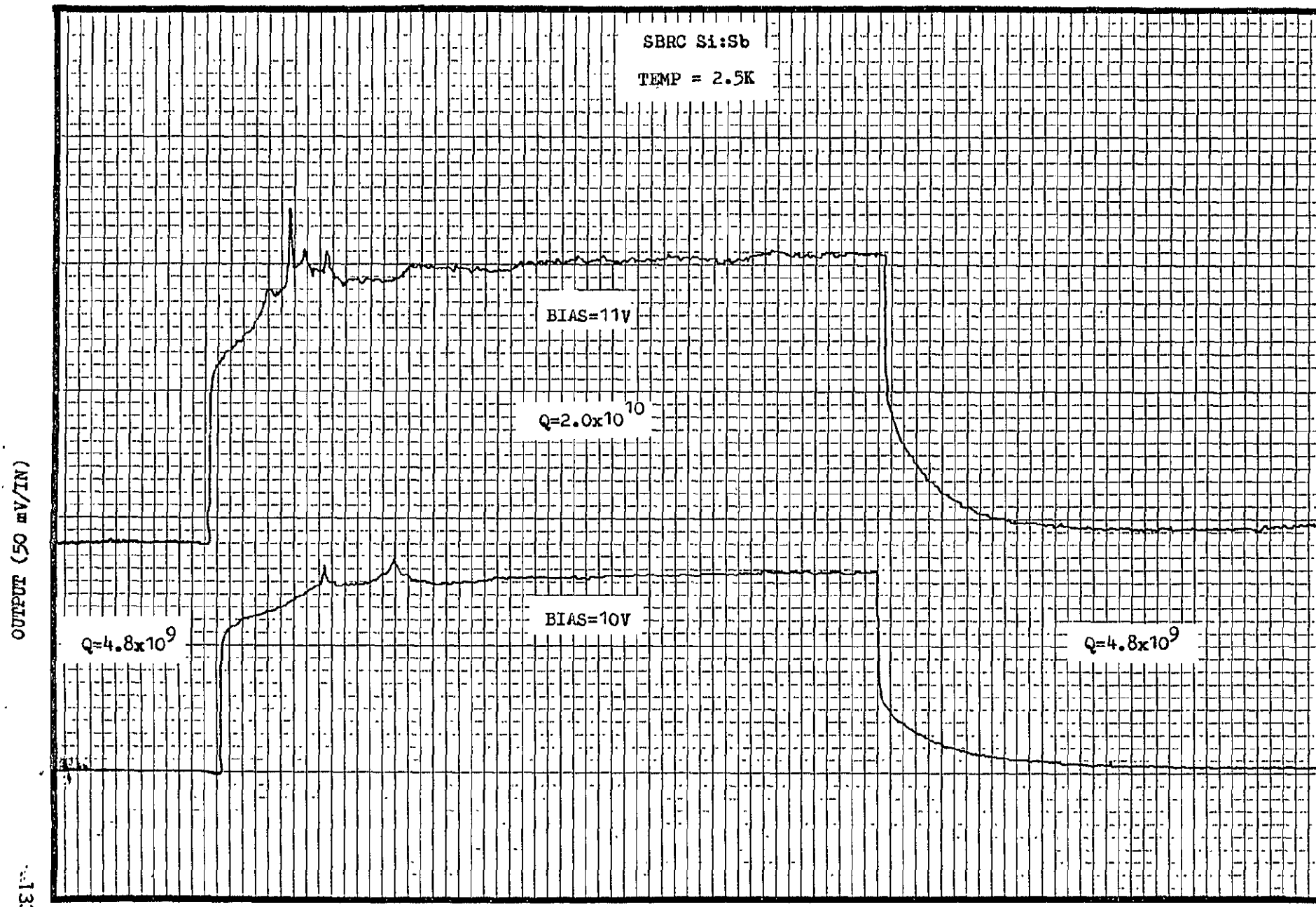


Figure 11a

TIME (0.5 SEC/IN)

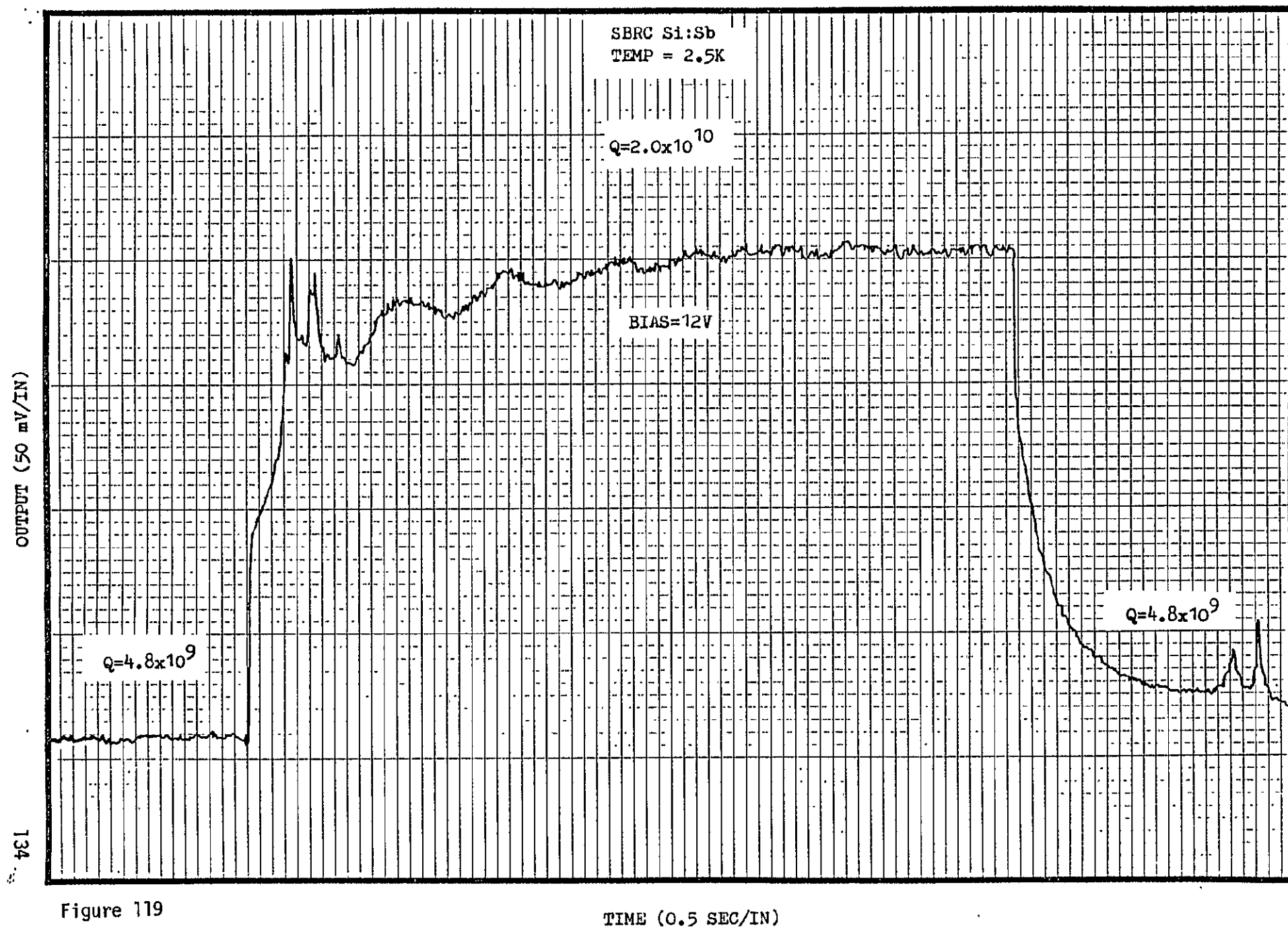


Figure 119

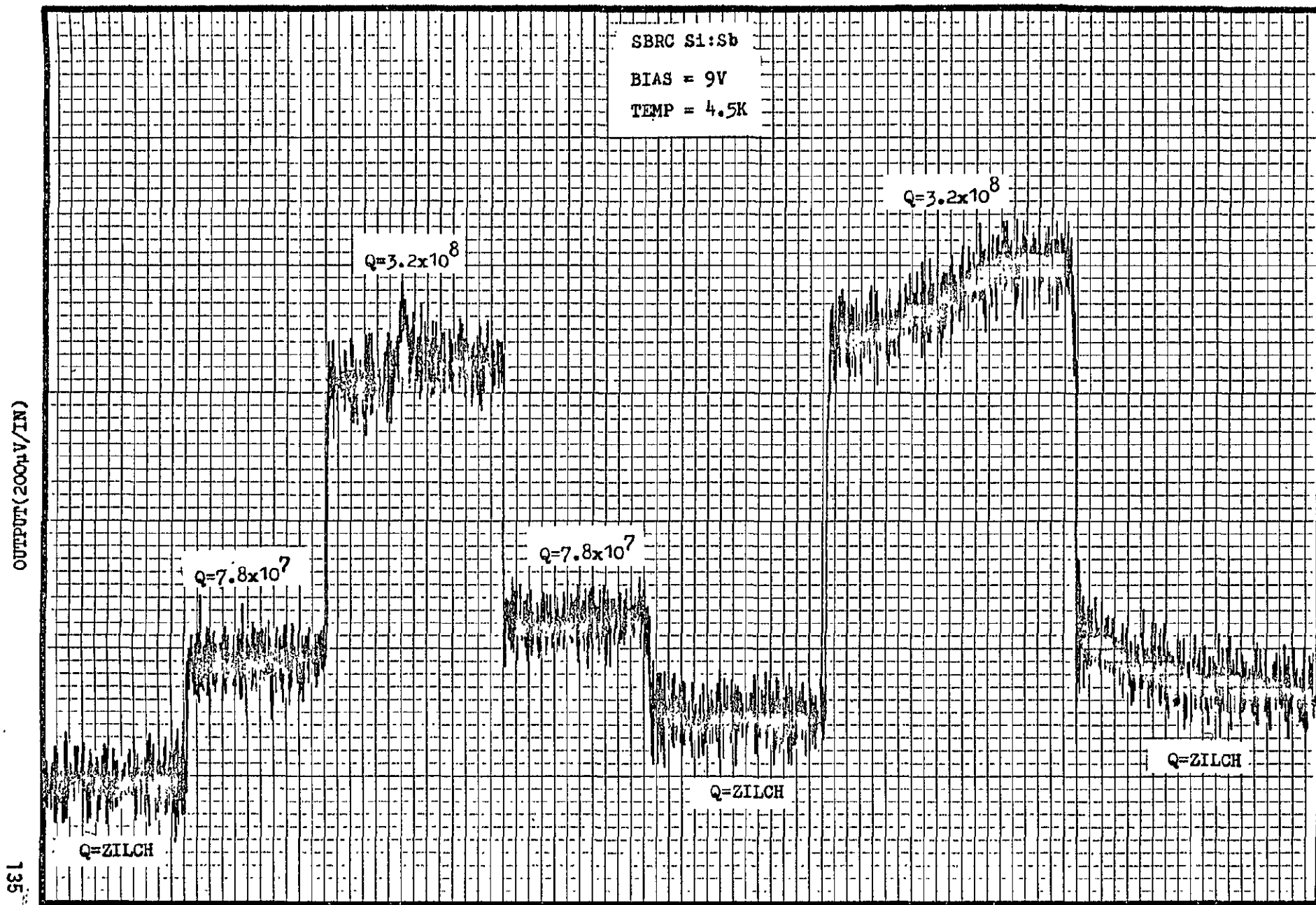


Figure 120

TIME (10 SEC/IN)

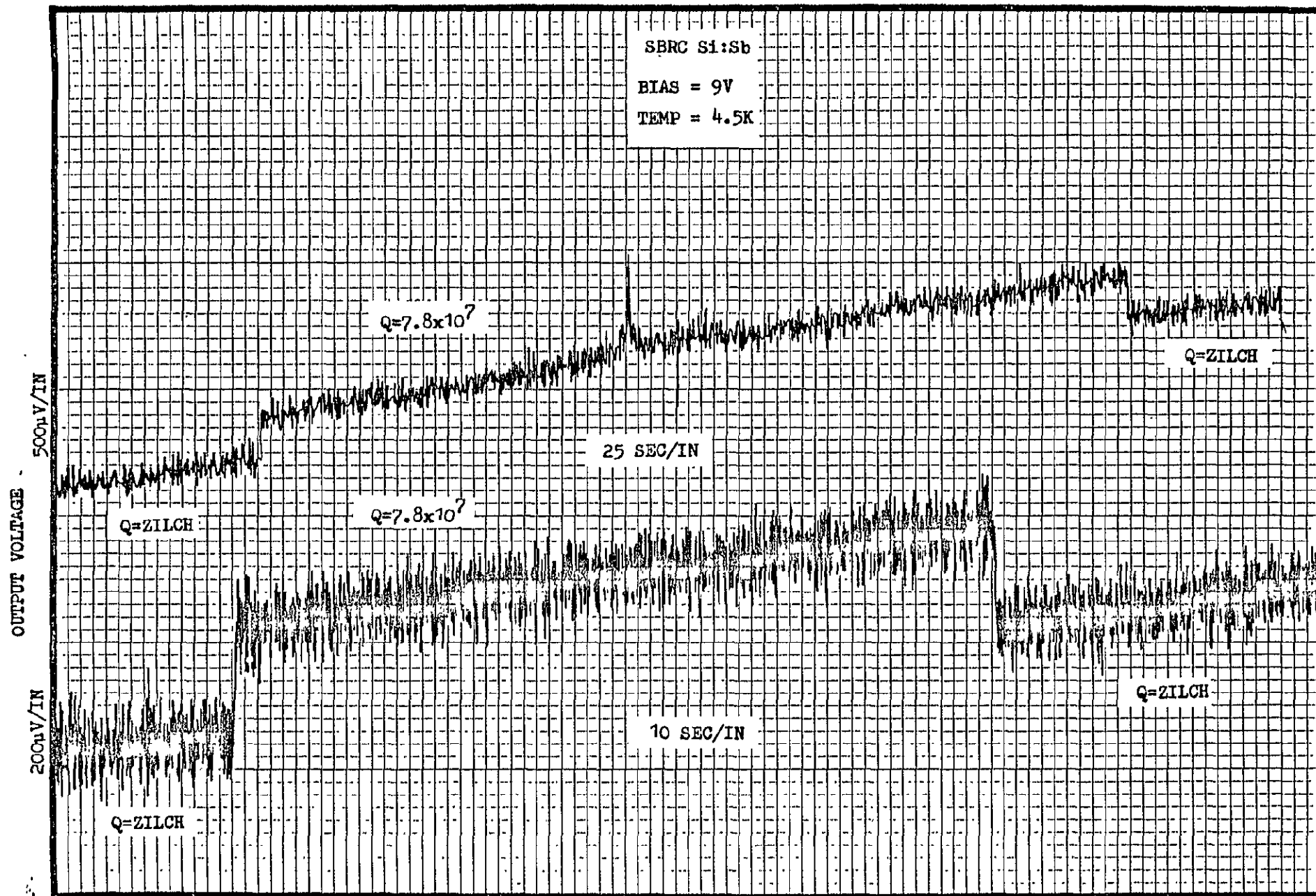


Figure 121

TIME

OUTPUT (500μV/IN)

SBRC Si:Sb

BIAS = 9V

TEMP = 4.5K

$Q=3.2 \times 10^8$

Q=ZILCH

Q=ZILCH

137

Figure 122

TIME (20 SEC/IN)

OUTPUT (500μV/IN)

138

SBRC Si:Sb

BIAS = 9V

TEMP = 4.5K

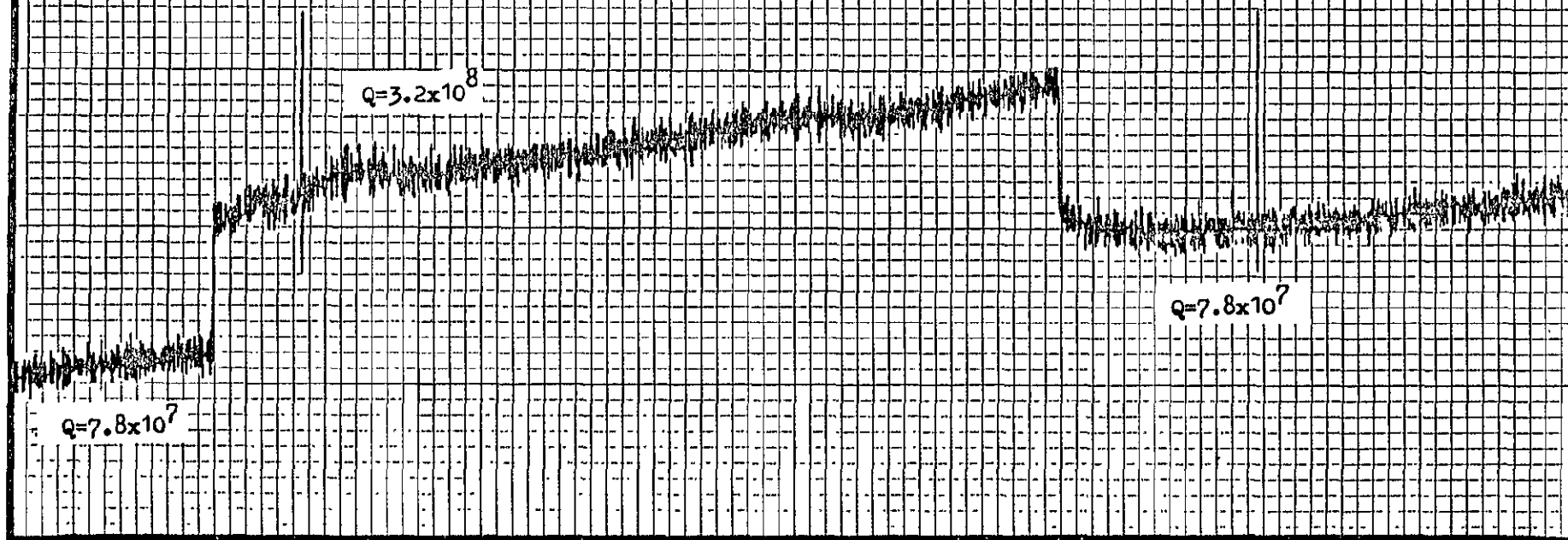


Figure 123

TIME (20 SEC/IN)



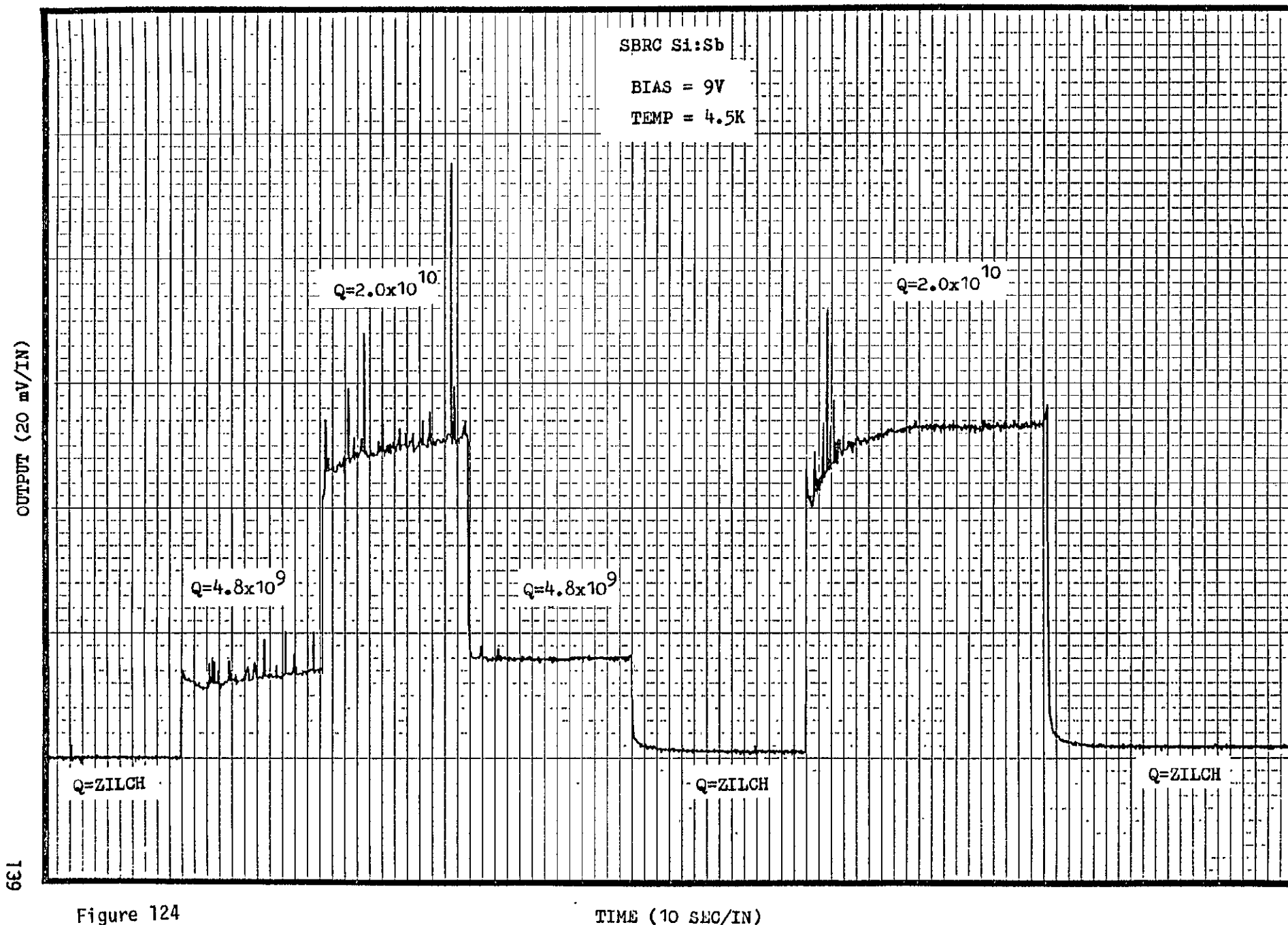


Figure 124

TIME (10 SEC/IN)

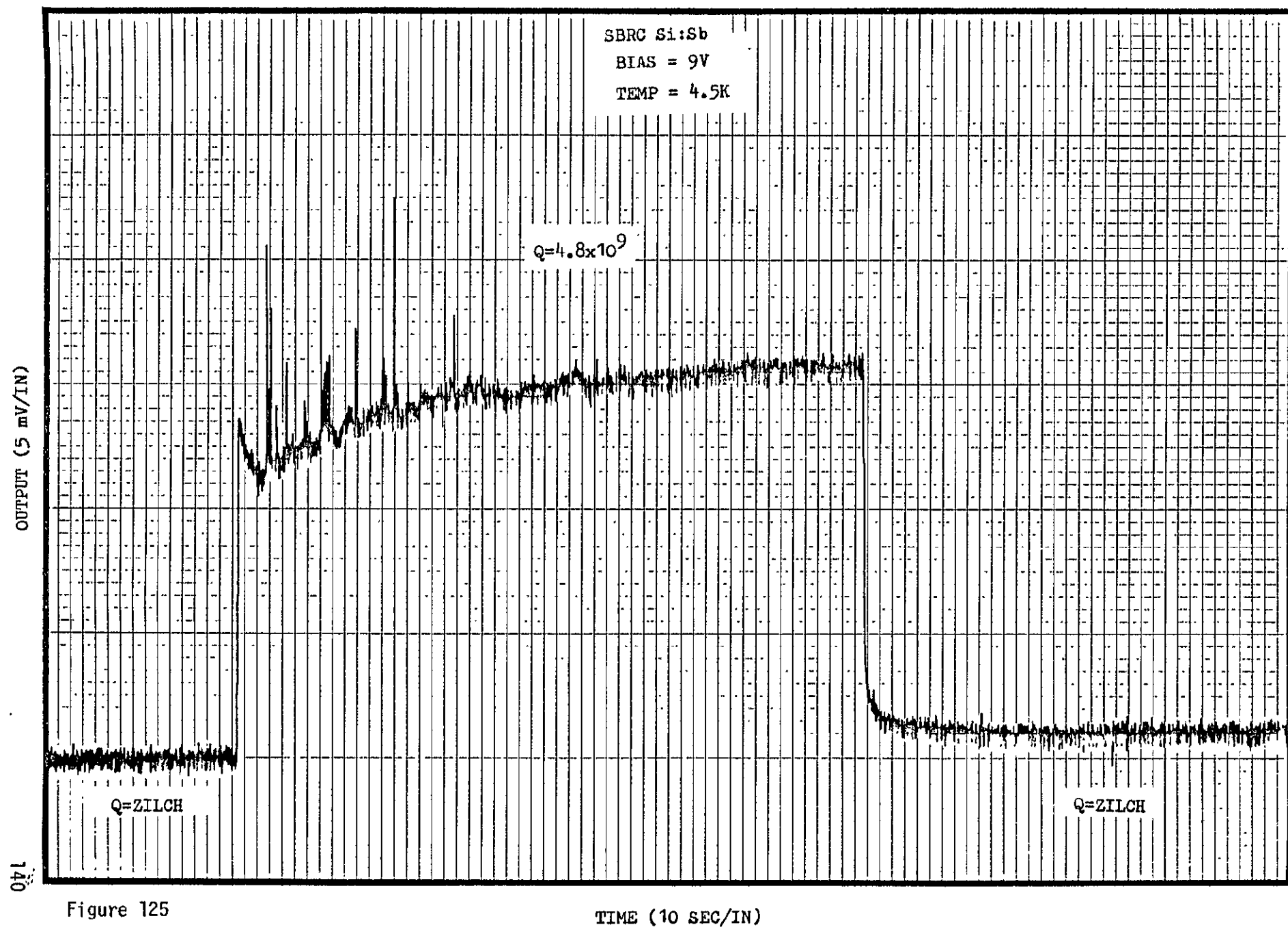


Figure 125

TIME (10 SEC/IN)

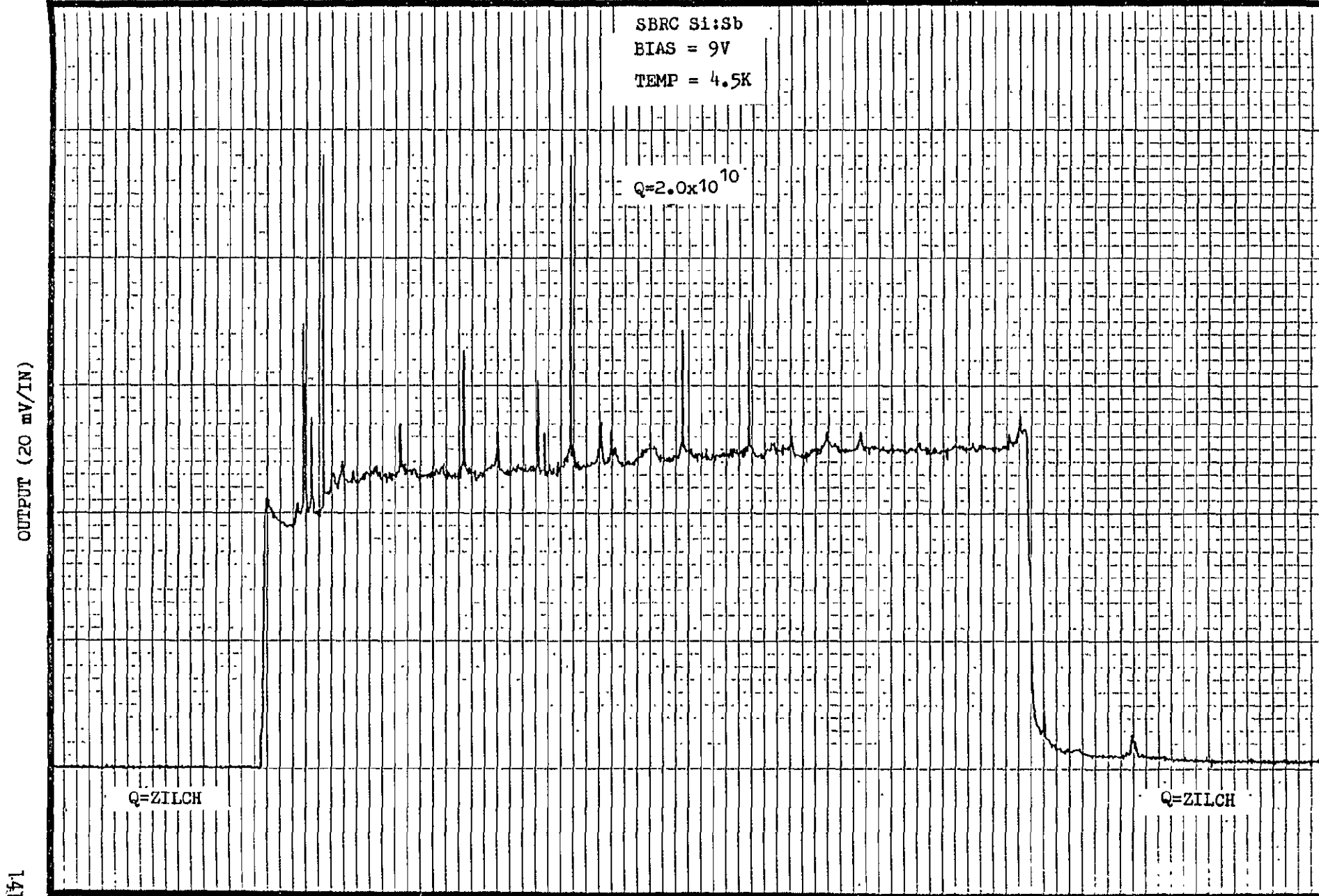


Figure 126

TIME (2 SEC/IN)

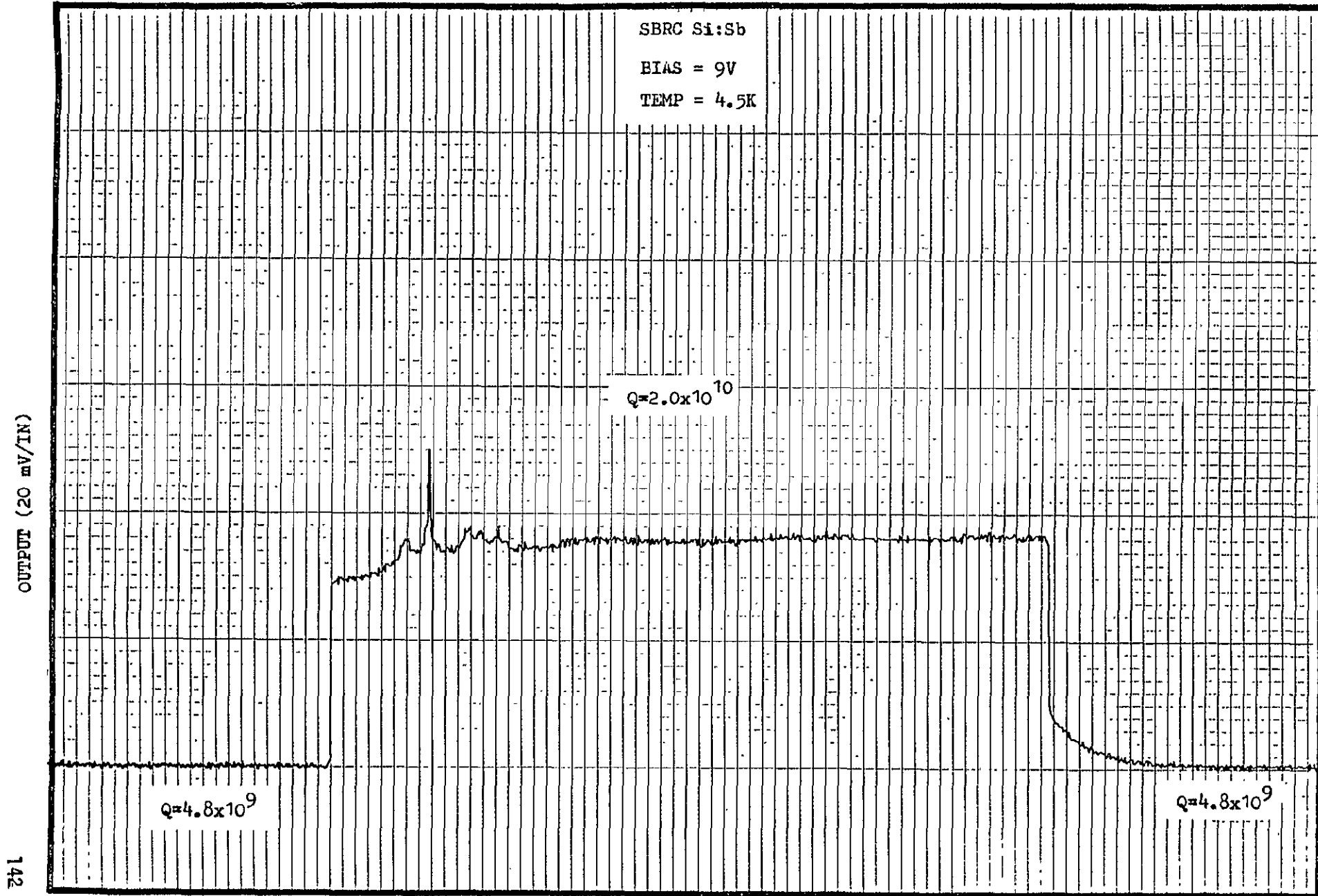


Figure 127

TIME (0.5 SEC/IN)

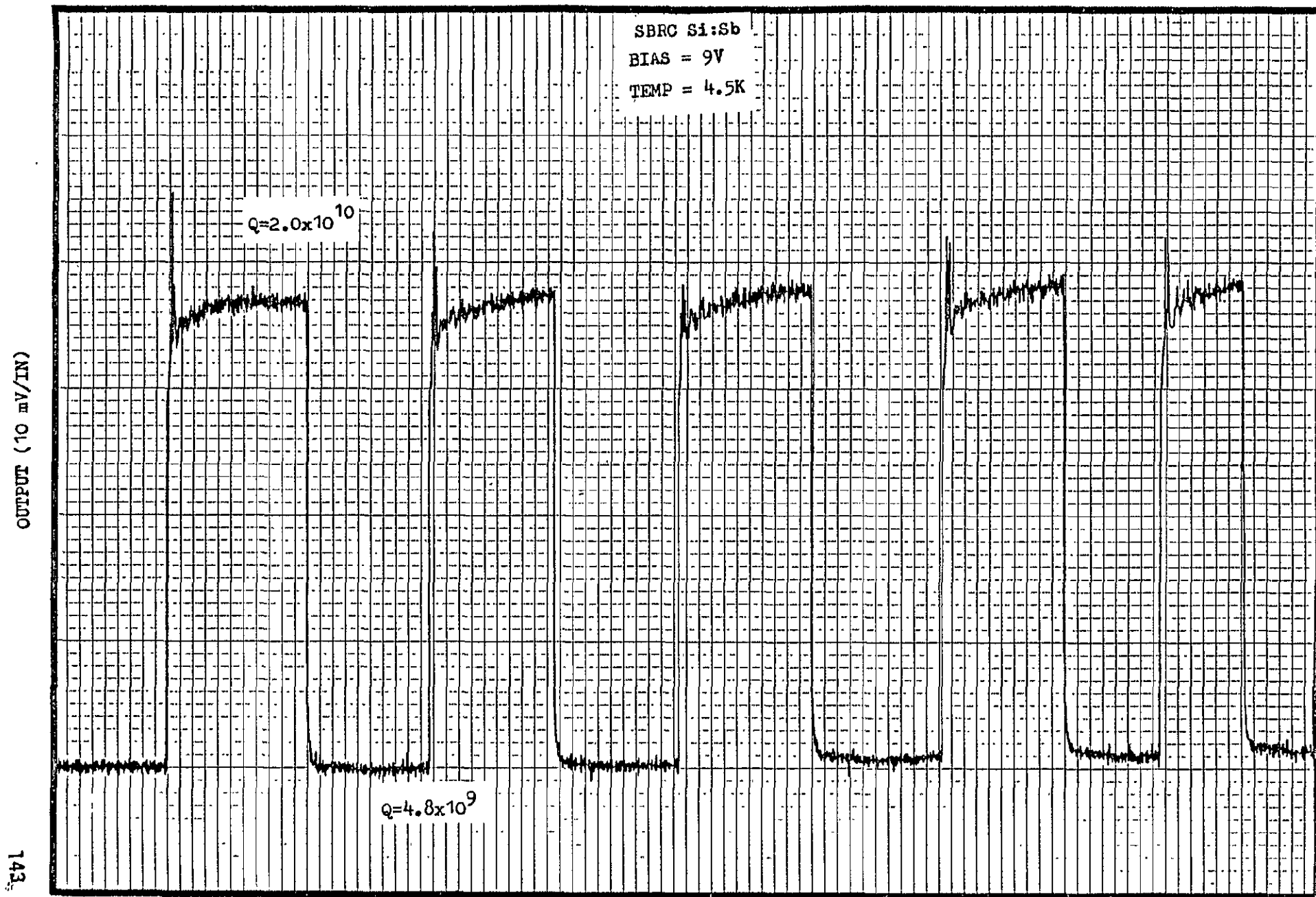
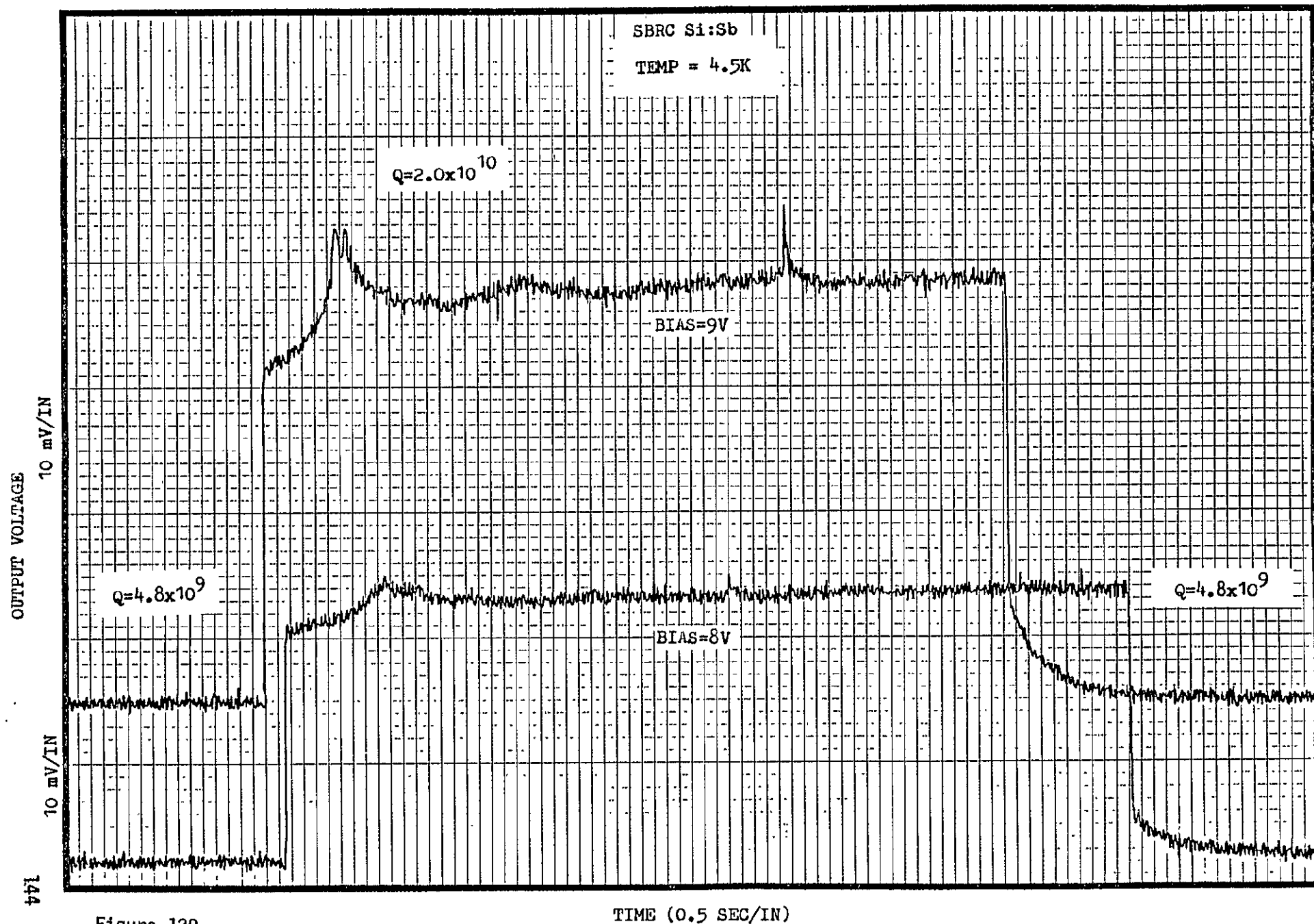


Figure 128

TIME (10 SEC/IN)



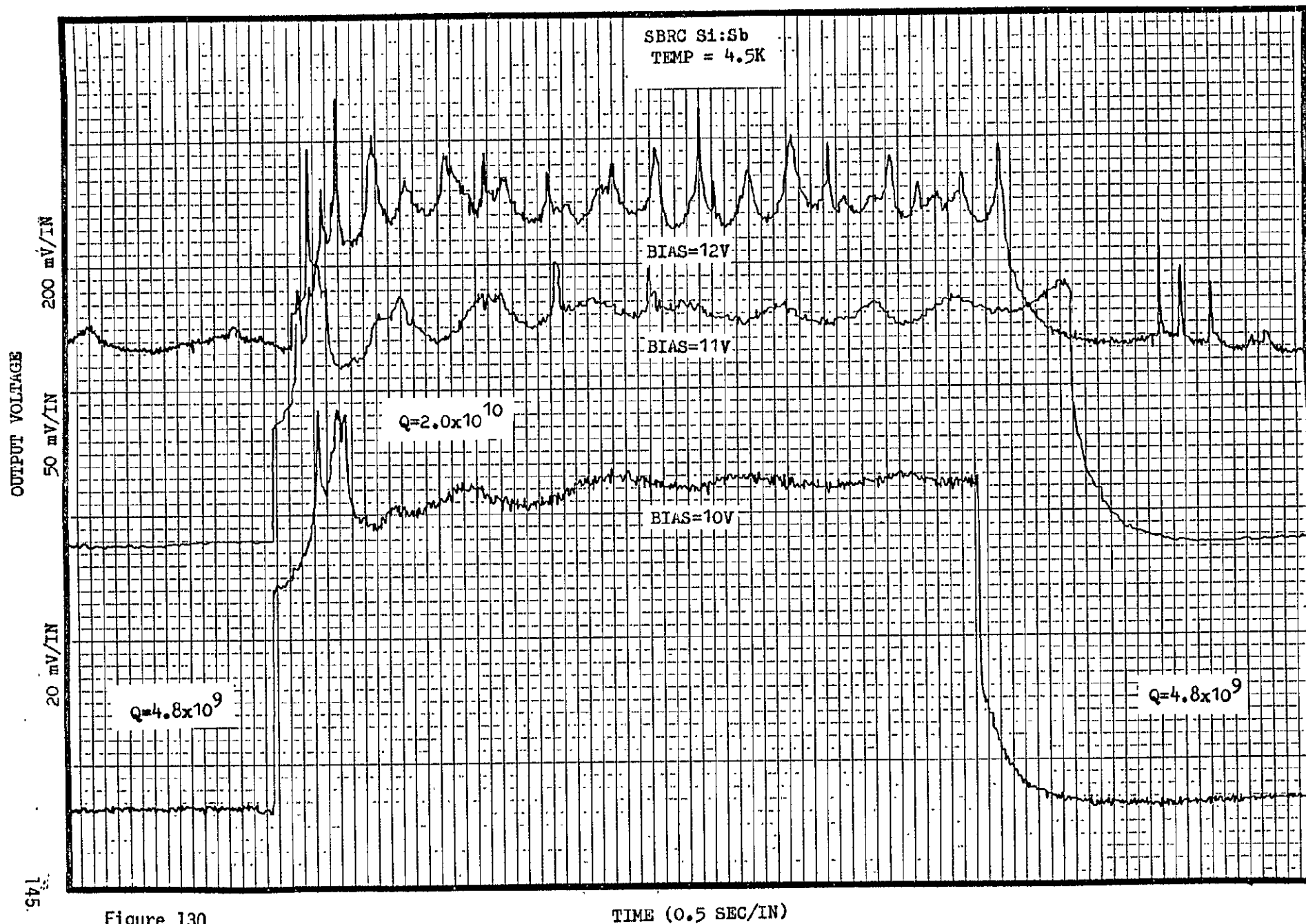


Figure 130